# The Neural Crest and Craniofacial Malformations

5

Hans J. ten Donkelaar, Christl Vermeij-Keers,
and Irene M.J. Mathijssen

## Contents



H.J. ten Donkelaar, M.D., Ph.D. (✉)
935 Department of Neurology,
Radboud University Nijmegen Medical Centre,
9101, 6500 HB Nijmegen, The Netherlands
e-mail: hans.tendonkelaar@radboudumc.nl,
hjtendonkelaar@gmail.com

C. Vermeij-Keers, M.D., Ph.D. • I.M.J. Mathijssen, M.D., Ph.D.
Department of Plastic and Reconstructive Surgery,
Erasmus MC, University Medical Centre Rotterdam,
Rotterdam, The Netherlands

## 5.1 Introduction

The **neural crest** is a temporary embryonic structure that is composed of a population of multipotent cells that delaminate from the ectoderm by epitheliomesenchymal tranformation (Duband et al. 1995; Hay 1995; Le Douarin and Kalcheim 1999; Francis-West et al. 2003; Thiery and Sleeman 2006; Acloque et al. 2009; Cordero et al. 2011; Liu et al. 2012; Dupin and Coelho-Aguiar 2013). Neural-crest-derived cells are called *mesectodermal* or *ectomesenchymal cells* (mesodermal cells of ectodermal origin) that have arisen through EMT. The neural crest was first described by His (1868) in the chick embryo as a *Zwischenstrang*, a strip of cells lying between the dorsal ectoderm and the neural tube. Classic contributions in amphibians identified interactions between tissues that lead to neural crest formation, and were reviewed by Hörstadius (1950). Cell labelling techniques, for example the quail-chick chimeric marker (Le Douarin 1969, 1973) and the *Cre-Lox* system (Chap. 2), showed that neural crest derivatives contribute to a large number of structures in the avian and mammalian species (Le Douarin and Kalcheim 1999; Le Douarin 2004; Dupin and Coelho-Aguiar 2013), including the spinal, cranial and autonomic ganglia, the enteric nervous system, the medulla of the adrenal gland, the melanocytes, dermal cells, corneal cells and many of the skeletal and connective tissues of the head. The whole facial and visceral skeleton and part of the neurocranium are formed from the neural crest (Wilkie and Morriss-Kay 2001; Morriss-Kay and Wilkie 2005). Many species-related discrepancies are present in the literature on the underlying developmental processes of the neural crest morphology and induction, EMT, neural crest cell migration and their targets.

In contrast to chick embryos, the neural crest in mammalian embryos is a less distinct structure and can be defined as the transition zone between the neuroectoderm and the presumptive epidermis from neural plate stages onwards (O'Rahilly and Müller 1999, 2007). In presomite murine embryos, however, the whole ectoderm, including the

H.J. ten Donkelaar et al., *Clinical Neuroembryology*,
DOI 10.1007/978-3-642-54687-7_5, © Springer-Verlag Berlin Heidelberg 2014

presumptive neural crest, is able to produce mesectodermal cells (Smits-van Prooije et al. 1985, 1987, 1988). These cells proliferate shortly after their migration into the mesodermal compartment (Vermeij-Keers and Poelmann 1980). In somite stages during the transformation of the cranial neuroectoderm of the head folds via the neural groove into the neural tube, there is a balance between the outgrowth of the neuroectoderm and the production of mesectodermal cells by the neural crest and only short-distance migration of these cells occurs.

In the past it was thought that the neural crest cells were pre-patterned (Noden 1978a, b, 1983a), but nowadays the neural crest cells are considered as stem cells. These multipotent cells have been identified during animal and human embryogenesis and can persist in many adult organs and tissues such as skin and teeth (Dupin and Coelho-Aguiar 2013). Additionally, it has been shown that the induction of the neural crest occurs much earlier than generally accepted, namely in gastrulation and neurulation stages (Basch et al. 2006; Steventon and Mayor 2012; Dupin and Coelho-Aguiar 2013).

The **cranial neural crest** provides the precursors of cartilage, bone, odontoblasts and connective tissue of the head (Vermeij-Keers 1990; Sulik 1996; LaBonne and Bronner-Fraser 1999; Le Douarin and Kalcheim 1999; Sperber 2002; Knecht and Bronner-Fraser 2002; Francis-West et al. 2003; Santagati and Rijli 2003; Cordero et al. 2011; Le Douarin and Dupin 2012; Dupin and Coelho-Aguiar 2013). During later developmental stages multiple places of EMT are recognized as well. In the head-neck area, for example, the neurogenic or surface ectoderm placodes and the optic neural crest are such areas. **Neurogenic placodes**, specialized regions of the embryonic ectoderm, are the major source of primary sensory neurons in the head (Johnston and Bronsky 1995; Graham and Begbie 2000; O'Rahilly and Müller 2007). The vasculature of the head is derived from mesoderm-derived endothelial precursors, whereas the neural crest provides the pericytes and smooth muscle cells of the vessels of the face and the forebrain (Etchevers et al. 2001; Dupin and Coelho-Aguiar 2013).

A number of craniofacial malformations have major neural crest involvement, and are usually referred to as ***neurocristopathies*** (Jones 1990; Johnston and Bronsky 1995, 2002; Gorlin et al. 2001; Cohen 2002; Etchevers et al. 2006; Dupin and Coelho-Aguiar 2013). The concept neurocristopathy was introduced by Bolande (1974) to explain the developmental relationships among a number of dysgenetic, hamartomatous and neoplastic disorders, including pheochromocytoma, von Recklinghausen's neurofibromatosis, Hirschsprung's aganglionic megacolon and the multiple endocrine adenomatoses. A neurocristopathy was defined as a condition arising from aberrations in the early migration, growth and differentiation of neural crest cells. Subsequently, an increasing number of disorders such as retinoic acid syndrome, hemifacial microsomia, Treacher Collins syndrome, DiGeorge sequence, cleft lip and palate, frontonasal dysplasia and Waardenburg syndrome have been included into the neurocristopathies, and more recently, the CHARGE syndrome (Vissers et al. 2004; Jongmans et al. 2006; Sanlaville et al. 2006; Sanlaville and Verloes 2007) and the Mowat-Wilson syndrome (Mowat et al. 1998, 2003). Apart from craniofacial malformations the neurocristopathies may be associated with developmental disorders of the CNS.

A group of craniofacial disorders are the result of defects in primary cilia. These ***craniofacial ciliopathies*** include Bardet-Biedl, Meckel-Gruber, oral-facial-digital type 1 and Joubert syndromes (Brugmann et al. 2010). Major craniofacial malformations are also found in the various types of holoprosencephaly (HPE) and in craniosynostoses. ***Holoprosencephaly*** is an early disorder of pattern formation that may lead to closely related forebrain and facial malformations. In the fetal period, ***craniosynostoses*** are frequent (approximately one in 2,500 children) craniofacial malformations due to agenesis or premature ossification of the cranial sutures, caused by mutations in *FGFR1-3* and other genes (Wilkie 1997; Cohen and MacLean 2000; Gorlin et al. 2001; Jabs 2002; Morriss-Kay and Wilkie 2005; Kweldam et al. 2011), that may interfere with normal brain development to varying degrees.

In this chapter, the neural crest and its derivatives (Sect. 5.2 and 5.3) and craniofacial development (Sect. 5.4) will be discussed, followed by an overview of the neurocristopathies (Sect. 5.5), craniofacial ciliopathies (Sect. 5.6), HPE (Sect. 5.7) and abnormal development of the skull (Sect. 5.8), leading to CNS malformations. The neuropathology of HPE will be discussed in Chap. 9.

## 5.2 Induction and Epitheliomesenchymal Transformation (EMT) of the Neural Crest

Neural crest cells are induced at the border between the neuroectoderm and the non-neural or surface ectoderm (Fig. 5.1). During the formation of the neural tube in the chick embryo, neural crest progenitors come to lie in or directly adjacent to the dorsal neural tube (Le Douarin and Kalcheim 1999; Creuzet et al. 2005). Depending on the species, neural crest cells leave the neuroepithelium before, during or after neural tube closure, and 'migrate' throughout the body. To do so, neural crest cells must lose their epithelial characteristics and take on the properties of migratory mesenchymal cells. Wheat germ agglutinin gold (WGA-Au) labelling experiments in murine embryos (Smits-van Prooije et al. 1985, 1987, 1988) and 1,1′-dioctadecyl–3,3,3′,3′-tetramethylindocarbocyanine (DiI) labelling in chick embryos (Kulesa and Fraser 1998)

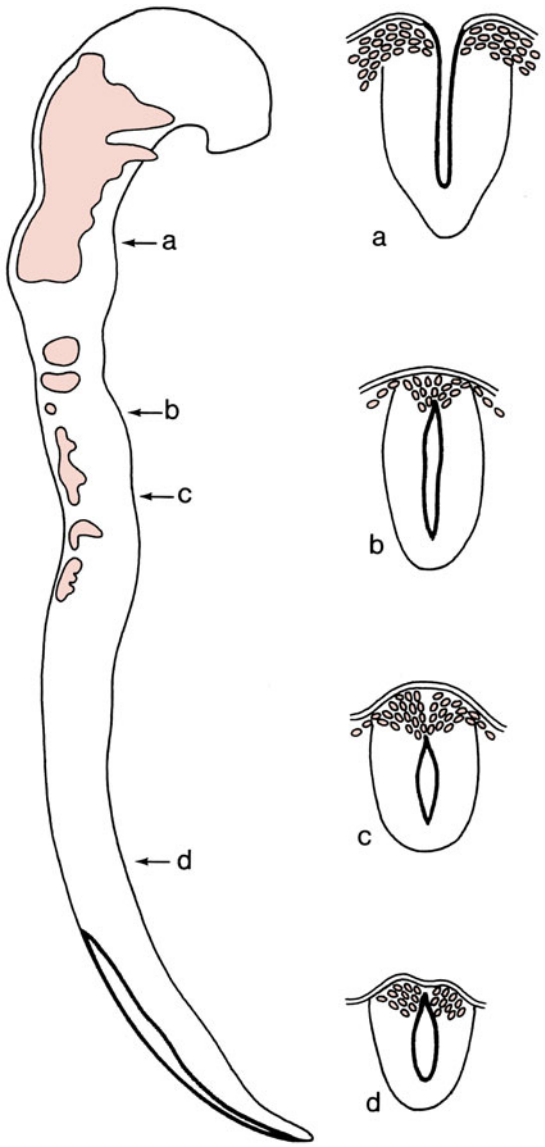


**Fig. 5.1** The early development of the human neural crest in a Carnegie stage 10 embryo. At rostral levels (**a**), crest material is formed before closure of the neural groove, whereas at more caudal levels (**b**–**d**) closure of the neural folds precedes migration of crest material (After Müller and O'Rahilly (1985))

have shown that migration of neural crest cells is random. In contrast, cell-free spaces underneath the chick neuroectoderm and surface ectoderm may, provide specific pathways for migrating neural crest cells (Le Douarin 1969, 1973). In quail-chick chimeras, however, cell-free spaces may be created artificially. Chemoattractive signals such as fibroblast growth factor (FGF) may also play a role in the control of neural crest cell migration (Kubota and Ito 2000; Francis-West et al. 2003), but the exact mechanism of migration remains unknown. Neural crest cells appear to form a reticular network and cooperate and proliferate during migration (Noden and Trainor 2005; Mayor and Theveneau 2013).

**Induction** of the neural crest appears to be a complex multistep process that involves many genes (LaBonne and Bronner-Fraser 1999; Aybar and Mayor 2002; Knecht and Bronner-Fraser 2002; Gammill and Bronner-Fraser 2003; Wu et al. 2003; Sauka-Spengler and Bronner-Fraser 2008; Steventon and Mayor 2012). Steventon and Mayor (2012) presented a three-step model for neural crest development: neural plate border induction, neural crest induction and neural crest maintenance. In these steps different levels of Wnt and/or BMP signalling are required. The neural plate border induction and neural crest induction, in chick and *Xenopus* embryos, require an inhibition and an increase in the level of Wnt signalling, respectively. For neural crest maintenance, activation of both Wnt and BMP is needed. In addition, FGFs and retinoic acid are likely to be important for the neural plate border induction. The neural crest can be distinguished by the expression of molecular markers, termed neural crest specifiers, such as the transcription factors of the *Snail* family, Snail and Slug, and *Sox9*, *Sox10*, *FoxD3 Twist* and *Id3* in *Xenopus*, zebrafish, chick and mouse (Mayor et al. 1995; Sefton et al. 1998; Linker et al. 2000; Aybar et al. 2003; Steventon and Mayor 2012). Many of these neural crest specifiers also control the EMT. The **generation** of **neural crest cells** appears towards the end of gastrulation (Steventon and Mayor 2012).

The **epitheliomesenchymal transformation** (**EMT**) of emerging neural crest cells is accompanied by the expression of the zinc-finger transcription factor Slug (Snail2). In chick and *Xenopus* embryos, its expression is maintained during the phase of crest cell migration (Nieto et al. 1994; LaBonne and Bronner-Fraser 2000; Basch et al. 2006). *Slug* mutant mice, however, do not show defects in either neural crest or mesodermal tissues (Jiang et al. 1998). In mice, another family member, Snail1, rather than Slug (Snail2) is expressed in the regions undergoing EMT (Cano et al. 2000; Locascio and Nieto 2001; Knecht and Bronner-Fraser 2002; Gammill and Bronner-Fraser 2003; Cordero et al. 2011). *Snail1* mutant mice die at gastrulation as a result of defects in mesoderm formation arising from deficient EMT.

EMT is a multi-step process: emerging neural crest cells must lose their apicobasal polarity, simultaneously disassemble intercellular adhesion complexes that are required for epithelial formation and degrade/disrupt their basal lamina (Thiery and Sleeman 2006; Acloque et al. 2009; Cordero et al. 2011; Theveneau and Mayor 2012; Mayor and Theveneau 2013). The disassembly of intercellular complexes involves members of the cadherin family. When the dynamic concert of cadherin gene expression fails to occur in the proper manner, neural crest cell migration is disrupted and the result is a perturbation in craniofacial development. SIP1, SNAIL (SNAIL1 and SNAIL2, formerly known as SLUG) (Comijn et al. 2001; Van de Putte et al. 2007) and *Foxd3* and *Sox9*/*10* are known genes that control cadherin

activation in the trunk neural crest cells, whereas in the cephalic region additional factors such as *Ets1*, *LSox5* and p53 are required (Mayor and Theveneau 2013). Vermeij-Keers and Poelmann (1980) described cell death (apoptosis) within the neural crest preceding the onset of its ectodermal disruption, which is confirmed by Smits-van Prooije et al. (1985). Furthermore, the first authors suggested that cell death is related to neural crest cell EMT. In cancer research studies this relationship has been established by TGF-β induction in mouse hepatocytes, which is determined by cell cycle stage (Song 2007), but independent of, for example p53 (Sheahan et al. 2008). Thiery and Sleeman (2006) suggested that EMT during embryogenesis is triggered by components of the extracellular matrix as well as soluble growth factors such as members of the TGF-β and FGF families. By contrast, they underlined the fact that *Sox9* and *Snail1* have an anti-apoptotic function as well, giving epithelial cells the needed protection from apoptosis during EMT.

Microdeletions or mutations in the *SIP* gene have been identified in patients with ***Mowat-Wilson syndrome*** (Dassot-Le Moal et al. 2007; Saunders et al. 2009), an autosomal dominant disorder characterized by distinct facial dysmorphisms, microcephaly, intellectual disability and epilepsy (Mowat et al. 1998, 2003).

Transcriptional misregulation of sets of genes involved in EMT is hypothesized to contribute to the pathogenesis of ***CHARGE syndrome***, a sporadic autosomal dominant disorder characterized by ocular coloboma, choanal atresia, heart malformations, growth restriction and genital and ear abnormalities (Verloes 2005; Sanlaville and Verloes 2007). Human mutations in the chromodomain helicase DNA-binding domain-7 member (CHD7) result in CHARGE syndrome (Vissers et al. 2004; Jongmans et al. 2006; Sanlaville and Verloes 2007). During human embryonic development *CHD7* is expressed in the CNS and neural crest mesenchyme of the pharyngeal arches (Sanlaville et al. 2006). Knockdown studies in *Xenopus laevis* embryos resulted in abnormal migration of neural crest cells into the pharyngeal arches and a phenotype consistent with CHARGE syndrome (Bajpai et al. 2010).

## 5.3 Derivatives of the Neural Crest

The neural crest is the major source of mesenchymal cells in the head and neck, and in addition gives rise to sensory ganglia, autonomic and enteric ganglia as well as to pigment cells of the skin. In the postcranial region, mesenchyme forming the connective tissues is mesodermal in origin (Table 5.1). The chick neural crest can be divided into four main domains (Le Douarin and Kalcheim 1999; Creuzet et al. 2005; Bronner and Le Douarin 2012): (1) the **cranial** or **cephalic neural crest**, giving rise to the craniofacial mesenchyme in particular; (2) the **trunk neural crest**, giving rise to the dorsal root and sympathetic ganglia; (3) the **vagal** and **sacral neural crest**, generating the parasympathetic (enteric) ganglia of the gut (the enteric nervous system); and (4) the **cardiac neural crest**, located between the cranial and trunk neural crests. In chick embryos, the cardiac neural crest produces the musculoconnective tissue for the large arteries arising from the heart and contributes to the separation of the truncus arteriosus into the pulmonary artery and aorta (Le Lièvre and Le Douarin 1975; Kirby 1987; Kirby and Waldo

**Table 5.1** Derivatives of neural crest cells

| | |
|---|---|
| Connective tissues | Ectomesenchyme of facial prominences and pharyngeal arches |
| | Bones and cartilage of facial and visceral skeleton |
| | Dermis of face and ventral aspect of neck |
| | Stroma of salivary, thymus, thyroid, parathyroid and pituitary glands |
| | Corneal mesenchyme |
| | Sclera and choroid optic coats |
| | Blood vessel walls; aortic arch arteries |
| | Dental papilla; part of periodontal ligament; cementum |
| Muscle tissues | Ciliary muscles |
| | Covering connective tissues of pharyngeal-arch muscles (masticatory, facial, faucial, laryngeal) |
| Nervous tissues | Supporting tissues: leptomeninges of prosencephalon and part of the mesencephalon; glia; Schwann's sheath cells |
| | Sensory ganglia: spinal dorsal root ganglia; and sensory ganglia of trigeminal, facial, glossopharyngeal and vagal nerves |
| | Autonomic nervous system: sympathetic ganglia and plexuses; parasympathetic ganglia |
| Endocrine tissues | Adrenomedullary cells and adrenergic paraganglia |
| | Calcitonin parafollicular cells of thyroid gland |
| | Carotid body |
| Pigment cells | Melanocytes in all tissues |
| | Melanophores of iris |

After Le Douarin and Kalcheim (1999), Sperber (2001)

1990; Bronner and Le Douarin 2012). The cranial neural crest is the only part of the neural crest that is able to produce cartilage and bone.

### 5.3.1 The Cranial Neural Crest

During neural tube closure in the chick embryo, cranial neural crest cells migrate into the underlying tissues as mesenchyme (**ectomesenchyme or mesectoderm**), forming a lineage of pluripotential stem cells that give rise to diverse tissues (Le Douarin and Kalcheim 1999; Creuzet et al. 2005; Bronner and Le Douarin 2012). In contrast, in mice the entire ectoderm of early presomite embryos and the ectoderm of the head folds (presumptive neurectoderm and surface ectoderm) in late presomite and early somite embryos are able to deposit mesectodermal cells into mesodermal compartments (Vermeij-Keers and Poelmann 1980; Smits-van Prooije et al. 1985, 1987; Tan and Morriss-Kay 1985; Boshart et al. 2000). Later, in 4–5-somite embryos the ectoderm of the head folds is differentiated into neurectoderm and surface ectoderm. From four-somite up to 20-somite murine embryos, that is even after the closure of the rostral neuropore, the cranial neural crest is active. In human embryos the first activity is seen in stage 9; from stage 9 (one to three somites) up to stage 10 (four to 12 somites), ectomesenchymal cells arise from parts of the head/neural folds, representing, the mesencephalic, trigeminal and facial crest (Müller and O'Rahilly 1983, 1985; O'Rahilly and Müller 2007). Thus in murine and human embryos the neural crest activity starts when the head/neural folds are wide open. In chick embryos, however, this activity coincides with the fusion of the neural folds (Theveneau and Mayor 2012).

O'Rahilly and Müller (2007) analysed the development of the neural crest in 185 serially sectioned staged human embryos. They found that: (1) a mesencephalic neural crest is discernible at stage 9, and trigeminal, facial and postotic components can be detected at stage 10; (2) crest was not present at the level of the diencephalon (D2); although the pre-otic crest from the neural folds is at first continuous (stage 10), *crest-free* zones are soon observable (stage 11) in rhombomeres 1, 3 and 5; (3) migration of the cranial neural crest from the neural folds begins before closure of the rostral neuropore, and later crest cells do not accumulate above the neural tube; (4) the trigeminal, facial, glossopharyngeal and vagal ganglia, which develop from crest that migrates before the neural folds have fused, continue to receive contributions from the roof plate of the neural tube after its closure; (5) the nasal crest and the terminalis-vomeronasal complex are the last components of the cranial crest to appear (stage 13) and they persist longer; (6) the optic, mesencephalic, isthmic, accessory and hypoglossal crest do not form ganglia. A summary of the neural crest streams for a stage 15, 33-day-old human embryo is shown in Fig. 5.2. In the literature, there is discussion about the existence of neural crest activity in the mammalian forebrain. In human embryos no contribution was found with the exception of the optic region (O'Rahilly and Müller 2007). In murine embryos, however, the neural crest of the whole forebrain deposits cells which contribute to the facial swellings (Smits-van Prooije et al. 1988; Morriss-Kay et al. 1993). Additionally, as a result of the mesectoderm formation, starting in presomite stages, nearly all cells of the mesodermal compartment of the head are mesectodermal cells, thus including those of the facial prominences. These cells are derived from both the neural and optic crest and the neurogenic placodes.

In contrast to murine embryos, the embryonic prominences of the chick face and neck (the so-called frontonasal process and the pharyngeal arches) are dependent on mesencephalic and rhombencephalic neural crest activity (Fig. 5.3; Couly and Le Douarin 1990). Recently, Le Douarin and co-workers described that only the most rostral part of the

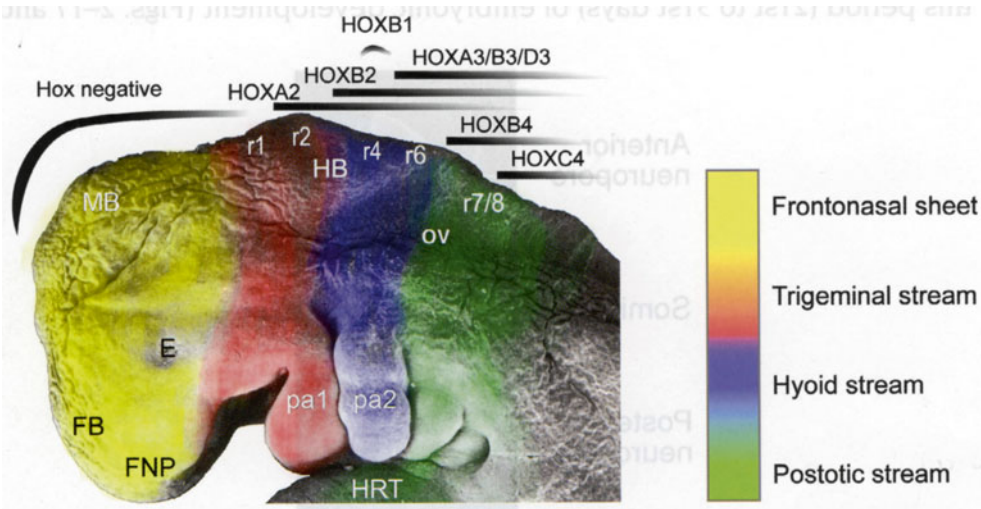


**Fig. 5.2** A stage 15, 33-day-old human embryo upon which are depicted the neural crest streams emanating from the rhombomeres, influenced by *HOX* gene expression patterns. *E* eye, *FB* forebrain, *FNP* frontonasal prominence, *HB* hindbrain, *HRT* heart, *MB* midbrain, *OV* otic vesicle, *r1–r8* rhombomeres, *pa1*, *pa2*, pharyngeal arches 1 and 2 (From Sperber et al. (2010); with permission)

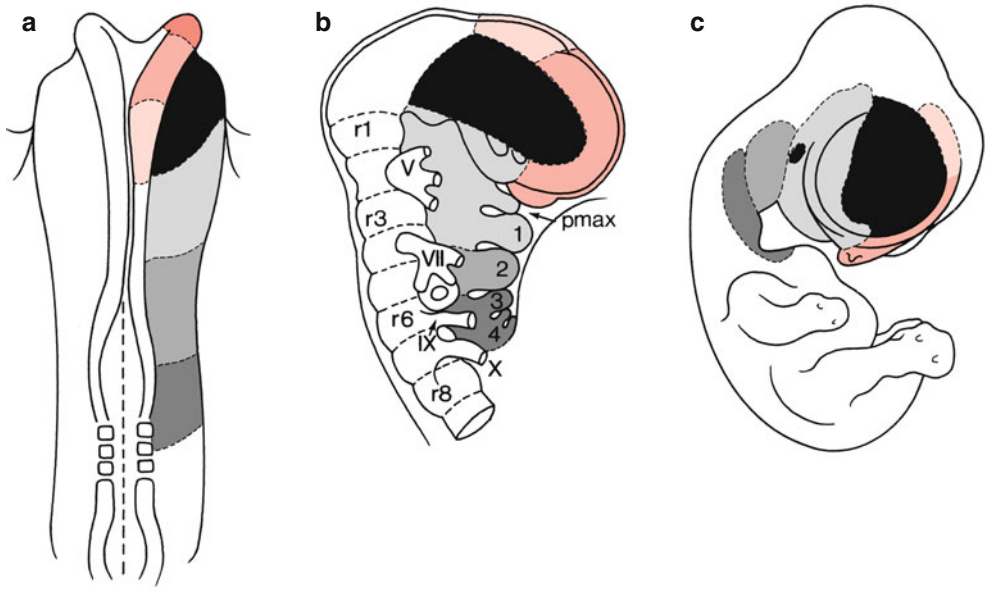


**Fig. 5.3** Fate map of the ectodermal territories in the chick embryo from the three-somite stage (**a**) to the 8-day embryo (**c**). (**b**) The rhombomeres (*r1*, *r3*, *r6*, *r8*) and the cranial nerves supplying the pharyngeal arches (*1–4*) are shown. *pmax* maxillary prominence, *V* trigeminal nerve, *VII* facial nerve, *IX* glossopharyngeal nerve, *X* vagus nerve (After Couly and Le Douarin (1990))

forebrain, instead of the whole forebrain, does not produce neural crest cells in chick embryos (Bronner and Le Douarin 2012; Le Douarin et al. 2012; Theveneau and Mayor 2012). As a consequence long-distance migration may be required to invade the prominences of the face and neck. This migration starts from regions rostral to rhombomere 6, taking one of three major **migratory pathways** or streams (Lumsden and Guthrie 1991; Sechrist et al. 1993; Kulesa and Fraser 2000; Creuzet et al. 2005; Noden and Trainor 2005; Theveneau and Mayor 2012; Fig. 5.4): (1) cells from the first and second rhombomeres migrate into the first pharyngeal (mandibular) arch, forming the mandibula, incus and malleus, and contributing to the trigeminal ganglion; these cells also generate the facial skeleton; (2) cells from the fourth rhombomere invade the second pharyngeal arch and form the hyoid cartilage and the facial and vestibulo-acoustic ganglia; and (3) cells from the sixth rhombomere migrate into the third and fourth pharyngeal arches and pouches to form the thymus, the parathyroid and thyroid glands, and the superior and jugular ganglia. Neural crest cells from the third and fifth rhombomeres enter the migrating streams of neural crest cells of the adjacent rhombomeres. Those that do not enter the various migratory streams will die (Graham et al. 1993, 1994; Sechrist et al. 1993). The apoptotic elimination of neural crest cells in the third and fifth rhombomeres involves the induction of high-level BMP expression in the neural crest, which stimulates expression of the homeobox gene *Msx2* (Graham et al. 1994; Creuzet et al. 2005). In mice, a similar pattern of neural crest migration pathways has been found (Golding et al. 2000; Trainor et al. 1994, 2002; Trainor and Krumlauf 2000). The separate streams are kept apart by ephrins (Golding et al. 2000; Trainor and Krumlauf 2000; Noden and Trainor 2005; Theveneau and Mayor 2012).

Experimental studies using transposition of the avian neural folds (Noden 1978a, b, 1983a) led to the concept that the spatial organization of cranial structures is the result of a **prepatterning mechanism** before cells migrate from the neural crest. The ordered domains of *Hox* gene expression in the neural tube and neural crest were later assumed to be a molecular correlate of the prepatterning mechanism. However, plasticity of *Hox* gene expression has been observed in the hindbrain and postotic neural crest of chick, mouse and zebrafish embryos (Trainor and Krumlauf 2000; Gammill and Bronner-Fraser 2003; Santagati and Rijli 2003; Creuzet et al. 2005; Noden and Trainor 2005). Although the neural crest seems to play an important role in arch patterning, there are also patterning mechanisms that are established independently in the pharynx. Therefore, the formation of the pharyngeal apparatus must result from integration between these patterning systems (Graham and Smith 2001; Graham et al. 2004). Recent studies, however, demonstrated that the neural crest of avian and mammals is a highly pluripotent structure. The cephalic as well as the trunk neural crest showed existence of multipotent precursors giving rise to all major neural crest lineages including self-renewing stem cells (Dupin and Coelho-Aguiar 2013).

The neural crest most probably plays a more prominent role in patterning the rostral, preotic arches but a lesser role in the caudal, postotic arches. The development of the branchial arches involves retinoic acid dependent mechanisms. Neural crest cells migrating into branchial arches 3–6, however, are not the primary targets of retinoic acid, but pharyngeal epithelial cells are. Retinoic acid signalling is indispensable for the development of the pharyngeal epithelia of these branchial arches (Niederreither et al. 2003; Mark et al. 2004).

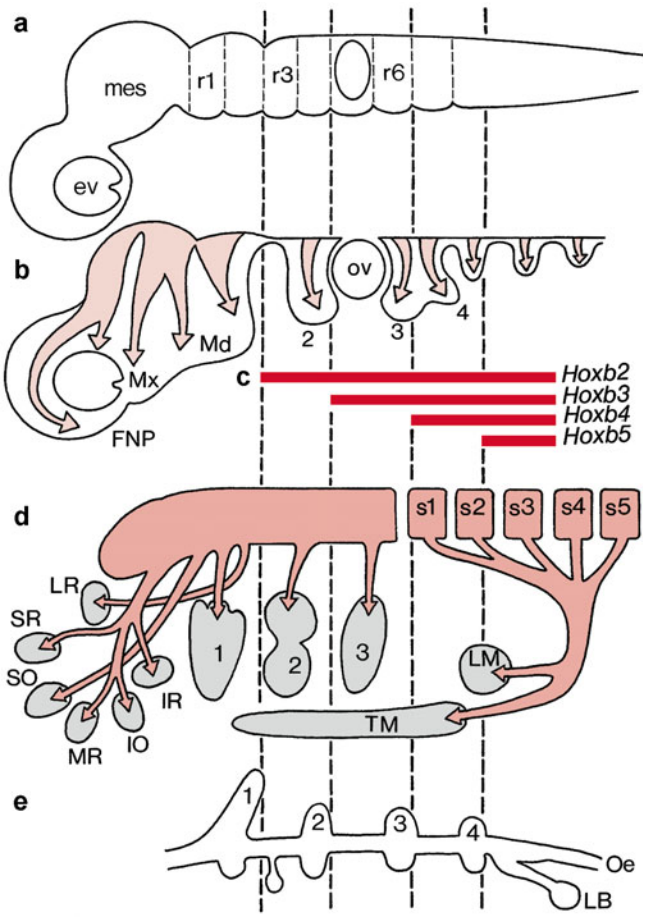


**Fig. 5.4** Neural crest progenitors, cranial nerves and myogenic primordia in an early avian embryo. (**a**) Lateral view of the brain; (**b**) neural crest movements indicated in *light red*; (**c**) *Hox* gene expressions (in *red*); (**d**) muscles (in *light grey*) arising from the unsegmented paraxial mesoderm (in *medium red*) and from the somitomeres (*s1–s5*, also in *medium red*); (**e**) pharynx and pharyngeal pouches. *ev* eye vesicle, *FNP* frontonasal prominence, *mes* mesencephalon, *IO* inferior oblique, *IR* inferior rectus, *LB* long bud, *LM* laryngeal muscles, *LR* lateral rectus, *Md* mandibular prominence, *MR* medial rectus, *Mx* maxillary prominence, *r1–r6* rhombomeres, *SO* superior obliqie, *SR* superior rectus, *TM* tongue muscles, *1–4* pharyngeal arches and pouches (After Noden and Trainor (2005))

The **segmented expression** of ***Hox* genes** in the hindbrain is reflected in the neural crest cells which express a complement of *Hox* genes characteristic for their level of origin (Hunt et al. 1991; Capecchi 1997; Favier and Dollé 1997; Rijli et al. 1998; Trainor and Krumlauf 2000; Santagati and Rijli 2003; Creuzet et al. 2005; Noden and Trainor 2005; Alexander et al. 2009; Barber and Rastegar 2010; Fig. 5.4). Each rhombomere and pharyngeal arch is characterized by its own complement of *Hox* genes, its ***Hox* code**. In the avian embryo, most of the skull and all of the facial and visceral skeleton are derived from the cephalic neural crest (Le Douarin et al. 2012). Neural crest cells participating in membranous bones and cartilages arise from the posterior half of the diencephalon, the mesencephalon and the rhombencephalon. They can be divided into an **anterior**, ***Hox*-negative**, **domain** (extending down including rhombomere 2) and a **posterior**, ***Hox*-positive**, **domain**. The transition between these two domains corresponds to rhombomere 3 (Fig. 5.4). The neural crest cells that form the facial skeleton belong exclusively to the anterior *Hox*-negative domain (the facial skeletogenic neural crest) and develop from the first branchial arch. Rhombomere 3 participates modestly to both the first and second branchial arches. Forced expression of *Hox* genes (*Hoxa2*, *Hoxa3* and *Hoxb4*) in the neural fold of the anterior domain inhibits facial skeleton development (Couly et al. 1998, 2002; Creuzet et al. 2002, 2005). Moreover, surgical excision of these anterior neural crest cells results in the absence of the facial skeleton. FGF8 also plays a key role in the development of the facial skeleton (Creuzet et al. 2004, 2005; Le Douarin et al. 2012).

In human embryos, Vieille-Grosjean et al. (1997) showed that the pattern of *HOX* gene expression in the rhombomeres and pharyngeal arches is similar to that observed in mice. The mouse *Hoxb2* gene, which is expressed in the hindbrain up to the boundary between the second and third rhombomeres, has an expression domain that extends caudally from the second pharyngeal arch (Fig. 5.4). *Hoxb3* is expressed as far rostrally as the rhombomere 4 – rhombomere 5 boundary and from the third pharyngeal arch caudally. *Hox* genes are required for the normal morphogenesis of arch-derived skeletal elements. Mice with targeted disruptions in the paralogous genes *Hoxa3* and *Hoxd3*, which are expressed in the third and fourth arches, display defects in the laryngeal cartilages (Condie and Capecchi 1994). Mice that lack the *Hoxa2* gene show a transformation of second arch skeletal elements into components of the first arch (Gendron-Maguire et al. 1993; Rijli et al. 1993), suggesting that specification of crest cells to first arch components requires the downregulation of *Hoxa2*. *Hoxa3* knockouts show specific deletions or hypoplasias of structures derived from the third arch, resembling DiGeorge syndrome. They lack a thymus and parathyroid glands, have a reduced thyroid gland and show malformations of the laryngeal cartilages and muscles, and of the heart (Chisaka and Capecchi 1991; Manley and Capecchi 1995). Decreased embryonic retinoic acid synthesis also results in a DiGeorge syndrome phenotype in newborn mice (Vermot et al. 2003; Mark et al. 2004). *Dlx* genes may be involved in intra-arch identity (Depew et al. 2005).

### 5.3.2 The Trunk Neural Crest

In the trunk of chick and mouse, neural crest activity is observed only after closure of the neural tube; it extends in a rostral to caudal direction following the fusing neural walls at some distance. In the trunk the neural crest activity started

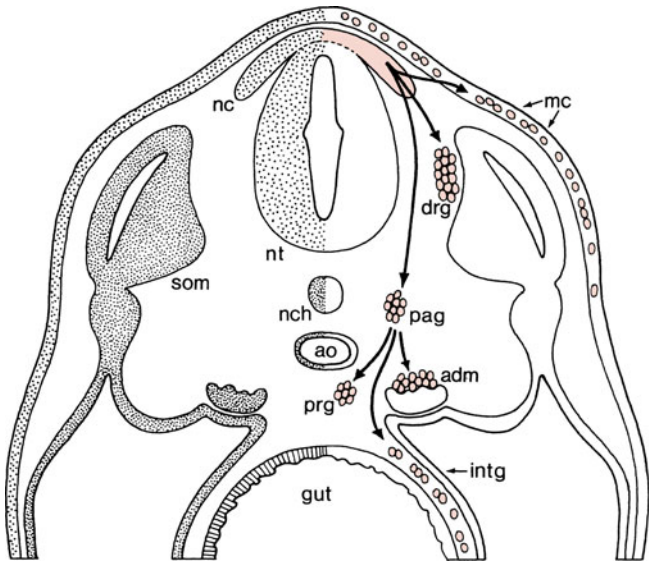


**Fig. 5.5** Migratory pathways of chick trunk neural crest cells. *adm* adrenal medulla (chromaffin cells), *ao* aorta, *drg* dorsal root ganglion cells, *intg* intestinal ganglion cells, *mc* melanocytes, *nc* neural crest, *nch* notochord, *nt* neural tube, *pag* paravertebral ganglion cells, *prg* prevertebral ganglion cells, *som* somite

relatively late and large amounts of cells were not produced (Smits-van Prooije et al. 1985; Theveneau and Mayor 2012). The **migratory pathways** of trunk neural crest cells are stereotyped and have been defined by various types of labelling experiments using grafts of Japanese quail crest into chick embryos, immunostaining for cell surface markers such as HNK-1 or fluorescent dyes such as DiI (Le Douarin and Kalcheim 1999) and more recently, using time-lapse techniques (Kulesa and Fraser 1998, 2000). Two main directions of movement were found (Fig. 5.5): a **dorsolateral pathway** for crest cells that differentiate into melanocytes, and a **ventral pathway** between neural tube and somites that gives rise to the dorsal root and sympathetic ganglia, to the enteric nervous system, to Schwann cells and to chromaffin cells for the adrenal gland (Le Douarin and Kalcheim 1999). Crest cells pass only via the anterior part of the sclerotome. The migration path taken by trunk neural crest cells is guided by extracellular matrix molecules surrounding the neural tube. Fibronectin, laminin, tenascin and proteoglycans promote their migration (Newgeen et al. 1986), whereas ephrin proteins present in the posterior part of the sclerotome restrict neural crest migration to the anterior part of the sclerotome (O'Leary and Wilkinson 1999). In human embryos, the trunk neural crest participates at stage 12 in the formation of the pia mater, the spinal ganglia and the sympathetic trunk and ganglia, and at stages 13–14 in the formation of the sheaths of the dorsal and ventral roots (O'Rahilly and Müller 1999). However, this long distance migration of the trunk neural crest cells has been challenged by Gasser (2006). Using reference points in rat and human embryos during successive developmental stages, he demonstrated that 'migration' of trunk crest cells can be explained by differential growth. This explanation, i.e. relative displacement of organs/tissues, was already suggested by Smits-van Prooije et al. (1988), using WGA-Au as a marker.

In avian embryos, neural crest cells that colonize the **gut** migrate from two regions of the neuraxis (Le Douarin and Teillet 1973; Le Douarin and Kalcheim 1999): neural crest cells arising at vagal levels (somites 1–7) colonize the entire length of the gut, whereas those arising at the sacral level contribute only to the innervation of the postumbilical part of the digestive tract. Comparable data were obtained in mouse embryos (Durbec et al. 1996). After homing at distinct levels of the gut, crest-derived cells differentiate into the ganglia of the myenteric Auerbach and the submucosal Meissner plexuses, forming the **enteric nervous system** (Furness and Costa 1987; Heaton et al. 1988). ***Aganglionic megacolon*** is characterized by the absence of enteric ganglion cells. In 1887, Hirschsprung described two patients with chronic obstipation and congenital megacolon. ***Hirschsprung disease*** or ***congenital aganglionosis*** appears to be due to absence of ganglion cells in variable lengths of the rectum and colon. It occurs in one in 5,000 live births with a male preponderance. Children with aganglionosis present with intestinal obstruction or chronic constipation. The severity of the presentation does not necessarily correlate to the length of the aganglionic segment. Aganglionic segments begin at the internal anal sphincter and extend proximally. The constant histological abnormality is the absence of ganglion cells in affected segments and the presence of large nerve trunks in the submucosal and myenteric plexuses (Howard and Garrett 1970; Kleinhaus et al. 1979; Clinical Case 5.1).

## Clinical Case 5.1. Congenital Aganglionosis

**Case Report**. After an uneventful pregnancy, a boy was born at 41 gestational weeks with a normal birth weight of 4,020 g. Shortly after birth, feeding problems with food refusal and recurrent vomiting became apparent. An X-rayof the abdomen showed much intestinal air and on contrast radiography of the colon, there was a charge of calibre at the rectal level. A suction biopsy revealed absence of ganglion cells at this level and confirmed the diagnosis ***Hirschsprung disease***. A transanal endorectal pull-through operation was performed and the last 32 cm of the rectum and colon was resected (Fig. 5.6). Postoperatively, the boy was without any problems. No ganglionic cells were found in the submucosal and muscular plexus of the distal rectum (Fig. 5.7).

This case was kindly provided by Martin Lammens (Antwerpen).

**Fig. 5.6** Subtotal colectomy specimen with distal narrowing of the lumen (at the *left*) and extreme widening of the colon above the stenotic region (**megacolon** at the *right*; courtesy Martin Lammens, Nijmegen; from ten Donkelaar et al. (2011))

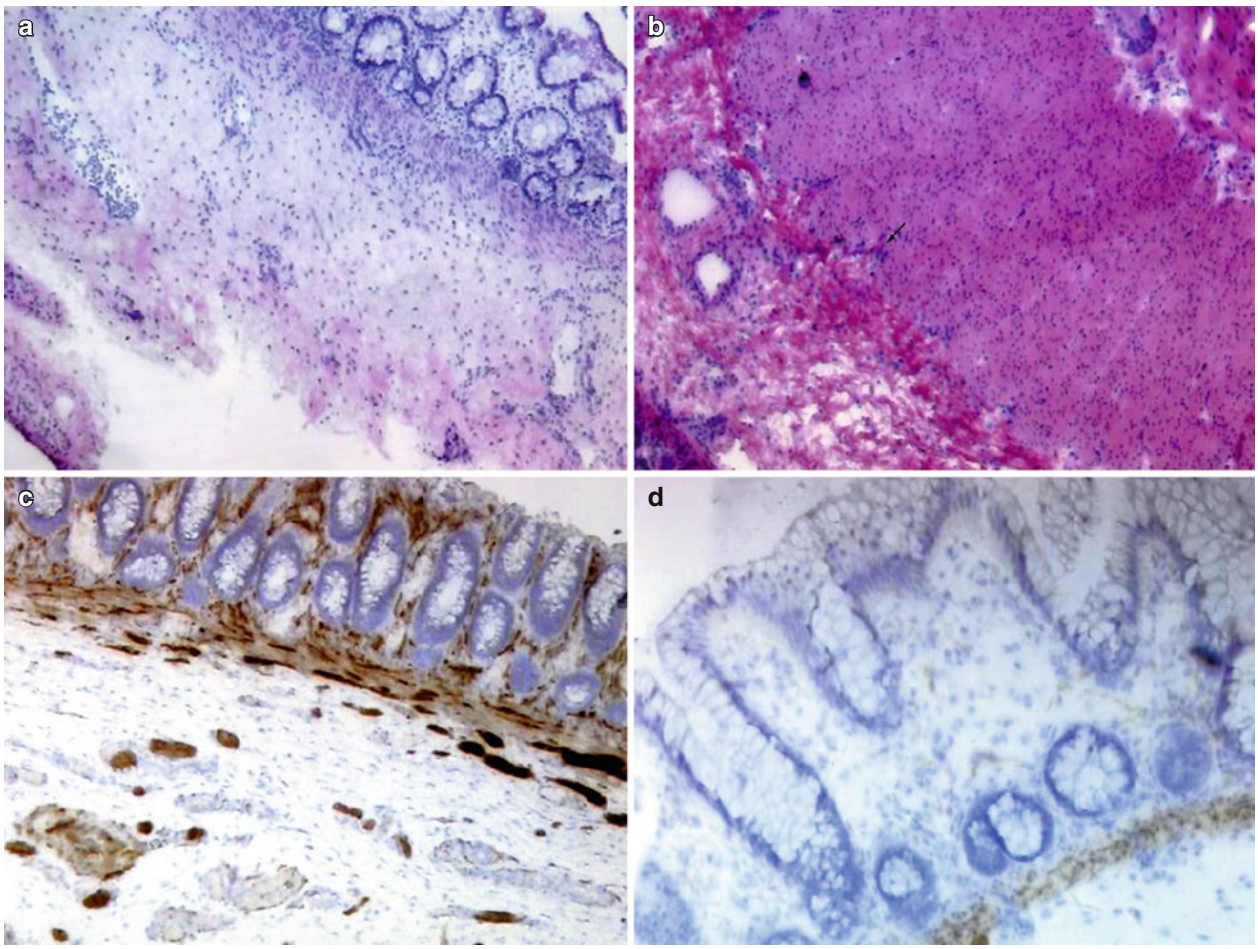


**Fig. 5.7** Biopsies of the specimen shown in Fig. 5.6: (**a**, **c**) biopsies of the stenotic region: no ganglion cells are present in the submucosa (**a**; HE-stained frozen section), whereas thickened nerve bundles are found in the submucosa and pathological staining of the thickened nerve fibres in the mucosa (**c**; acetylcholinesterase histochemistry); (**b**, **d**) biopsies of the dilated proximal part with presence of ganglion cells in the submucosa (*arrow* in **b**; HE-stained frozen section) and almost absent staining of mucosal nerve fibres (**d**; acetylcholinesterase histochemistry; courtesy Martin Lammens, Nijmegen; from ten Donkelaar et al. (2011))

## 5.4 Craniofacial Development

Prior to a discussion of neurocristopathies and other craniofacial malformations involving the CNS, the development of the face, the pharyngeal arches and the skull will be briefly discussed. Knowledge of the normal developmental events that shape the craniofacial region is necessary for understanding the changes that result in malformations of this region. The following description is largely based on Hinrichsen (1985, 1990) and Vermeij-Keers (1990).

### 5.4.1 Early Development of the Face

The early development of the forebrain and face is characterized by the formation and subsequent transformation of the so-called head folds (Vermeij-Keers 1990): first, the neural walls with the eye primordia, than the otic disc, the pharyngeal arches and, finally, the lens placode and the nasal placode. These transformations show a rather basic pattern of development, outgrowth of swellings forming and surrounding a cavity or groove that is subsequently closed partly or totally as a result of fusion of the swellings. The first slightly lordotic shape of the human embryo facilitates the initial fusion process of the neural walls transforming the neural groove into the neural tube (Chap. 4). Later, the lordosis changes into a kyphosis, enabling the transformation of the pharyngeal arches and the formation of the neck. The development of the **head** or **cephalic folds** in human and murine embryos is comparable (van Oostrom 1972; Vermeij-Keers 1990; Sulik 1996). In human embryos, the development of the head folds takes place during stages 8–9 (O'Rahilly 1973; O'Rahilly and Müller 1981; Müller and O'Rahilly 1983), and in mouse embryos around 7.5 days *post coitum* (E7.3-E7.7) at which time the head folds are covered with columnar epithelium (van Oostrom 1972). The border of the head folds is the transition of the surface ectoderm and the amnion. At stage 8, O'Rahilly and Müller (1981) described the head folds already as **neural folds**. They are the first rostral structures to appear in the embryo, and continue caudally as the neural plate. In four- to seven-somite mouse embryos, the head folds grow out rapidly, and a separation into lateral, thin (surface ectoderm of the head-neck region) and medial, thick (neuroectoderm of the forebrain, midbrain and hindbrain) parts becomes evident. At the transition of both parts, the **cranial neural crest**, the neuroectoderm produces mesectodermal or ectomesenchymal cells.

In amphibians, Adelmann (1936) showed that within the rostral neural plate a median population of cells, the **eye field**, segregates into two lateral primordia, the future optic vesicles. Experimental removal of the prechordal plate resulted in failure of separation of the midline structures of the rostral neural plate, leading to cyclopia as is also found in the most severe forms of HPE. The separation of the eye field is dependent upon interactions with the underlying mesoderm. The resulting degree of bilateralization of the eyes and forebrain has a profound effect on the subsequent morphogenesis of the face. In amphibian and chick embryos, the primordia of the eyes are found in the rostral neural plate, just caudal to the anterior neural ridge (Couly and Le Douarin 1988; Eagleson and Harris 1990; Eagleson et al. 1995; Chap. 2). Cyclopic animals such as the zebrafish mutant *cyclops* (Hatta et al. 1991, 1994; Varga et al. 1999; Schier 2001) have a defect in the development of the optic stalk and chiasm. The single vertebrate eye field is characterized on the molecular level by the expression of the so called eye-field transcription factors (Zuber et al. 2003; Graw 2010). Subsequently, this field is separated into two optic primordia under the control of the *cyclops* gene. This gene is expressed in the prechordal plate mesoderm and contributes to the signal that establishes the ventral midline of the brain. Mice lacking the *Shh* gene demonstrate cyclopia and abnormal axial patterning (Chiang et al. 1996). Secreted factors such as Sonic hedgehog (SHH; Chiang et al. 1996) and FGF8 (Sun et al. 1999) play important roles before and during patterning of the neural plate (Chap. 9). In chick embryos, FGF8 and SHH signalling pathways are also required during early morphogenesis of the forebrain and frontonasal process (Schneider et al. 2001). The *Distal-less* related gene *Dlx5* is also required for normal development of the frontonasal process (Acampora et al. 1999). In human embryos, O'Rahilly and Müller (1999) suggested a single eye field at stage 8 that is situated directly above the prechordal plate. The prechordal plate suppresses the median part, so that bilateral optic primordia are formed, presumably still in stage 8 embryos. Vermeij-Keers et al. (1987) found evidence for the existence of bilateral optic primordia in human cyclopia cases.

During the transformation of the head folds into the cranial neural walls or neural folds, the **optic primordia** (optic sulci) develop within the neuroectoderm as two separate shallow grooves (Fig. 5.8a, b; mouse, seven-somite embryo: Smits-van Prooije et al. 1985; man, stage 10: Müller and O'Rahilly 1985). Close to the margin of the neuroectoderm the **otic disc** develops as a concavity of columnar epithelium in the surface ectoderm (three-somite mouse embryo: Verwoerd and van Oostrom 1979; man, stage 9: Müller and O'Rahilly 1983). Meanwhile, the caudal part of the neural folds transforms via the neural groove into the neural tube. The initial contact between the neural walls takes place in the caudal part of the rhombencephalic folds or in the upper cervical neural folds (mouse, five-somite embryo: Smits-van Prooije et al. 1985; man, stage 10: Müller and O'Rahilly 1985; Nakatsu et al. 2000). Rostrally, in the head other points of closure occur in the mouse embryo (Geelen and Langman 1977; Sakai 1989; Golden and Chernoff 1993) as well as in the human embryo (Müller and O'Rahilly 1985; Golden and

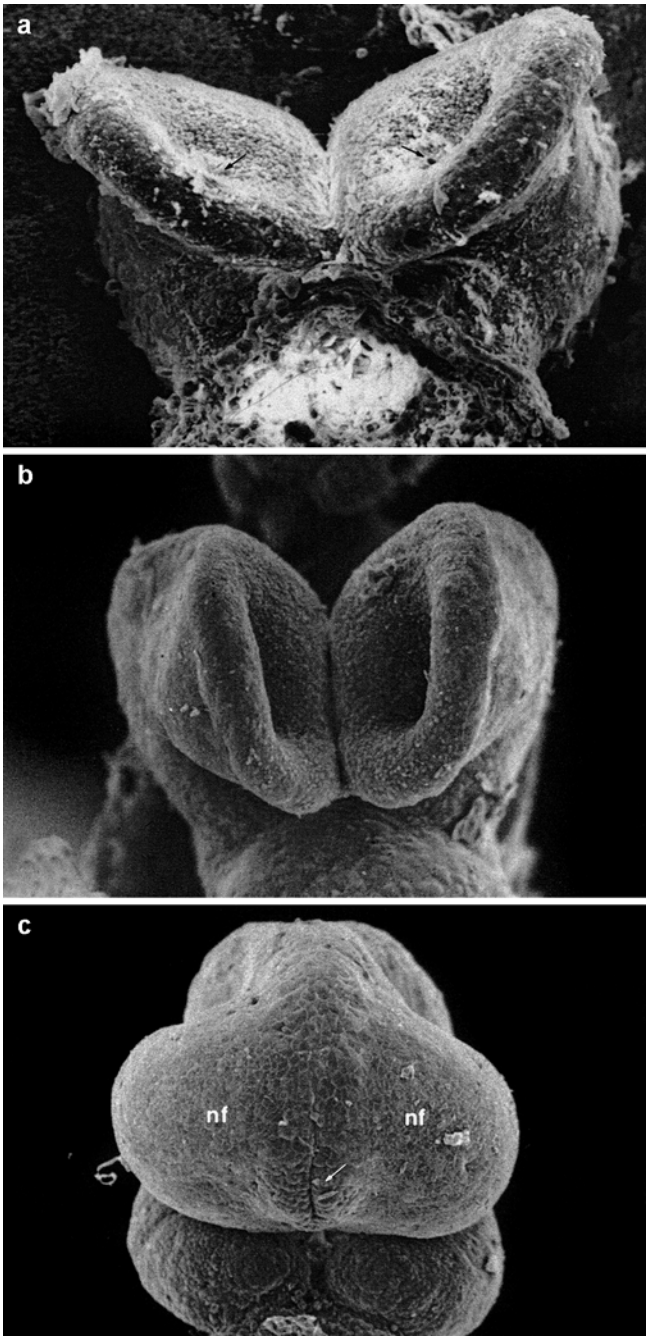


**Fig. 5.8** Scanning electron micrographs of the developing face of mouse embryos in frontal view (the heart was removed in **a** and **c**): (**a**) E8.0-embryo, *arrows* indicate the optic sulci as bilateral grooves in the head folds; (**b**) E8.3-embryo, showing the prosencephalon with the evaginating optic vesicles; (**c**) E8.7-embryo in which the prosencephalon is fused except for the rostral neuropore (*arrow*) which separates the two nasal fields (*nf*)

Chernoff 1995; Nakatsu et al. 2000; Chap. 4). The final closure of the rostral neuropore is located between two areas of ectodermal, cuboidal or columnar epithelium, the **nasal fields** (the *Nasenfelder* of His 1885), in mice in 15-somite embryos (Vermeij-Keers et al. 1983; Fig. 5.8c), in human embryos at stage 11 (O'Rahilly and Gardner 1971; Müller and O'Rahilly 1986). This location corresponds with the presumptive internasal groove (Vermeij-Keers 1990).

In human embryos, the first visible appearance of the bilateral **optic primordia** is seen in eight-somite embryos (Bartelmez and Blount 1954; O'Rahilly 1966) as a thickened area of each neural wall in which a shallow sulcus is present. Subsequently, each **optic sulcus** widens and changes into an **optic vesicle** after closure of the neural walls. Within each nasal field two local thickenings develop, the **lens placode** (mouse: E8.8, 15–16-somite embryos; stage 13 human embryos: Müller and O'Rahilly 1988a) and the **nasal placode** (mouse: E9.8; stage 14 human embryos: Hinrichsen 1985; Müller and O'Rahilly 1988b). The lens placode is adjacent to the optic vesicle and is transformed into the lens vesicle, whereas the optic vesicle becomes the optic cup. *Pax6* plays an important role during eye development including the lens (Chiang et al. 1996; Huang et al. 2011). In stage 15 human embryos, the lens vesicle detaches from the surface ectoderm (O'Rahilly 1966). The cavity of the optic vesicle communicates via the lumen of the short optic stalk with that of the forebrain. During the formation of the optic cup, its external layer grows out into the direction of the internal layer. This process is influenced by the lens placode (Chap. 9).

The mesodermal component of the head region is not only supplied by the cranial and optic neural crest but also by cells deposited by the **surface ectoderm** or **neurogenic placodes**: the nasal placodes (Verwoerd and van Oostrom 1979), the acoustic or otic placode (Batten 1958) and the epibranchial placodes of the pharyngeal arches (Adelmann 1925; Graham and Begbie 2000; Lleras-Forero and Streit 2012; Graham and Shimeld 2013). Neurogenic placodes are specialized regions of the cephalic embryonic ectoderm from which among others neuroblasts for the cranial sensory systems are generated. Neurons in cranial sensory ganglia have a dual origin from the neural crest as well as from placodes (Noden 1991a, b; Le Douarin and Kalcheim 1999). The origin of neurogenic precursors and the pattern of expansion of the surrounding surface ectoderm were defined using the quail-chick chimera technique (D'Amico-Martel and Noden 1983; Couly and Le Douarin 1985, 1987, 1990).

The **otic disc** is the first ill-defined appearance of the developing ear (three- to five-somite mouse embryo: Verwoerd and van Oostrom 1979; stage 9 human embryo: Müller and O'Rahilly 1983). At the end of stage 10, the otic disc becomes incorporated and transforms via the **otic pit** into the **otic vesicle** or **otic cyst** (O'Rahilly 1983; Müller and O'Rahilly 1985; Van De Water et al. 1988). Subsequently, the otic vesicle becomes separated from the surface ectoderm by apoptosis, and induces the condensation of its surrounding mesenchyme into the **otic capsule**. The otic vesicle forms the membranous labyrinth and the otic capsule the osseous labyrinth (Streeter 1906, 1918; Chap. 7). Placodal cells,

given off from the walls of the otic vesicle, form the vestibular and possibly the cochlear (spiral) ganglia (O'Rahilly and Müller 2001). The **cavity** of the **middle ear** develops from the **tubotympanic recess** of the first pharyngeal pouch (Kanagasuntheram 1967). Recently, however, using transgenic mice, it was shown that the middle ear develops through cavitation of a mass of neural crest cells. These cells -without cilia- form a lining continuous with the endodermal cells -with cilia- derived from the auditory (Eustachian) tube, which connects the middle ear to the pharynx (Thompson and Tucker 2013). As a consequence the mesenchyme of the auditory ossicles may also originate as a whole or in part from the neural crest (Thompson et al. 2012). Furthermore, the origin of the auditory ossicles in relation to the two pharyngeal arches is not entirely clear (Anson et al. 1948, 1960; Hanson et al. 1962; O'Rahilly and Müller 2001; O'Gorman 2005). Presumably, the head of the malleus and the body and short crus of the incus arise from the first pharyngeal arch, whereas the handle of the malleus, the long crus of the incus and the head and crura of the stapes develop from the second arch. Thompson et al. (2012) suggested that the stapedial footplate is composed of cells of neural crest and mesodermal origin. The base of the stapes appears in the lateral wall of the otic capsule. The **external ear** arises from a series of small swellings, the **auricular hillocks**, around the first pharyngeal groove (Streeter 1922; Hinrichsen 1985, 1990).

### 5.4.2 Development of the Pharyngeal Arches

A prominent feature of human embryos is the presence of a series of bulges on the lateral surface of the head and neck, the **pharyngeal arches** (Fig. 5.9). Each arch has an outer covering of ectoderm, an inner covering of endoderm and a mesenchymal core derived from the neural crest, and most likely the surface ectoderm placodes and mesoderm. Between the arches, the ectoderm and endoderm are in close apposition and form the **pharyngeal membranes**. The externally situated **pharyngeal grooves** have internal counterparts, the **pharyngeal pouches**. During the process of outgrowth of the embryo, the wide lumen of the foregut is transformed into pharyngeal pouches by outgrowing swellings into this lumen. The first pharyngeal pouch develops in the early somite stages. Between the first pharyngeal pouch and its complementary pharyngeal groove the first pharyngeal membrane, the future tympanic membrane, develops. Initially, the groove is shallow and wide but deepens subsequently during the outgrowth of the first pharyngeal arch. The different germ layers generate distinct components of the pharynx. The ectoderm produces the epidermis and the sensory neurons of the arch-associated ganglia (Verwoerd and van Oostrom 1979; D'Amico-Martel and Noden 1983; Couly and Le Douarin 1990), whereas the

**Fig. 5.9** Scanning electron micrograph of the development of the human pharyngeal arches at stage 15 (From Jirásek (2001), with permission)

endoderm gives rise to the epithelial cells lining the pharynx and the endocrine glands forming from the pharyngeal pouches (Graham et al. 2005). The neural crest forms the connective and skeletal tissues (Noden 1983b; Couly et al. 1993), whereas the mesoderm forms the musculature and the endothelial cells of the arch arteries (Noden 1983b, 1991a, b; Couly et al. 1992; Trainor et al. 1994; Francis-West et al. 2003; Chap. 7).

In human embryos, five **pharyngeal** or **visceral arches** (also known as branchial or aortic arches) develop successively. Four pairs are visible on the outside of the human embryo at 4 weeks and are separated from each other by three grooves (Fig. 5.9). More caudally, their arrangement is less clear-cut but it is customary to label a fifth and even a sixth arch. The first pharyngeal arch is the biggest, develops cranial to the heart primordium of the embryo and forms only the mandibular processes of the facial swellings (Vermeij-Keers et al. 1983). The maxillary prominence expands around the stomodeum below the optic vesicle and is unrelated to the pharynx (Vermeij-Keers 1990; Noden 1991a, b). The mandibular processes keep their positions, grow out and form a groove in the midline between the two swellings. They actually do not fuse but merge because no epithelial plate is formed (Oostrom et al. 1996). The second arch grows caudally and laterally from the side of the second pharyngeal groove, covering the third and fourth arches. The third pharyngeal arch does the same with respect to the fourth. The retrobranchial ridge, incorporating the fifth arch, grows rostrally into the direction of the second arch (Starck

1975; Vermeij-Keers 1990). Via contacts with the fourth and third arches this swelling adheres and fuses with the second pharyngeal arch. Initially, slit-like cavities, remnants of the pharyngeal grooves, remain present between these contact places. Inside the embryo, the slit-like cavities obliterate and ectodermal epithelial plates are formed at the contact places between the swellings. These plates disappear by apoptosis. The outgrowing pharyngeal arches and their subsequent shifting do not only cause transformations of the pharyngeal grooves but also of their corresponding pouches. The successive organs developing from these pouches (Fig. 5.10; Table 5.2) do not migrate to their definite position, as is generally stated in the literature, but in the first instance they attain their positions during the outgrowth and transformation of the pharyngeal arch system. Then, differential growth causes the shift of the organs (Vermeij-Keers 1990; Gasser 2006). Later, they differentiate and form, among others, the thymus (derivative of the third pouch) and the superior (fourth pouch) and inferior (third pouch) parathyroid glands (Weller 1933; Norris 1937, 1938).

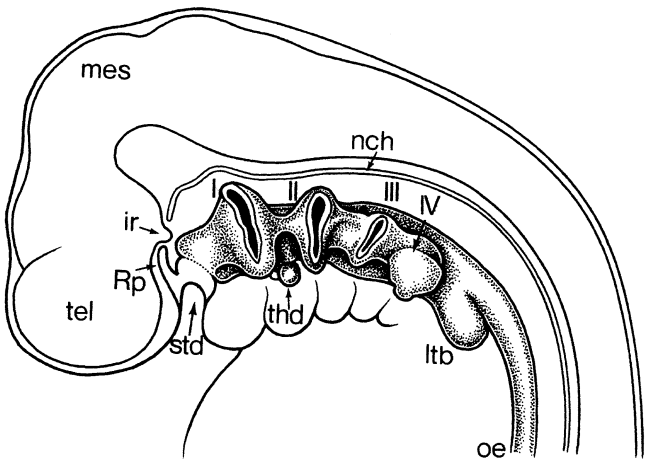


**Fig. 5.10** Development of the pharyngeal pouches (*I–IV*) in a 4-week-old human embryo. The *stippled line* caudal to the stomodeal depression indicates the position of the buccopharyngeal membrane before its resorption. *ir* infundibular recess, *ltb* laryngotracheal bud, *mes* mesencephalon, *nch* notochord, *oe* oesophagus, *Rp* Rathke's pouch, *std* stomodeal depression, *tel* telencephalon, *thd* thyroid diverticulum, *I–IV* pharyngeal pouches (After Weller (1933))

### 5.4.3 Further Development of the Face

The formation of the nose – including its cavities – has a key role during the further development of the human face, which is determined by the development of the primary palate and secondary palate, respectively. In the literature, there is consensus that the development of the secondary palate is based on fusion of the palatal shelves. By contrast, different developmental processes were described for the five swellings (bilateral maxillary and mandibular processes, and the frontonasal prominence) surrounding the stomodeum and forming the primary palate: fusion, merging or a combination of both (His 1885; Hochstetter 1891; Bardeen 1910; Politzer 1952; Hinrichsen 1985, 1990; Sulik 1996; Liu et al. 2007; Jugessur et al. 2009; Figs. 5.11 and 5.12). However, the cell biological mechanisms observed during the fusion process of the secondary palate are similar to those of the primary palate. The difference between fusion and merging will be explained below. Additionally, the origin of the maxillary process and the interpretation of the frontonasal prominence are under discussion. Following the morphology of the early embryonic head-neck area the outgrowth of the maxillary processes is not coupled with changes in the shape of the first pharyngeal arch. Therefore, both **maxillary processes** represent ***separate swellings*** and do not form part of the mandibular arches (Vermeij-Keers 1972, 1990). Furthermore,

**Table 5.2** Derivatives of the pharyngeal arches, grooves, and pouches

| Pharyngeal arch | Ectodermal groove | Endodermal pouch | Skeleton | Muscles | Nerves |
|---|---|---|---|---|---|
| First (mandibular) | External acoustic meatus; ear hillocks; pinna | Auditory tube; tympanic membrane | Meckel's cartilage: malleus, incus, mandibula template | Masticatory, tensor tympani, mylohyoid, anterior belly digastric | nV |
| Second (hyoid) | Disappears | Tonsillar fossa | Reichert's cartilage: stapes, styloid process; superior part body hyoid | Facial, stapedius, stylohyoid, posterior belly digastric | nVII |
| Third | Disappears | Inferior parathyroid glands; thymus | Inferior part body hyoid; greater cornu hyoid | Stylopharyngeus | nIX |
| Fourth | Disappears | Superior parathyroid glands | Thyroid and laryngeal cartilages | Pharyngeal constrictors, palate muscles, cricothyroid | nX |
| Sixth | Disappears | Ultimopharyngeal body | Cricoid, arytenoid, corniculate cartilages | Laryngeal, pharyngeal constrictors | nX |

After Sperber (2001)


**Fig. 5.11** Early development of the human face in Carnegie stages 14 (**a**), 16 (**b**) and 17 (**c**), shown in frontal views. *Arrows* indicate the interplacodal area (From the Kyoto Collection of Human Embryos; courtesy Kohei Shiota)

the term frontonasal prominence is used differently. In some studies it is used as an equivalent for the *mittlere Stirnfortsatz* of His (1885), but in many recent textbooks on human embryology, the frontonasal prominence approximately covers both nasal fields. In each nasal field a **nasal placode** develops, separated by the **interplacodal area** (Vermeij-Keers et al. 1983; Vermeij-Keers 1990). Around the nasal placode three facial swellings, defined as mesenchymal proliferations covered by ectoderm and separated by grooves, will grow out. At the medial side of each placode the medial nasal process and, laterally, the lateral nasal and maxillary processes develop. The nasal placodes, thereby, evaginate and are turned over by the outgrowth of the lateral nasal and maxillary processes. The first contact between the facial swellings is between the maxillary and medial nasal processes (Vermeij-Keers 1972, 1990; Rudé et al. 1994). Later, the lateral nasal process will contact the medial process both surrounding the external nasal aperture (nostril). At the site of adhesion between the three facial swellings the **epithelial plate** of Hochstetter (1891) or nasal fin develops in an occipito-frontal direction. Cell death occurs before, during and after formation of the epithelial plate followed by epitheliomesenchymal transformation and migration. Subsequently, the first disruption of the plate appears halfway, right above the frontally expanded stomodeum that is now called the primitive oral cavity. Cell death continues and gradually the fusion of the mesenchymal cores of the three swellings becomes obvious by 7 weeks of development (17 mm CRL). At that stage the various facial processes are still distinguishable by grooves. One of them, the internasal groove, develops in the median of the interplacodal area between both outgrowing medial nasal processes (Vermeij-Keers et al. 1983; Figs. 5.11 and 5.14). From these structures, the tip and dorsum of the nose, the nasal septum, the columella and philtrum are formed after outgrowth of the presumptive nasal septum in fronto-caudal direction.

The facial swellings transform both nasal placodes via the nasal grooves into the nasal tubes, leading to the formation of the primary palate and primitive oral cavity. This transformation is not only accompanied by considerable morphogenetic changes in the developing facial region itself, but also by changes in the nasal lumens and the bilateral anlage of **nasolacrimal duct**. This duct develops by cell death from a narrow epithelial plate formed by fusion of the lateral nasal and maxillary prominences corresponding to the nasolacrimal groove. The posterior part of each nasal tube is initially separated from the primitive oral cavity by the oronasal or bucconasal membrane (part of Hochstetter's epithelial plate) at the end of the fifth week, which disintegrates by apoptosis at the end of the seventh week to form the primitive choanae. Failure of membrane disintegration leads to ***choanal atresia***, one of the common congenital

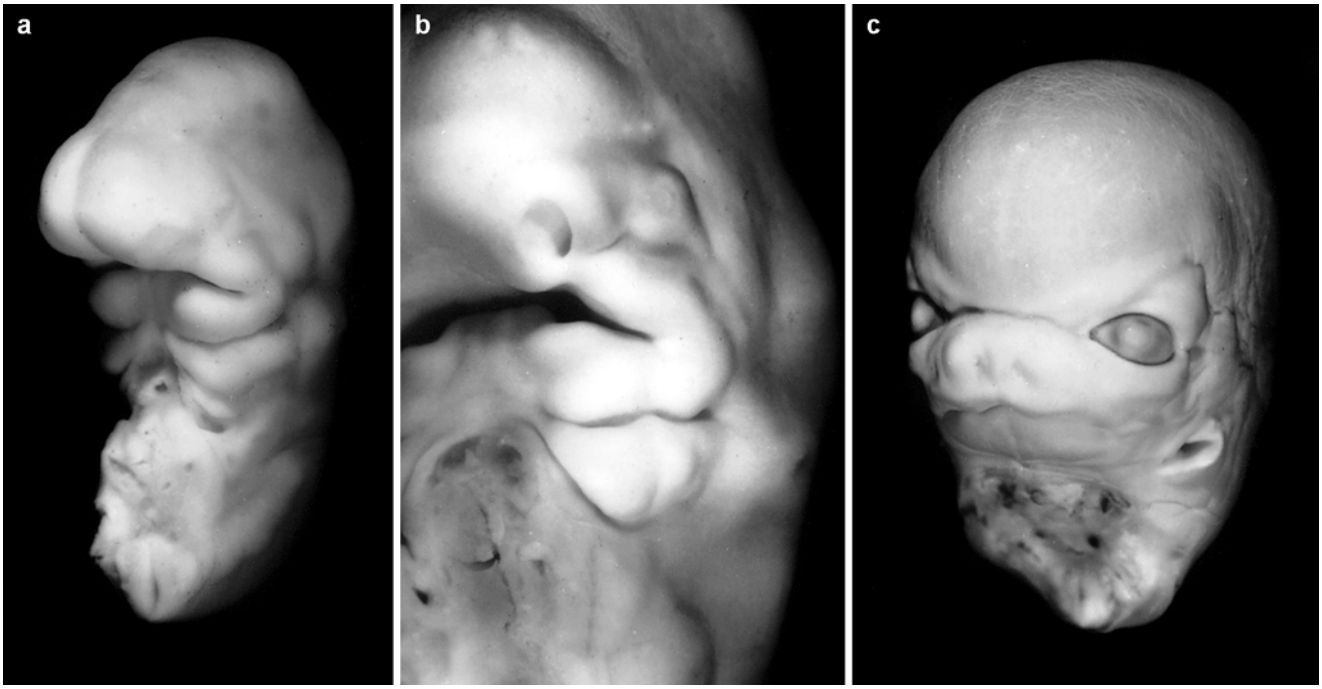


**Fig. 5.12** Early development of the human face in Carnegie stages 15 (**a**), 16 (**b**) and 21 (**c**), shown in oblique-lateral views (From the Kyoto Collection of Human Embryos; courtesy Kohei Shiota)

nasal anomalies (approximately 1 in 8,000 births; Sperber and Gorlin 1997; Sperber 2002).

The **secondary palate** develops after the fusion of the primary palate and starts as outgrowing palatal shelves from the maxillary prominences. These swellings grow out at either side of the tongue, shift from a vertical to a horizontal position and fuse in fronto-occipital direction with the primary palate, with each other and the nasal septum and form the roof of the oral cavity (Hinrichsen 1985). So the definitive nasal cavities are developed from the nasal tubes and from part of the primitive oral cavity (captured through fusion of the palatal shelves); their openings into the pharynx are called now the secondary choanae.

After 7 weeks of development, the facial grooves are eliminated by proliferation of the underlying mesenchyme, i.e. merging (Hinrichsen 1985, 1990; Vermeij-Keers 1990). At the same time the presumptive lip and alveolus grow out in caudal direction from the primary palate, resulting in the formation of the labial groove. Additionally, the mesenchymal differentiation of the lip, alveolus, and hard and soft palates starts. This differentiation concerns the bilateral development of the various bone centers of the upper jaw, i.e. the maxilla (a single center at 17 mm CRL), palatal bone (a single center at 23 mm CRL), and the premaxilla bearing both incisors (two centers at 23 and 50 mm CRL, respectively) and of the musculature. These bone centers grow out fuse with each other (maxilla and premaxilla) or form sutures (hard palate).

The above described complexity of control of embryogenesis of the primary palate and secondary palate is reflected by the common occurrence of oral clefts, approximately 1 in 700 live births (Mossey et al. 2009). Based on recent studies, the oral clefts are subdivided into three categories: cleft lip/alveolus, cleft lip/alveolus and palate, and cleft palate because of differences with respect to embryonic development, prevalence, risk factors and associated congenital malformations (Harville et al. 2005; Rittler et al. 2008; Luijsterberg and Vermeij-Keers 2011; Bush and Jiang 2012; Maarse et al. 2012). These three cleft categories consist of multiple subphenotypes, which can be explained by the successive developmental processes, time and place related (Rozendaal et al. 2012; Luijsterberg et al. 2014; Fig. 5.13):

1. If there is no fusion of the swellings or shelves at all, a complete cleft lip/alveolus or a complete cleft hard and soft palate including the uvula is the result.
2. If the fusion process stops somewhere along the fusion lines, then with respect to the primary palate a complete cleft of the lip and an intact or an incomplete cleft alveolus develops. The secondary palate shows an intact hard palate and a complete or incomplete cleft soft palate with complete cleft uvula or an incomplete hard palate with a complete cleft soft palate and uvula.
3. An incomplete cleft of the lip shows always a tissue bridge under the nostril, which means that the facial swellings are fused during early developmental stages. An incomplete cleft lip is, therefore, the result of

insufficient outgrowth of the lip in caudal direction during later stages. This cleft type can be associated with an intact alveolus, an incomplete cleft, hypoplasia or a submucous cleft of the alveolus. The latter is caused by insufficient outgrowth of the bone centers of the premaxilla and/or maxilla.

4. A submucous/subcutaneous cleft lip develops by defective differentiation of the mesenchyme into musculature at the fusion line.
5. Differentiation defects of the secondary palate concern: agenesis or hypoplasia of the palatine bones, submucous cleft hard and/or soft palate, hypoplasia soft palate and hypoplasia of the musculature.

All combinations of the various cleft types are possible and explainable, for example the incomplete cleft lip (differentiation defect) and a complete cleft alveolus (fusion defect), indicated as Simonart's band (Luijsterberg et al. 2014). Oral clefts – unilateral and bilateral types – occur as isolated anomalies, but also in association with other anomalies, often as part of a chromosomal defect or syndrome (Maarse et al. 2012). In early developmental stages the nose can be considered as two separate organs, which may develop asymmetrically. This asymmetrical development of the nose is expressed perfectly in the unilateral clefting of the lip and/or alveolus (Rozendaal et al. 2012; Luijsterberg et al. 2014).

Several distinct genetic and environmental risk factors have been identified for non-syndromic cleft lip and palate (Mossey et al. 2009; Cordero et al. 2011; Dixon et al. 2011). In view of the complexity of the developmental processes of the primary and secondary palate it is most likely that multiple genes are involved. With regard to non-syndromic oral clefts the strongest current evidence exists for mutations of the following genes: *FOXE1*, *MSX1*, *FGFR2* and *BMP4*. Additionally, genome-wide association studies supported by analysis of mouse models resulted in the identification of *IRF6*, *VAX1*, 8q24 locus, *MAFB*, *ABCA4*, and 17q22 locus genes (Dixon et al. 2011). Furthermore, there is evidence that lifestyle factors such as smoking, maternal alcohol consumption and folate deficiency are risk factors of oral clefts. However, the studies of alcohol consumption and folic acid supplementation are controversial and both links remain to be confirmed (Dixon et al 2011).

Other nasal malformations may vary from a simple depression to complete separation of the nostrils (Sperber and Gorlin 1997; Sperber 2002), and various degrees of aplasia of the wings of the nose and atresia of the nasal cavities (Van der Meulen et al. 1990; Nishimura 1993).

After **rupture** of the **buccopharyngeal membrane**, the **stomodeum** communicates with the foregut. The largest part of the primitive oral cavity is derived from the stomodeum. The roof of the stomodeum makes contact with the floor of the prosencephalon, just in front of the still intact buccopharyngeal membrane. After its rupture, initiated by apoptosis (Poelmann et al. 1985) the surrounding tissues grow out into the primitive oral cavity, leading to the formation of **Rathke's pouch** (Chap. 9). Subsequently, the walls of the pouch make contact and form a solid stalk that disappears through apoptosis. The primitive mouth opening becomes reduced by proliferating ectomesenchyme, fusing the maxillary and mandibular prominences to form the corners of the definitive mouth. Inadequate fusion results in ***macrostomia*** (unilateral or bilateral), whereas tension of the fusion process may produce ***microstomia***. The lower lip is rarely defective, but if so, it is clefted in the midline (Oostrom et al. 1996).

Apart from the nasolacrimal and internasal grooves, the interorbital groove develops gradually by outgrowth of the lateral nasal processes and the rapidly growing telencephalic vesicles (Vermeij-Keers 1972; Vermeij-Keers et al. 1984; Figs. 5.13 and 5.14). This groove runs from one eye cup to the other over the now-visible nasal root, and connects the future medial angles of the eyes. The outgrowth and differentiation of the nasal septum in fronto-caudal direction (17–27 mm CRL) leads to the disappearance of the internasal and interorbital grooves, i.e. merging. Additionally, the distance between the eyes and both nasal anlages shows a relative decrease due to a relative lag in transverse growth.

Insufficient relative decrease of the midfacial part leads to ***hypertelorism*** (Fig. 5.14). The most common form of human hypertelorism is found in ***frontonasal dysplasia*** also known as median cleft face syndrome, bifid nose with median cleft lip or internasal dysplasia (Van der Meulen et al. 1990; Gorlin et al. 2001). Severe median nasal clefting, hypertelorism and abnormal embryonic apoptosis were found in *Alx3*/*Alx4* double-mutant mice (Beverdam et al. 2001). *Aristaless*-like homeobox genes form a distinct gene family, characterized by a paired-type homeobox and the presence of a small conserved C-terminal domain in the proteins encoded, known as aristaless or OAR domain (Meijlink et al. 1997). During embryogenesis, a subset of these genes, including *Alx3*, *Alx4*, *Prx1*, *Prx2* and *Cart1*, are expressed in neural-crest-derived mesenchyme of developing craniofacial regions and in the mesenchyme of developing limbs (Leussink et al. 1995; Qu et al. 1997; ten Berge et al. 1998a, b). Mice with *Alx4* mutations have strong preaxial polydactyly, and mild craniofacial abnormalities in the rostral skull base and parietal and frontal bones (Qu et al. 1997). In double *Alx3*/*Alx4* mutants, most facial bones and many other neural-crest-derived skull elements are malformed, truncated or absent (Beverdam et al. 2001). *Cart1* mutant mice have major cranial defects including acrania and meroanencephaly (Zhao et al. 1996). These severe malformations are discussed in Chap. 4. In man, *ALX4* haploinsufficiency is associated with ossification defects in the parietal bones (Wu et al. 2000; Wuyts et al. 2000a; Mavrogiannis et al. 2001) and a homozygous mutation in *ALX4* gene is accompanied with mild or more severe frontonasal dysplasia phenotypes,

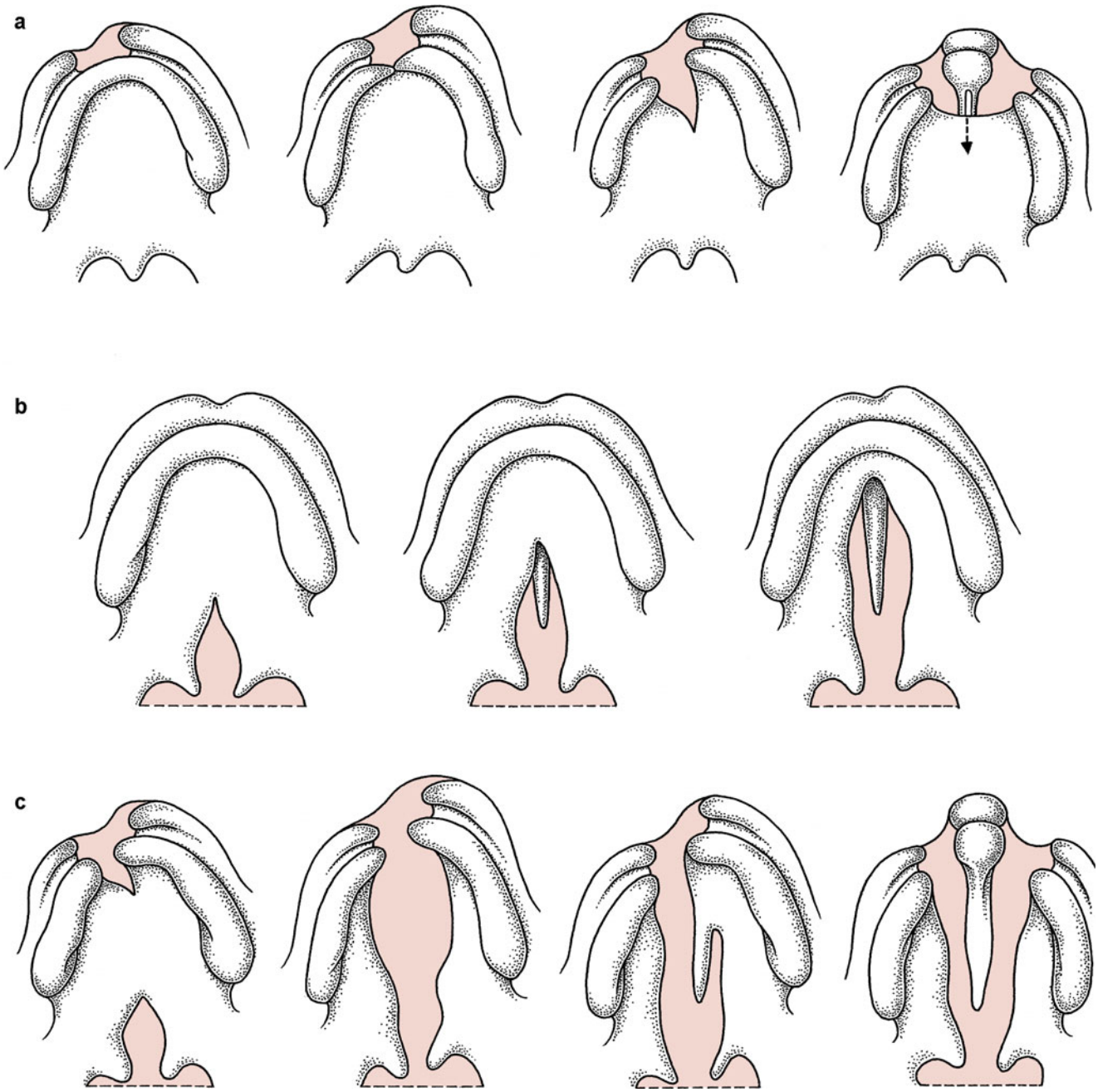


**Fig. 5.13** Classification of the various types of cleft lip and cleft palate (indicated in *light red*). (**a**) Clefts of the primary palate, from left to right: unilateral incomplete cleft lip, unilateral incomplete cleft lip with incomplete cleft of alveolus, unilateral complete cleft lip and alveolus, and bilateral complete cleft lip and alveolus; (**b**) clefts of the secondary palate, from right to left: uvula bifida with complete cleft of palatum molle, uvula bifida with complete cleft of palatum molle and incomplete cleft of palatum durum, and complete cleft of all parts of secondary palate; (**c**) clefts of the primary and secondary palate, from left to right: unilateral complete cleft of lip and alveolus with uvula bifida and complete cleft of palatum molle, the same but now with a complete cleft of palatum durum at the right, the same but now in combination with an incomplete cleft of the palatum durum at the left, and complete clefts on both sides of lips and all parts of palate (After Van der Meulen et al. (1990) and ten Donkelaar et al. (2007))

i.e. parietal foramina or severe cranium bifidum, and mild or severe midline brain malformations, respectively (Kayserili et al. 2009, 2012). Mutations in *ALX3* were found to cause autosomal recessive frontorhiny, a distinctive presentation of frontonasal dysplasia (Twigg et al. 2009). Mutations in the *GLI3* gene cause ***Greig cephalopolysyndactyly syndrome***, a rare form of hypertelorism that is associated with polysyndactyly (Mo et al. 1997; Shin et al. 1999; Gorlin et al. 2001).

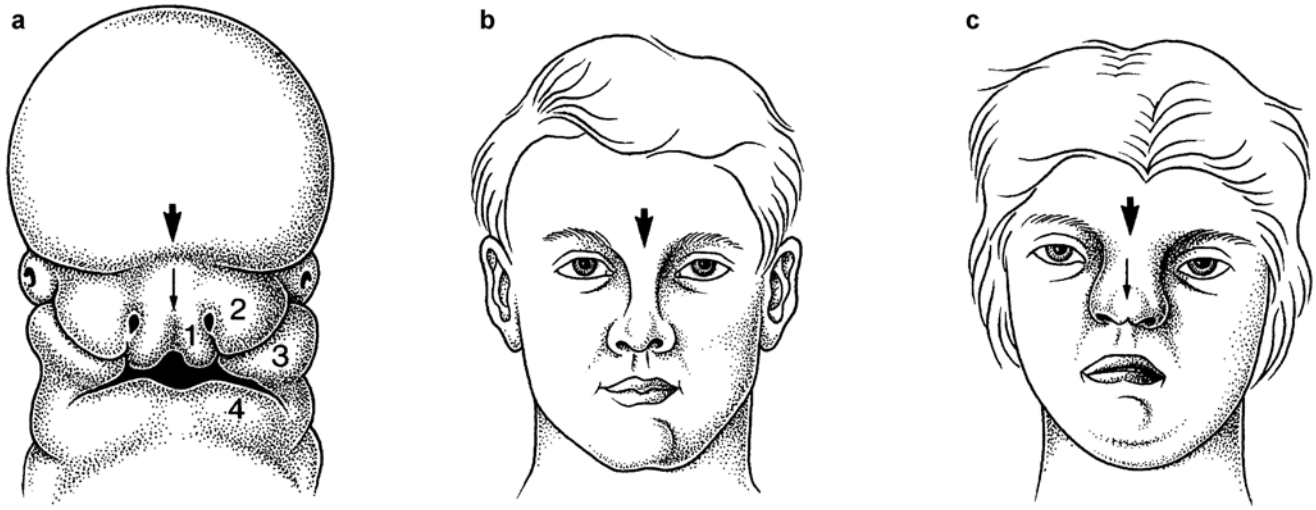


**Fig. 5.14** The face of a stage 17/18 human embryo (**a**), an adult face (**b**) and the face of an adolescent with orbital hypertelorism (**c**), showing the relative positions of the eyes and nose components. The internasal groove is indicated by a *small arrow* and the interorbital groove by a *larger arrow*. The facial prominences are numbered: *1* medial nasal process, *2* lateral nasal process, *3* maxillary prominence, *4* mandibular prominence (From Vermeij-Keers et al. 1984)

### 5.4.4 Development of the Skull

The development of the skull is influenced by environmental as well as genetic factors (Kjaer et al. 1999; Sperber 2001, 2002; Sperber et al. 2010). Its development is greatly influenced by brain growth. Initial neurocranial development is dependent on the formation of a membrane surrounding the neural tube, whose prior existence is essential for normal development. Persistence of the cranial neural fold stage (***anencephaly***) results in ***acalvaria*** (Sperber et al. 1986). The surrounding membrane subdivides into an outer **ectomeninx** and an inner **endomeninx**. The ectomeninx produces an outer osteogenic layer, in which bone forms, and an inner dura mater. The endomeninx subdivides into the outer arachnoid and the inner pia mater. The skull consists of the neurocranium, surrounding the brain, and the facial and visceral skeleton, which form the bones of the face and the lower jaw and the auditory ossicles, respectively. The skull develops from paraxial mesoderm (the sphenoid), the cranial neural crest and surface ectoderm placodes, occipital somites (parts of the occipital bone) and, presumably, mesenchyme from the prechordal plate. The skull ossifies in part endochondrally and in part intramembranously.

The **neurocranium** comprises the vault of the skull, i.e. the calvaria, and the cranial base (Fig. 5.15). The **chondrocranium** forms the cartilaginous base of the embryonic and fetal skull, in which endochondral ossification occurs. It arises from mesenchymal condensations. At stage 17, the first cartilage of the neurocranium develops around the membranous labyrinth and forms the **otic capsule** (Müller and O'Rahilly 1980). The occipital component of the chondrocranium also arises very early, and corresponds to the first

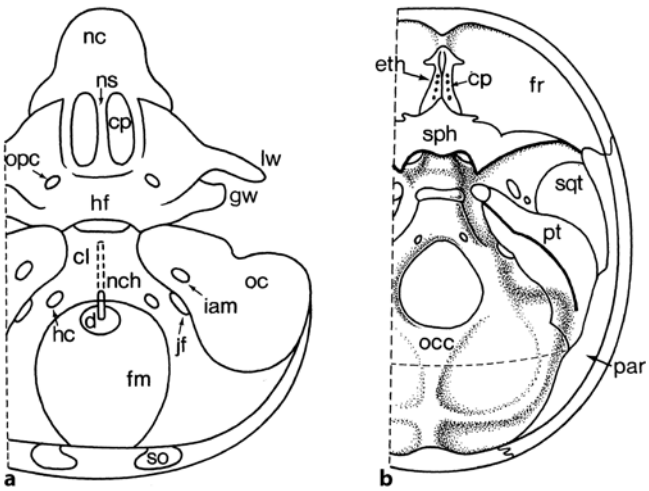


**Fig. 5.15** Development of the skull base from above: (**a**) chondrocranium at the end of the embryonic period; (**b**) the calvaria at birth. *cl* clivus, *cp* (site of) cribriform plate, *d* dens, *eth* ethmoid, *fm* foramen magnum, *fr* frontal bone, *gw* greater wing of sphenoid, *hc* hypoglossal canal, *hf* hypophysial fossa, *iam* internal acoustic meatus, *jf* jugular foramen, *lw* lesser wing of sphenoid, *nc* nasal capsule, *nch* notochord, *ns* nasal septum, *oc* otic capsule, *occ* occipital bone, *opc* optic canal, *par* parietal bone, *pt* petrous part of temporal bone, *so* supra-occipital, sph sphenoid, *sqt* squamous part of temporal bone (After O'Rahilly and Müller 2001)

four sclerotomes (Müller and O'Rahilly 1994; O'Rahilly and Müller 2001). Other primary chondrogenic centres are the area of the future clivus (basi-occipital) and the sphenoid, presented by the hypophysial fossa, the dorsum sellae and the greater and lesser wings. The foramen magnum arises at the end of the embryonic period. Intramembranously ossified components of the neurocranium (**desmocranium**) are the

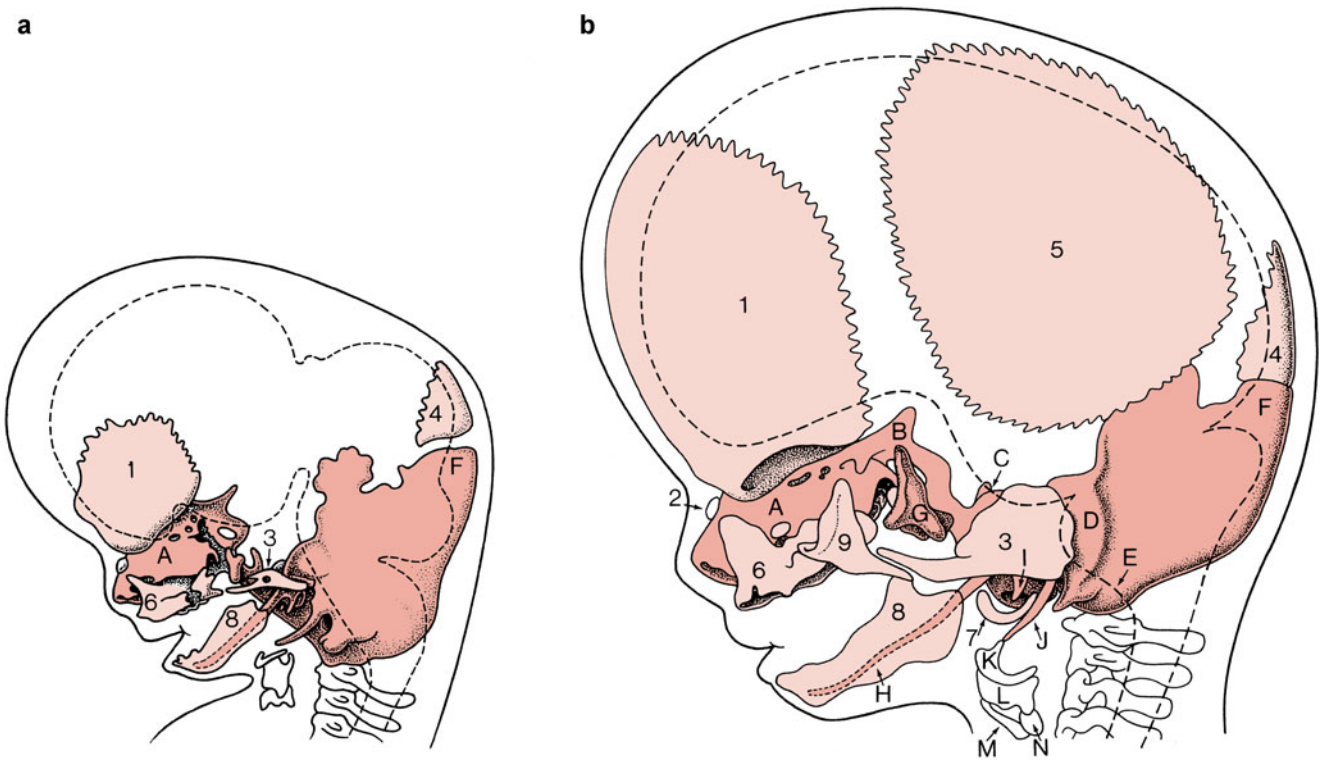


**Fig. 5.16** Development of the human desmocranium: (**a**) a 40-mm embryo; (**b**) an 80-mm embryo (After Williams et al. 1995). The contours of the CNS are indicated by broken lines. Chondral elements (*red*): *A* nasal capsule, *B* orbitosphenoid, *C* postsphenoid, *D* otic capsule, *E* exoccipital, *F* supra-occipital, *G* alisphenoid, *H* Meckel's cartilage, *I* carilage of malleus, *J* styloid cartilage, *K* hyoid cartilage, *L* thyroid cartilage, *M* cricoid cartilage, *N* arytenoid cartilage. Dermal elements (*light red*): *1* frontal bone, *2* nasal bone, *3* squama of temporal bone, *4* squama of occipital bone, *5* parietal bone, *6* maxilla, *7* tympanic ring, *8* mandibula, *9* zygomatic bone

bone plates of the skull such as the frontal and parietal bones. The **ossification centres** that develop in the membrane form the frontal, parietal, squamous temporal and squamous occipital bones. In general, each of these bones develops out of one bone centre. The parietal bone, however, develops from two bone centres that fuse with each other and subsequently function as one centre. The intervening areas form fibrous **sutures** and **fontanelles**, termed anterior, posterior, anterolateral and posterolateral. Defects of calvarial intramembranous ossification are recognized as ***cranium bifidum*** and ***foramina parietalia permagna***, and are due to mutations in the *ALX4* and *MSX2* genes (Cargile et al. 2000; Wuyts et al. 2000a, b). The calvarial sutures are the sites at which the skull expands to accommodate itself to the enlarging brain. Growth takes place in the direction perpendicular to the sutures (Smith and Töndury 1978; Vermeij-Keers 1990; Opperman 2000). Most volume expansion of the skull occurs in utero and within the first 2 years of life, although most sutures do not ossify before adulthood (Sperber 2001, 2002).

The **facial skeleton** can be subdivided into an upper third, predominantly of neurocranial composition and incorporating the orbits, a middle portion incorporating the nasal complex, maxillae, zygomata and temporal bones, and a lower third, composed of the mandibula, i.e. part of the viscerocranium.

The **facial skeleton** develops intramembranously (**desmocranium**) from ossification centres in the ectomesenchyme of the facial prominences (Fig. 5.16). During the third intrauterine month, centres appear for the nasal, lacrimal, pterygoid, palatine, zygomatic and premaxillary (incisive bone) bones (Vermeij-Keers 1990; Sandikcioglu et al. 1994; Kjaer et al. 1999). Mesenchymal precursors such as those for the auditory ossicles of the visceral skeleton are present early and later become cartilaginous. They are partly replaced by intramembranously ossified bone. The cartilage of the first pharyngeal arch (Meckel's cartilage) is largely replaced by the mandibula. The mandibula ossifies intramembranously from a single centre on each side (Mérida-Velasco et al. 1993). The facial skeleton is largely laid down in mesenchyme at the end of the embryonic period (O'Rahilly and Müller 2001).

Deficient mandibular development (***micrognathia***) is characteristic of the Pierre Robin sequence, and several syndromes such as cri du chat, Treacher Collins and Goldenhar syndromes. In the Pierre Robin sequence, the underdeveloped mandibula usually demonstrates catch-up growth in the child. In Treacher Collins syndrome, deficiency of the mandibula is maintained throughout growth (Sperber 2001). Patients with hemifacial microsomia (Goldenhar syndrome)

start and end with a smaller mandible, but show a growth pattern similar to normal controls (Ongkosuwito et al. 2013). The *Prx1*/*Prx2* genes play a role in mandibular arch morphogenesis (ten Berge et al. 2001). ***Agnathia*** is found in the ***otocephalies***, ranging from milder forms in which derivatives of the skeletal and dental portions of the first arch are absent to the more severe form in which little more than external ears ('ear head') are apparent (Duhamel 1966; Vermeij-Keers 1990; Fig. 5.21).

***Agnathia-otocephaly*** was described as a lethal developmental field complex, characterized by extreme hypoplasia or absence of the mandibula, astomia, aglossia and synotia (Bixler et al. 1985). It is most likely caused by a persistent buccopharyngeal membrane (Vermeij-Keers 1990) and is frequently associated with HPE (Pauli et al. 1983; Siebert et al. 1990; Cohen and Sulik 1992). In inbred strains of guinea pigs, otocephaly is probably a neural crest problem (Wright and Wagner 1934). In a substrain of C57B1 mice with a balanced chromosomal translocation, Juriloff and coworkers (1985) found that in the less severely affected embryos the first evidence of cell death was in the mesodermal cores of the first pharyngeal arch. The balanced translocation may hasten cell death. In more severe cases, cell death was also found in the mesoderm underlying the neural tube. *Otx2* heterozygous mouse mutants display otocephalic phenotypes, the severity of which is dependent on the genetic background of a C57BL/6 strain (Hide et al. 2002). *Otx2* is not only expressed in the forebrain and the mesencephalon (Acampora et al. 1995, 1998), but also in the cephalic mesenchyme, including mesencephalic neural crest cells that are distributed to the mandibula (Kimura et al. 1997). Therefore, *Otx2* heterozygous mutant defects relate primarily to *Otx2* function in the formation of mesencephalic neural crest (Kimura et al. 1997). Recently, it is demonstrated that *OTCX2* and *PRRX1* are involved in otocephaly/dysgnathia in humans (Sergi and Kamnasaran 2011; Celik et al. 2012; Chassaing et al. 2012). Most *Otx2*+/− mutant mice also display HPE (Matsuo et al. 1995), but a role for *OTX2* in human HPE has not been found so far.

## 5.5 Neurocristopathies

A number of craniofacial malformations have major neural crest involvement, and are usually referred to as ***neurocristopathies*** (Jones 1990; Johnston and Bronsky 1995, 2002). The concept neurocristopathy was introduced by Bolande (1974) to explain the developmental relationships among a number of dysgenetic, hamartomatous and neoplastic disorders, including pheochromocytoma, von Recklinghausen's neurofibromatosis, Hirschsprung's aganglionic megacolon (Clinical Case 5.1) and the multiple endocrine adenomatoses. A neurocristopathy was defined as a condition arising from aberrations in the early migration, growth and differentiation of neural crest cells. Subsequently, an increasing number of disorders such as retinoic acid syndrome (RAS), hemifacial microsomia, Treacher Collins syndrome, DiGeorge sequence, cleft lip and palate, frontonasal dysplasia and Waardenburg syndrome have been included into the neurocristopathies (Table 5.3). The CHARGE and Mowat-Wilson syndromes may be added. Recently, the idea that neural crest abnormalities underlie the pathogenesis of the DiGeorge sequence has been challenged (Sect. 5.5.4). The same holds for Treacher Collins syndrome (Sect. 5.5.3).

**Table 5.3** Some neurocristopathies and related disorders

| Syndrome | Ear abnormalities | Facial bone malformations | Cardiovascular malformations | Pharynx glands | Facial clefts | Other associated malformations |
|---|---|---|---|---|---|---|
| Retinoic acid syndrome | Microtia/anotia; low-set ears; stenosis external meatus | Mandibular (micrognathia) and other deficiencies | Conotruncal defects | Thymus deficient or absent | Cleft palate (8 %) | Brain (particularly cerebellum) |
| DiGeorge syndrome | Low-set ears | Variable maxillary and mandibular deficiencies (micrognathia) | Conotruncal defects | Thymus deficient or absent | Cleft lip and/or palate (10 %) | Brain |
| Hemifacial microsomia | Microtia; accessory auricles; abnormal ear ossicles | Usually asymmetrical deficiencies of mandibula, squamous temporal and other bones | Conotruncal defects | None reported | Cleft lip and/or palate (7–22 %) | Eye, brain (in severe cases), vertebrae in oculo-auriculo-vertebral variant |
| Treacher Collins syndrome | Pinna anomalies; abnormal ear ossicles; hypoplasia or atresia external meatus | Symmetrical deficiencies or absence of zygoma, underdevelopment of posterior maxilla and mandibula | No increase in cardiovascular malformations | None reported | Cleft palate (35 %) | Eyelid coloboma; rarely with limb defects, e.g. Nager syndrome |

After Sperber and Gorlin (1997), Johnston and Bronsky (2002)

Several syndromes specifically affect derivatives of the face and the first and second branchial arches (Passos-Bueno et al. 2009; Johnson et al. 2011a, b). Treacher Collins syndrome affects bilaterally the ear, the lower eyelid, the zygoma, the maxilla and the mandibula. Related disorders are the oculo-auriculo-vertebral syndrome (Sect. 5.5.2) and the auriculo-condylar syndrome (Passos-Bueno et al. 2009). Hemifacial microsomia shows unilateral malformation of nearly the same structures. Some patients who were exposed to thalidomide during a restricted period of development had a malformation similar to mandibulofacial dysostosis and hemifacial microsomia (Kleinsasser and Schlothane 1964; Jacobson and Granström 1997; Gorlin et al. 2001).

### 5.5.1 Retinoic Acid Syndrome

***Retinoic acid syndrome*** (***RAS***) malformations first appeared shortly after the introduction of Accutane (13-*cis*-retinoic acid), a drug used for the treatment of severe cystic acne (Lammer et al. 1985). Although the retinoids (the normal biologically active retinoic acid and related compounds such as vitamin A, the dietary precursor of retinoic acid) had long been known to be potent teratogens, and the drug Accutane was not to be taken during pregnancy, in the USA many accidental exposures occurred, resulting in a surprisingly high incidence of very severe malformations involving craniofacial structures. Teratogenic doses of retinoic acid given to mice at early stages of neurulation yielded craniofacial malformations that are strikingly similar to those in children with retinoic acid embryopathy (Webster et al. 1986; Willhite et al. 1986; Sulik et al. 1988; Sulik 1996; Morriss-Kay and Ward 1999). The defects observed in children with RAS include abnormalities of the external and middle ear, sometimes underdevelopment of the mandibula and cleft palate, facial nerve paralysis, cerebellar defects, outflow tract defects of the cardiovascular system, and defects of the thymus and parathyroid glands. Such defects are usually fatal within the first years of life (Johnston and Bronsky 1995, 2002). The unexpectedly severe nature of RAS malformations relates to the very poor ability of humans to clear retinoic acid metabolites (Webster et al. 1986). Teratogenic studies in mice (Goulding and Pratt 1986; Webster et al. 1986; Pratt et al. 1987) suggested that the timing of exposure for the most severe facial malformations coincided with the onset and period of migration of first and second arch crest cells (about day 21 in human embryos), whereas the sensitive period for cardiovascular malformations coincided with the migration of third and fourth arch crest cells (about day 23 in man).

**Local retinoid** (**RA**) **signalling** coordinates forebrain and facial morphogenesis by maintaining FGF8 and SHH expression (Schneider et al. 2001; Niederreither and Dollé 2008). FGF8 and SHH act as survival factors in the brain and facial primordia (Ahlgren and Bronner-Fraser 1999; Helms et al. 1997; Hu and Helms 1999; Laue et al. 2011; Rhinn and Dollé 2012). Experiments in chick embryos (Schneider et al. 2001) show that, in the absence of an intact RA signalling pathway, FGF8 and SHH expression is lost, cells fail to proliferate and undergo apoptosis, and the forebrain and frontonasal process cease their morphogenesis, suggesting a critical period of the morphogenesis of the forebrain and the frontonasal process dependent upon RA signalling correlated with the timing of RA production in the frontonasal ectoderm. Forebrain and frontonasal process-derived tissue are sensitive to disruptions in RA signalling during early development, but later become insensitive.

### 5.5.2 Oculoauriculo-Vertebral Spectrum

The predominant defects in the non-random association of anomalies known as the ***oculoauriculo-vertebral spectrum*** are problems in the morphogenesis of the face, the first and second pharyngeal arches, sometimes accompanied by vertebral anomalies (most commonly cervical hemivertebrae or hypoplasia of vertebrae) and/or ocular anomalies (Jones 1997; Gorlin et al. 2001; Passos-Bueno et al. 2009). The association with epibulbar dermoid and vertebral anomaly is known as ***Goldenhar syndrome*** (Fig. 5.17a–c), and the predominantly unilateral occurrence as ***hemifacial microsomia***. The occurrence of various combinations and gradations of these anomalies, both unilateral and bilateral, with or without epibulbar dermoid and vertebral anomaly, suggested that hemifacial microsomia and the Goldenhar syndrome may simply represent gradations in severity of a similar disorder of morphogenesis. Their frequency of occurrence is estimated to be 1 in 3,000 to 1 in 5,000, with a slight (3:2) male predominance (Jones 1997; Gorlin et al. 2001). CNS malformations include intellectual disability, hydrocephalus, Chiari type II malformation, occipital encephalocele, facial nerve paralysis, agenesis, hypoplasia and lipoma of the corpus callosum, and hypoplasia of the septum pellucidum (Aleksic et al. 1984; Jacobson and Granström 1997). Severe abnormalities of the pons were found in two infants with Goldenhar syndrome (Pane et al. 2004). The syndrome can be detected by prenatal ultrasound examination on the frequent presence of a lipoma on the corpus callosum (Jeanty et al. 1991; Wong et al. 2001).

The main facial features of ***hemifacial microsomia*** (HFM) include a small lower jaw, sometimes with an absent jaw joint, a malformed or absent external ear with accessory tags and facial clefts (Cousley and Calvert 1997). Recently, Ongkosuwito et al. (2014) demonstrated that the maxilla is also involved in HFM patients, especially in the more severe cases. Experimental studies in rodents suggest that this pattern of malformation is often caused by bleeding in the region of the stapedial artery, transitorily supplying the


**Fig. 5.17** Craniofacial dysmorphology syndromes in neurocristopathies: (**a**–**c**) Goldenhar syndrome in a 2-year old boy, showing bilateral microtia (*left* lobar type; *right* concha type), conductive hearing loss, left facial nerve paresis, left-sided mandibular hypoplasia, craniosynostosis, defects of vertebrae and ribs and various heart defects: ventricular septal defect, atrial septal defect, pulmonary stenosis and patent ductus arteriosus; (**d**–**f**) Treacher Collins syndrome in a 10-year-old boy with the following bilateral craniofacial abnormalities: microtia, agenesis of external acoustic meatus, conductive deafness, dysplasia of os petrosum, aplasia of zygoma, hypoplasia and crowding of maxilla and mandibula, hypoplasia of mastoid and maxillary sinus, and colobomata of lower eyelids (Courtesy Michiel Vaandrager, Rotterdam)

second pharyngeal arch (Poswillo 1973). Such events are usually sporadic, but genetic predisposition can occur, as shown by the *Hfm* mouse, in which a chromosome 10 transgene integration is associated with a small ear or an asymmetric jaw in 25 % of progeny heterozygous for the transgene (Naora et al. 1994). At E9.5, rupture of the dorsal vasculature of the second pharyngeal arch has been found in *Hfm*+/– mutants. In man, genetic linkage to chromosome 14q32 was reported in a family with hemifacial microsomia in which first-arch abnormalities segregate with unusually high penetrance (Kelbermann et al. 2000).

### 5.5.3 Treacher Collins Syndrome

***Treacher Collins syndrome*** (Treacher Collins 1900) or ***mandibulofacial dysostosis*** (Franceschetti and Klein 1949) is an autosomal dominant inherited syndrome that is localized on chromosome 5q32-33.1. Its incidence is approximately 1 in 50,000 live births and its clinical features include the following (Fig. 5.17d–f): (1) abnormalities of the external ears, atresia of the external auditory canals and malformation of the middle ear ossicles through to a complete absence of the middle ear, resulting in bilateral conductive

hearing loss (Phelps et al. 1981); (2) lateral downward sloping of the palpebral fissures, frequently with colobomas of the lower eyelids and a paucity of lid lashes medial to the defect; (3) hypoplasia of the mandibula, maxilla and zygoma; and (4) cleft palate (Dixon et al. 1994; Marres et al. 1995; Jacobson and Granström 1997; Jones 1997; Gorlin et al. 2001; Marsh and Dixon 2001; Trainor 2010; van Gijn et al. 2013). The Treacher Collins Syndrome Collaborative Group (1996) identified the molecular basis of this rare disorder by positional cloning. Although the causative gene (*TCOF1* after Treacher Collins-Franceschetti syndrome) has a somewhat variable penetrance, malformations are usually very consistent. *TCOF1* appears to be poorly conserved among mammals compared with other developmental genes. *TCOF1* encodes for a nuclear phosphoprotein known as Treacle. The majority of mutations in *TCOF1* lead to truncations of the C-terminal end of Treacle (Dixon et al. 2007). Mouse *Tcof1* shows only 62 % amino acid identity with the human protein (Dixon et al. 1997). *Tcof1* is widely expressed, most highly at the edges of the neural folds (Dixon et al. 1997). Heterozygous mice show exencephaly associated with extensive apoptosis in the prefusion neural folds (Dixon et al. 2000). The Treacher Collins syndrome has not been associated with neural tube defects. This discrepancy may be due to species-specific differences between mice and man.

Studies on the pathogenesis of RAS defects in mice have also provided data relevant to Treacher Collins syndrome (Poswillo 1975; Wiley et al. 1983; Webster et al. 1986; Sulik et al. 1987; Osumi-Yamashita et al. 1992; Evrard et al. 2000). In mice, the spatiotemporal expression of *Tcof1* coincides with the formation and migration of neural crest cells, implying that *Tcof1* plays an important role in their development (Dixon et al. 2006). Cell lineage studies in E8.5 wild type and *Tcof1*$^{+/-}$ mouse embryos revealed no defects in cranial neural crest cell migration, however, 25 % fewer migrating neural crest cells were observed in the TCS embryos compared to their wild-type littermates (Dixon et al. 2006). The deficiency in neural crest cell number arises from extensive neuroepithelial apoptosis from E8.0 to E10.5, which diminishes the neural stem cell pool from which neural crest cells arise. This process is p53 dependent (Jones et al. 2008). Therefore, the general cranioskeletal hypoplasia observed in patients with Treacher Collins syndrome arises *not* because of a neural crest migration defect, but rather as a *deficiency* in neural crest cell number (Trainor 2010). So, *Tcof1*/Treacle plays a critical role in neural crest cell formation and is required for neuroepithelial survival and neural crest cell proliferation (Dixon et al. 2006). Remarkably, *Tcof1*$^{+/-}$ embryos treated in utero from E6.5 onwards with a specific inhibitor of p53, exhibited a dose-dependent inhibition of neuroepithelial apoptosis and rescue of cranioskeletal development (Jones et al. 2008).

### 5.5.4 DiGeorge Sequence and Related Disorders

The ***DiGeorge sequence*** or ***syndrome*** (DiGeorge 1965) variably includes defects of development of the face, the thymus, parathyroids and great vessels (Conley et al. 1979; Lammer and Opitz 1986; Jones 1997; Gorlin et al. 2001; Yutzey 2010), i.e. tissues in particular of the third and fourth branchial arches, and their associated pouches. Hypoplasia or aplasia of the thymus leads to a deficit in cellular immunity allowing severe infectious diseases. Hypoplasia to absence of the parathyroids results in severe hypocalcemia and seizures in early infancy. Common cardiovascular malformations are aortic arch anomalies, including right aortic arch, interrupted aorta, conotruncal anomalies such as truncus arteriosus and ventricular septal defect, patent ductus arteriosus and tetralogy of Fallot. Specific to partial monosomy 22q are lateral displacement of inner canthi with short palpebral fissures, short philtrum, micrognathia and ear anomalies. The DiGeorge sequence is aetiologically heterogeneous. It has been associated with prenatal exposure to alcohol and Accutane, and a variety of chromosome abnormalities (Gorlin et al. 2001; Johnston and Bronsky 2002). The majority of cases, however, result from partial monosomy of the proximal arm of chromosome 22 due to a microdeletion of 22q11.2 (Fig. 5.18), detectable by molecular or fluorescence in situ hybridization analysis (Lindsay 2001). Therefore, the DiGeorge sequence and related malformations with chromosome 22 deletions such as the velocardiofacial or Shprintzen syndrome (Shprintzen et al. 1978; Goldberg et al. 1993; also known as Sedlacková syndrome: Sedlacková 1967) and conotruncal anomaly face syndrome are combined to the chromosome 22 deletion (*del22q11*) syndrome (Driscoll et al. 1992a, b; Emanuel et al. 2001; Lindsay 2001). The velocardiofacial syndrome is characterized by hypoplasia or a cleft of the secondary palate, cardiac defects, a typical face, microcephaly and hearing and learning disabilities. The occurrence of the *del22q11* syndrome is estimated as 1 in 4,000 live births (Scambler 1994, 2000; Lindsay 2001). The symptoms of *del22q11* syndrome are diverse. Distinct features can show variable expressivity and incomplete penetrance. Depending on the key symptoms, two phenotypes may be distinguished (Ryan et al. 1997; Scambler 2000; Lindsay 2001). The 'pharyngeal' phenotype encompasses the most characteristic features of *del22q11* syndrome, including congenital cardiovascular defects, craniofacial anomalies and aplasia or hypoplasia of the thymus and parathyroids. The 'neurobehavioural' phenotype becomes manifest in early childhood as learning difficulties, cognitive defects and attention-deficit disorder. In adolescence and adulthood, some patients develop various psychiatric disorders, including schizophrenia, schizoaffective and bipolar disorders. The basis of the neurobehavioural phenotype is

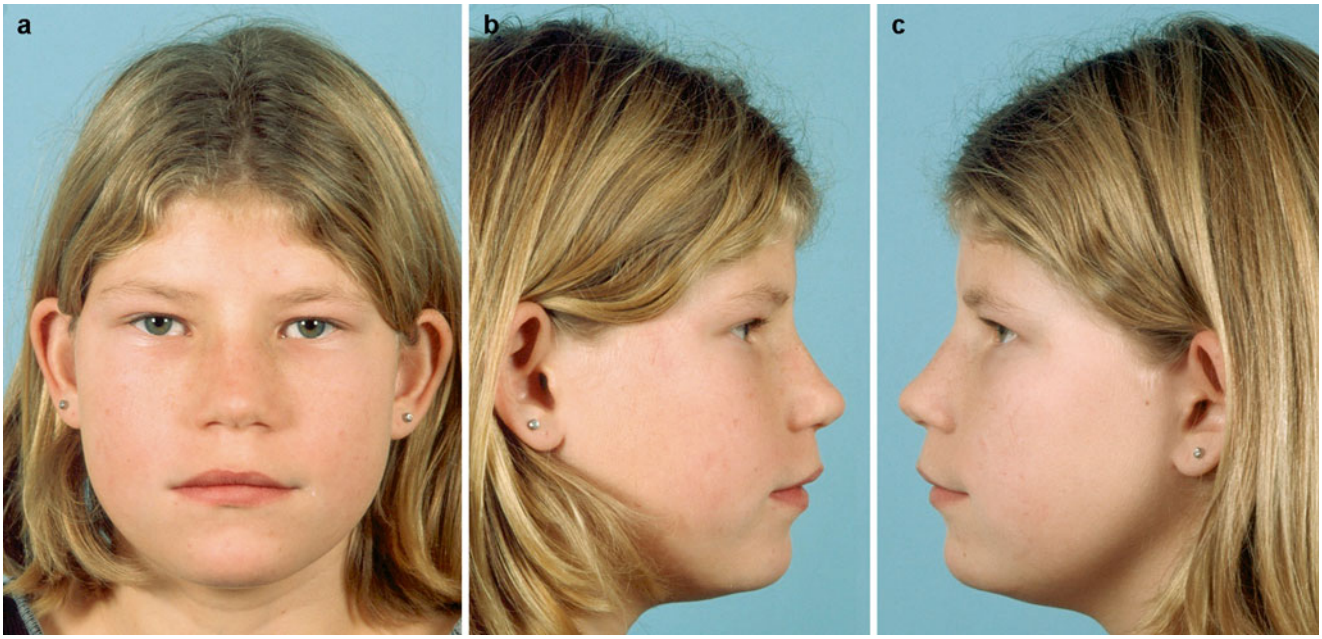


**Fig. 5.18** (**a**–**c**) Craniofacial dysmorphology in a 10-year-old girl with a 22q11-deletion. At birth, the patiënt showed a flat occiput, short neck, wide but closed palate, tetralogy of Fallot and slight dysmorphic toes. In 1994, a velopharyngeal insufficiency was found, followed by DNA analysis, and the diagnosis of a 22q11 deletion in 1996. Apart from bilateral hearing loss, due to chronic inflammation of the middle ears, no other abnormalities of the derivatives of the pharyngeal arches were found. A general developmental delay of the patiënt required special education (Courtesy Jeannette M. Hoogeboom, Rotterdam)

unknown. All patients with the *del22q11* syndrome manifest at least some components of the pharyngeal and neurobehavioural phenotypes with varying degrees of severity. In contrast to the clinical heterogeneity of this syndrome, the *del22q11* genetic lesion is remarkably homogeneous in affected individuals. Approximately 90 % of patients have a typical deleted region of some 3 Mb, encompassing 30 genes, whereas about 8 % of patients have a smaller deletion of some 1.5 Mb, involving 24 genes (Lindsay 2001).

Treatment of pregnant mice with ethanol at the time of migration of the first and second arch crest cells leads to massive cell death, resulting in malformations very similar to those of the DiGeorge sequence (Daft et al. 1986; Sulik et al. 1986). This suggested that the DiGeorge sequence may be secondary to an abnormality in the neural crest (Scambler 1994). A number of gene knockouts produce the DiGeorge sequence. *Hoxa3* knockout mice show some resemblance to the DiGeorge sequence (Chisaka and Capecchi 1991; Manley and Capecchi 1995; Capecchi 1997). They lack a thymus and parathyroid glands, have a reduced thyroid and show malformations of the laryngeal cartilages and muscles, and of the heart. Lindsay and co-workers (1999), Lindsay and Baldini (2001) developed a mouse model heterozygous for the 22q11.2 deletion. Neural crest migration into the pharyngeal arches appeared to be normal but there was severe underdevelopment of the fourth arch aortic vessels in all of the embryos studied. The gene content of the human 22q11 region was found to be highly conserved in a region of mouse chromosome 16. The first mouse deletion generated, *Df1* (Lindsay et al. 1999), encompassing mouse homologues of 18 out of the 24 genes that are deleted in patients with the 1.5-Mb deletion, led to cardiovascular defects similar to those in patients. The T-box transcription factor *Tbx1* plays a crucial role in the fourth arch abnormality in mice (Lindsay 2001; Lindsay et al. 2001). *Tbx1*-null mice die at birth and have a persistent truncus arteriosus, a hypoplastic pharynx, lack a thymus and parathyroids, and have ear, jaw and vertebral anomalies. The embryological basis of these abnormalities is maldevelopment of the pharyngeal arches and arch arteries 2–6, and of the pharyngeal pouches 2–4 (Lindsay et al. 2001). The severity and extent of the embryological lesion indicate that *Tbx1* may be required for the segmentation of the pharyngeal endoderm, an event that initiates the development of the entire pharyngeal apparatus (Lindsay 2001). Chordin secreted by the mesendoderm is required for the correct expression of *Tbx1* and other transcription factors involved in the development of the pharyngeal region (Bachiller et al. 2003). Chordin mutant mice either die early during development or die perinatally, showing an extensive array of malformations that encompass most features of the human DiGeorge and velocardiofacial syndromes. FGF8 is also required for pharyngeal arch and cardiovascular development in mice (Abu-Issa et al. 2002; Frank et al. 2002). *Fgf8* mutants resemble *Tbx1*−/− mouse embryos, probably due to a common signalling pathway (Vitelli et al. 2002).


**Fig. 5.19** (**a**, **b**) Waardenburg syndrome in a 32-year-old male patiënt with a 558-559delCA mutation in exon 4 of the *PAX3* gene, compatible with Waardenburg type 1. The patiënt shows typical craniofacial dysmorphology, early temporal greying, has severe bilateral congenital hearing loss, mental retardation, and no verbal communication (Courtesy Jeannette M. Hoogenboom, Rotterdam)

The hypothesis that neural crest abnormalities underlie the pathogenesis of the DiGeorge sequence seems however unlikely since pharyngeal patterning is not affected in chick embryos in which the neural crest has been ablated (Bockman et al. 1989; Veitch et al. 1999). Moreover, *Tbx1* is not expressed in the neural-crest-derived mesenchyme of the pharyngeal arches. Neural crest cells may, however, play a secondary role in the disorder as targets of *Tbx1*-driven signalling (Lindsay 2001; Cordero et al. 2011). Yagi et al. (2003) showed that a *TBX1* mutation is responsible for five major phenotypes in *del22q11* syndrome. In view of these data, the DiGeorge sequence should not be viewed any longer as a neurocristopathy.

### 5.5.5 Waardenburg Syndrome

The term ***Waardenburg syndrome***, originally described by Waardenburg (1951), is used for a heterogeneous set of auditory-pigmentary syndromes, the primary cause of which is a patchy lack of melanocytes in the hair, eyes, skin and stria vascularis (Read 2001; Spritz et al. 2003; Pingault et al. 2010). Four subtypes can be distinguished: (1) type 1 with dystopia canthorum, caused by mutations in the *PAX3* gene (Fig. 5.19); (2) type 2 without dystopia is heterogeneous, some cases are due to changes in the *MITF* and *SLUG* genes; (3) the rare type 3, resembling type 1 but with additional contractures or hypoplasia of the upper-limb joints and muscles, also results from *PAX3* mutations; and (4) type 4 with Hirschsprung's disease, again heterogeneous and due to mutations in the *EDN3*, *EDNRB* and *SOX10* genes. Most forms are inherited as autosomal dominant traits. The hearing loss in all types is congenital, sensorineural and non-progressive (Chap. 7). Waardenburg syndrome types 1, 3, and 4 are neurocristopathies, affecting more than one neural crest derivative. Type 2 appears to be melanocyte-specific. Auditory-pigmentary syndromes and mouse models are further discussed in Chap. 7.

## 5.6 Cranial Ciliopathies

A ***ciliopathy*** is defined as a disorder that results from aberrant form or function of primary cilia. As a class of diseases, ciliopathies have a rather broad range of clinical manifestations (Badano et al. 2006; Chap. 3). A number of ciliopathies result in malformations of the craniofacial complex, including the Bardet-Biedl, oral-facial-digital type 1, Meckel-Gruber (Chap. 3), Joubert (Chap. 8) and Ellis-van Creveld syndromes (Brugmann et al. 2010).

The ***Bardet-Biedl syndrome*** (***BBS***) is an autosomal, genetically heterogeneous disorder that is characterized by obesity, polydactyly, renal anomalies, retinal degeneration and intellectual disability. A subgroup presents with characteristic facial features including deep set eyes, hypertelorism, downward slanting palpebral fissures, a flat nasal bridge with anteverted nares and prominent nasolabial folds, a long philtrum and a thin upper lip. BBS patients may have a wide, prominent forehead and a small mouth with a slightly everted lowerlip and retrognathia (Beales et al. 1999). Zebrafish models have been used to explore the consequence of mutations in *Bbs* genes on craniofacial development. Defects in

zebrafish *Bbs* genes cause shortening of the anterior neurocranium, partial cyclopia and micrognathia, attributed to lack of neural crest cell migration into the facial prominences (Tobin et al. 2008).

The ***oral-facial-digital syndrome type 1*** (***OFDS1***) is an X-linked dominant disorder caused by mutations in *OFD1*. This male lethal disorder is characterized by digital abnormalities, polycystic kidneys, CNS malformations and facial anomalies (Ferrante et al. 2001, 2009; Macca and Franco 2006; Thauvin-Robinet et al. 2006, 2009). The most common craniofacial abnormalities of OFDS1 include hypertelorism, a broad nasal bridge, facial asymmetry, cleft palate, lingual hamartomas and hypodontia. CNS malformations frequently observed in this disorder include agenesis of the corpus callosum, abnormal gyration, grey matter heterotopia, cerebellar and brain stem abnormalities and intellectual disability. In a murine model system, knockout of *Ofd1* generates phenotypes highly reminiscent of the OFDS in humans, yet more severe. The craniofacial complex in *Ofd1* mutant mice is characterized by a shortened skull and facial region, cleft palate and exencephaly and defective cilia in various tissues (Ferrante et al. 2006).

## 5.7 Holoprosencephaly

The ***holoprosencephalies*** encompass a range of phenotypes that vary in severity and involve malformations of the brain and upper face among the midline (DeMyer et al. 1963, 1964; Cohen 1989a, b; Cohen and Sulik 1992; Norman et al. 1995; Golden 1998; Muenke and Beachy 2001; Cohen and Shiota 2002). HPE is aetiologically extremely heterogeneous. Its formation may depend on the interaction of both genetic and environmental factors. Specific teratogens such as maternal diabetes increase the risk for HPE 200-fold (Norman et al. 1995; Cohen and Shiota 2002). About 1–2 % of newborn infants of diabetic mothers develop HPE. Numerous other teratogens are known to cause HPE in various animal models (Cohen and Sulik 1992; Cohen and Shiota 2002). The incidence of HPE in live-born children with normal chromosomes has been estimated to be 0.48–0.88 per 10,000. In contrast, the rate among human abortions was estimated at 40 per 10,000, indicating a very high rate of embryonic and fetal loss (Matsunaga and Shiota 1977; Shiota 1993). In a large epidemiologic study in a Californian population, Croen et al. (1996) observed an overall prevalence of 1.2 per 10,000 live births and fetal deaths (121 HPE cases in 1,035,386 live births/fetal death deliveries), whereas the prevalence for live births was 0.88 per 10,000. In another perinatal study from Scotland, Whiteford and Tolmie (1996) found 50 HPE cases in 694,950 live births and stillbirths (a prevalence of 0.7 per 10,000).

Although the majority of HPE cases are sporadic, familial HPE has been described in pedigrees, suggesting autosomal dominant, autosomal recessive, and possibly X-linked inheritance. The clinical variability can be striking even within a single pedigree. In pedigrees with clinically unaffected parents and multiple affected siblings autosomal recessive inheritance is suggested. Since abnormal HPE genes are not fully penetrant and germ line mosaicism may happen, some of these cases may actually be autosomal dominant (Nanni et al. 1999). The causes of HPE in man are summarized in Table 5.4. Certain chromosomes, chromosome 13 in particular, display recurrent involvement in HPE. HPE may be present in as many as 70 % of trisomy 13 cases (Taylor 1968; Cohen and Sulik 1992; Norman et al. 1995). Cytogenetically verified chromosome abnormalities in perinatal studies range from 34 % in Scotland (Whiteford and Tolmie 1996) to 37 % in California (Croen et al. 1996). A similar frequency was observed in prenatally diagnosed HPE (Berry et al. 1990; Blaas et al. 2002). Cytogenetic studies of HPE patients suggest at least 13 different autosomal dominant loci (Roessler and Muenke 1998, 2010; Nanni et al. 2000; Bendavid et al. 2010; Table 9.10), giving rise to 15–20 % of all cases of HPE (Cohen and Shiota 2002). Several HPE genes have been identified: *SHH* (also known as HPE3: Belloni et al. 1996; Roessler et al. 1996; Nanni et al. 1999), *SIX3* (HPE2: Wallis et al. 1999; Domené et al. 2008), *ZIC2* (HPE5: Brown et al. 1998; Roessler et al. 2009), *TGIF* (HPE4: Gripp et al. 2000; El-Jaick et al. 2007), *Patched*/*PTCH* (Ming and Muenke 1998; Ming et al. 2002), *GLI2* (Roessler et al. 2003) and *NODAL* (Roessler et al. 2008). Of these defective genes in human HPE, three exhibit a ventrodorsal gradient of expression (*SHH*, *SIX3* and *TGIF*) and two a dorsoventral gradient (*GLI2* and *ZIC2*). Patients with HPE3 (*SHH*) and HPE2 (*SIX3*) mutations exhibit the HPE spectrum with major facial malformations ((Wallis et al. 1999), whereas *ZIC2* mutations show only minimal facial malformations, such as slanting of the frontal bones as a result of microcephaly (Brown et al. 1998). Heterozygous carriers for mutations in either *SHH* or *SIX3* can appear phenotypically normal, whereas other heterozygous mutation carriers within the same family may be severely affected (Nanni et al. 1999). Nanni and co-workers identified three HPE patients with an *SHH* mutation and an additional *ZIC2* or *TGIF* mutation. The first patient exhibited microcephaly due to semilobar HPE but with normal midfacial dimensions and, therefore, this corresponds best with the *ZIC2* phenotype. The other two cases showed major craniofacial abnormalities matching the *SHH* HPE spectrum. HPE may occur in a large number of syndromes and associations (Siebert et al. 1990; Cohen and Sulik 1992; Norman et al. 1995; see Table 5.4 for some examples). Syndromal (not chromosomal) conditions with HPE include such diverse

**Table 5.4** Aetiology of human holoprosencephaly

| Causes | Examples | Notes |
|---|---|---|
| Chromosomal abnormalities | Most frequently involved:<br>Chromosomes 13 and 18<br>Trisomy 13<br>Trisomy 18<br>Numerous deletions, duplications, and ring chromosomes | <br><br>In 70 % HPE (Taylor 1968)<br><br>Examples of deletions and duplications (in order of frequency): del(13)(q22), del(18p), del(7)(q36), dup(3)(p24-pter), del(2)(p21), del(21)(q22.3); for further data see Schinzel (1983), Cohen and Sulik (1992) and Norman et al. (1995) |
| Identified genes | *SHH* (HPE3)<br>*SIX3* (HPE2)<br>*ZIC2* (HPE5)<br>*TGIF* (HPE4)<br>*Patched/PTCH*<br>*GLI2*<br>*NODAL* | See text for explanation |
| Teratogens | Diabetic embryopathy<br>Ethyl alcohol (alcohol abuse)<br><br><br>Retinoic acid | HPE in 1–2 % of newborn infants of diabetic mothers<br>In 28 autopsies with HPE, Jellinger et al. (1981) found one case in which the mother had a history of alcohol abuse; Ronen and Andrews (1991) found HPE in 3 such cases<br>HPE has been noted (Lammer et al. 1985; Rosa et al. 1994) |
| Syndromes with HPE | Meckel syndrome<br>Pallister-Hall syndrome<br><br><br>Lambotte syndrome<br><br>Smith-Lemli-Opitz syndrome<br><br>Velocardiofacial syndrome<br>Aicardi syndrome | May have HPE with median or lateral cleft lip (Hsia et al. 1971)<br>Congenital hypothalamic hamartoblastoma hypopituitarism, other anomalies including HPE (Hall et al. 1980), due to mutations in *GLI3* (Kang et al. 1997)<br>Microcephaly, intellectual disability, ocular hypotelorism (Verloes et al. 1990)<br>Deficiency (DCHR7) in cholesterol biosynthesis (Kelley and Hennekam 2001)<br>HPE in 1 out of 61 cases (Wraith et al. 1985)<br>Flexion spasms, intellectual disability and agenesis of corpus callosum; arhinencephaly in several instances; rarely HPE (Sato et al. 1987; Donnenfeld et al. 1989) |
| Associations | Anencephaly<br>Frontonasal dysplasia<br>Agnathia-otocephaly | Cases with holoprosencephalic facies (Lemire et al. 1981)<br>Median cleft syndrome (DeMyer 1967; Sedano et al. 1970)<br>Cyclopia/HPE may occur (Pauli et al. 1983; Siebert et al. 1990) |

After Cohen and Sulik (1992), Norman et al. (1995), Blaas et al. (2002), Cohen and Shiota (2002)

disorders as Meckel-Gruber, Pallister-Hall, Smith-Lemli-Opitz and Aicardi syndromes. The ***Smith-Lemli-Opitz syndrome*** is due to a deficiency in the final step of cholesterol biosynthesis (Tint et al. 1994; Kelley et al. 1996; Kelley and Hennekam 2001; Chap. 3).

The **brain malformations** in HPE will be discussed in Chap. 9. In brief, forebrain malformations range from the ***alobar***, ***complete form*** with one single ventricle, undivided thalami and corpora striata, and absence of the olfactory bulbs and corpus callosum, to the ***semilobar***, ***incomplete form***, in which hypoplastic cerebral lobes with an interhemispheric posterior fissure and a hypoplastic corpus callosum may be present, to the ***lobar type***, in which a distinct interhemispheric fissure is present with some midline continuity and the olfactory bulbs may vary from normal to absent. HPE can be detected prenatally by ultrasound (Kurtz et al. 1980; Blaas et al. 2000, 2002; Clinical Case 5.2). In the California study (Croen et al. 1996), 46 % of HPEs were of the alobar type, 20 % semilobar and 5 % lobar.

The **facial anomalies** in HPE are usually categorized into four main types (DeMyer et al. 1964; Cohen and Sulik 1992; Figs. 5.20 and 5.21): (1) cyclopia with a single eye or various degrees of doubling of the eye anlage, with or without a proboscis; (2) ethmocephaly with ocular hypotelorism and proboscis located between the eyes; (3) cebocephaly with ocular hypotelorism and a single-nostril nose; and (4) median cleft lip and palate (premaxillary agenesis) and ocular hypotelorism. Less severe facial dysmorphism, microsigns such as a single central incisor and/or ocular hypotelorism, and HPE without facial malformations are also found (DeMyer et al. 1964; Cohen and Sulik 1992; Brown et al. 1998). Five out of the six cases shown in

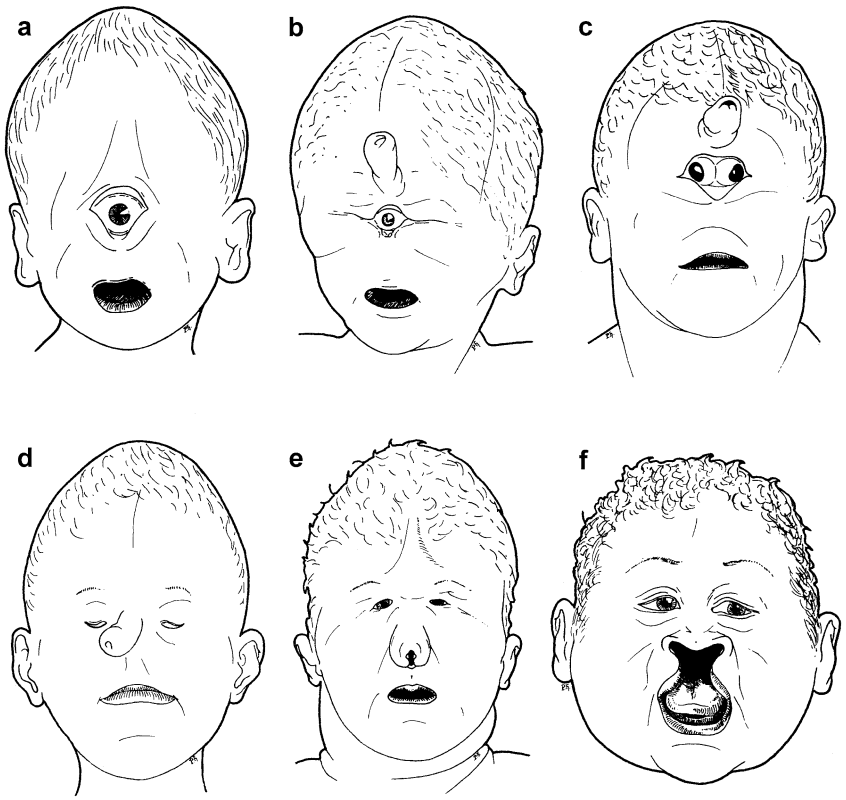


**Fig. 5.20** Holoprosencephaly, main types of facial malformation: (**a**) cyclopia; (**b**, **c**) single median eye with various degrees of doubling of ocular structures; (**d**) ethmocephaly; (**e**) cebocephaly; (**f**) median cleft lip with arhinencephaly (After Duhamel 1966)

Fig. 5.21 exhibited major facial malformations, varying from agenesis of the eyes to hypotelorism and were holoprosencephalic and, as a consequence, microcephalic. In these five cases the developing forebrain is too narrow, indicating a lack of outgrowth of the ventral neurectoderm during early embryogenesis (Müller and O'Rahilly 1989) and, as a consequence, insufficient EMT in presomite and early somite stages (Vermeij-Keers 1990). As a result the interplacodal area (the area between the nasal placodes) is either absent (resulting in agenesis of the eyes and orbits, cyclopia, synophthalmia, synorbitism, hypotelorism without a nasal septum) or too narrow (hypotelorism with a nasal septum). During normal embryonic development, both medial nasal processes grow out from the interplacodal area, and give rise to the premaxilla, the prolabium, the vomer and other parts of the nasal septum. The mesectoderm of this area originates from the cranial neural crest and surface ectodermal placodes (Smits-van Prooije et al. 1988).

The embryological background of HPE cases with major facial malformations is an abnormally narrow prosencephalon, particularly along its ventral midline, causing agenesis or non-separation of the eye primordia, non-separation of the thalami and lack of proper outgrowth of the telencephalic hemispheres, leading to agenesis of the olfactory bulbs and the corpus callosum. This is in keeping with experimental studies in animals on the teratogenic effects of drugs and other chemicals (Cohen and Sulik 1992; Cohen and Shiota 2002) and data from mice lacking *Shh* (Chiang et al. 1996). *Shh* expression has been detected in the mouse prechordal plate and the ventral neuroectoderm. In chick embryos, *Shh* expression in the ectoderm of the craniofacial primordia is essential for outgrowth of the facial swellings (Helms et al. 1997; Hu and Helms 1999). Moreover, *Six3* participates in midline forebrain and eye formation (Bovolenta et al. 1996). In contrast, in mice *Zic2* is expressed along the dorsal neuroectoderm up to the rostral end of the future telencephalon, and reduction of *Zic2* expression causes a neurulation delay and inhibition of EMT, which results in HPE and various neural tube defects (Nagai et al. 1997, 2000). These different expression patterns, *Shh* and *Six3* in the ventral neuroectoderm and *Zic2* in the dorsal neuroectoderm, suggest that these genes affect the outgrowth and differentiation of the forebrain in different ways. Mutations of genes expressed dorsally in the neural tube give rise to either inappropriate division of the prosencephalon into cerebral hemispheres with agenesis of the telencephalic roof plate, resulting in HPE with normal midfacial dimensions (Brown et al. 1998; Fig. 5.21f), or defects in the fusion process of the prosencephalic neural walls, causing exencephaly and anencephaly (Nagai et al. 2000).


**Fig. 5.21** Holoprosencephaly, spectrum of craniofacial malformations. (**a**) Alobar or complete holoprosencephaly was diagnosed by ultrasound at 22 weeks of gestation, after which pregnancy was terminated at 24 weeks. At autopsy, the female fetus showed agenesis of both eyes and orbits, arhinia and microstomia. (**b**) Frontal view of a cyclopic face of a female fetus of approximately 35 weeks of gestation. The fetus had a single eye in a single orbit and fused optic nerves, arhinia without proboscis, and agnathia with astomia and synotia. The brain showed a complete holoprosencephaly. (**c**) Frontal view of a male fetus of 32 weeks of gestation with synorbitism, arhinia with proboscis, agnathia with astomia and synotia. The brain showed a semilobar or incomplete holoprosencephaly with a dorsal sac (Chap. 9). (**d**) Frontal view of a female fetus of 32 weeks gestation with hypotelorism, arhinia with a septated proboscis, agnathia with astomia and synotia. The brain showed an incomplete holoprosencephaly. (**e**) A hypoteloric male fetus of 34 weeks of gestation with a flat nose, cleft palate and agenesis of the premaxillae, the prolabium and the nasal septum. An incomplete holoprosencephaly was found. (**f**) A case of alobar, complete holoprosencephaly with a normal face (**a** Courtesy Annemarie Potters, Deventer; **b–e** from the collection of the Museum of Anatomy, University of Leiden; courtesy Christl Vermeij-Keers; **f** courtesy Raoul Hennekam)

## Clinical Case 5.2. Alobar Holoprosencephaly

***Alobar holoprosencephaly*** (***HPE***) and other forms of HPE can be detected prenatally by ultrasound. Blaas et al. (2000) presented a case of alobar HPE with cyclopia in an embryo with a gestational age of 9 weeks and 2 days with a crown-rump length (CRL) of 22 mm. Three-dimensional ultrasound improved the imaging (see Case Report).

**Case Report**. An 31-year-old gravida 6 para 1 was referred to a university hospital because of habitual abortion. Her husband had a balanced chromosomal translocation (46, XY, t(8;14)(p21.1;q24.1). At the first examination at the gestational age of 9 weeks and 2 days, ultrasound examination showed an embryo of 22-mm CRL with abnormal development of the brain with a small monoventricular forebrain (Fig. 5.22a) and a proboscis (Fig. 5.22b). Seven days later, CRL was 33 mm (Fig. 5.22d). Three-dimensional reconstructions were made from both examinations (Fig. 5.22c, g). The body, including the proboscis and the brain cavities, were outlined by manual segmentation and given different colours. Two eye anlagen, lying closely together below the proboscis, could be identified

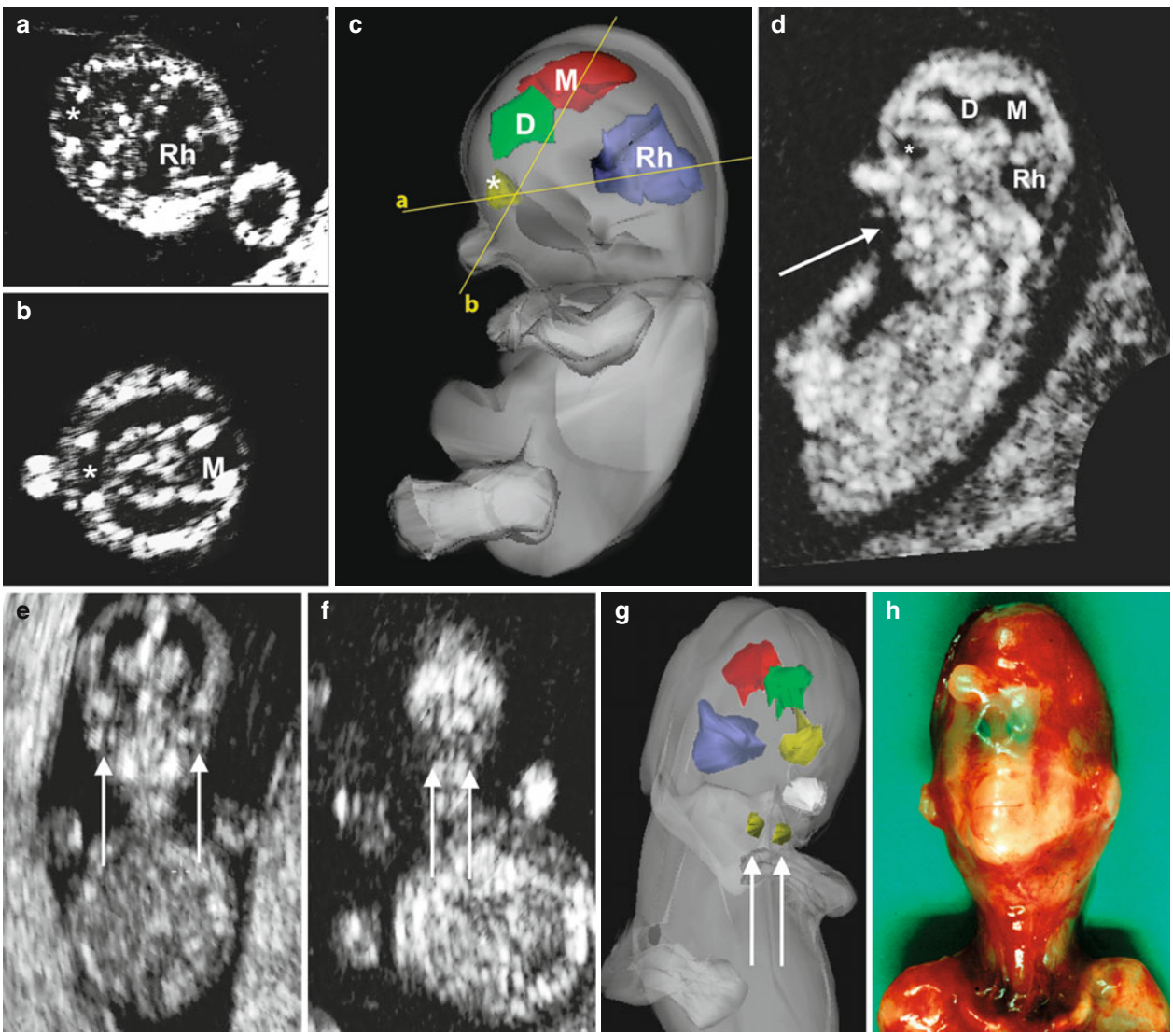


**Fig. 5.22** Alobar holoprosencephaly at 9 weeks of gestation visualized by two- and three-dimensional ultrasound: (**a**–**c**) ultrasound sections showing the non-separation of the forebrain (*asterisks* in **a** and **b**) of the 9-week and 2-day-old embryo (crown-rump length, *CRL*, 22 mm), and three-dimensional reconstruction of the embryo with volume presentation of body and brain cavities (**c**); (**d**) three-dimensional reconstruction 7 days later, the *arrow* points at the cyclopia; (**e**) coronal section through the face of a normal fetus (CRL 30 mm), showing the normal hypertelorism of the eyes (*arrows*) at that age; (**f**) fetus with holoprosencephaly (CRL 33 mm) with the two eye anlagen lying close together (*arrows*); (**g**) three-dimensional reconstruction of the same fetus with the holosphere (*yellow*) and the cavities of the diencephalon (*D*, *green*), the mesencephalon (*M*, *red*) and the rhombencephalon (*Rh*, *blue*), and the eye anlagen (*yellow*, *arrows*); (**h**) postabortem photograph of the fetus with cyclopia, two eye anlagen and a proboscis (Reproduced with permission from Blaas et al. (2000); copyright 2000, John Wiley & Sons Ltd.)

at 10 weeks of gestation (Fig. 5.22f). There was a small monoventricular holosphere, connected to the diencephalon by a narrow duct (Fig. 5.22c, d, f). Chorion villus biopsy at 10.5 weeks revealed the same balanced translocation as that of the father. The patient was informed about the diagnosis of alobar HPE at the first visit. With the informed consent of the patient, the pregnancy continued until 12.5 weeks of gestation before it was terminated. This was done to confirm the diagnosis by ultrasound, by karyotyping and by postabortem autopsy. The autopsy confirmed the diagnosis of alobar HPE, associated with cyclopia with two eye anlagen, a proboscis and a small monoventricular holosphere (Fig. 5.22h).

This case was kindly provided by Harm-Gerd Blaas (Trondheim).

### References

Blaas H-GK, Eik-Nes SH, Berg S, Torp H (1998) *In-vivo* three-dimensional ultrasound reconstructions of embryos and early fetuses. Lancet 352:1182–1186

Blaas H-GK, Eik-Nes SH, Vainio T, Isaksen CV (2000) Alobar holoprosencephaly at 9 weeks gestational age visualized by two- and three-dimensional ultrasound. Ultrasound Obstet Gynecol 15:62–65

## 5.8 Abnormal Development of the Skull with CNS Manifestations

Developmental defects of the cranial vault and face are relatively common, such is the case in craniosynostoses, whereas congenital defects of the skull base and sensory capsules (nasal and otic) are relatively rare (Sperber 2002). During postnatal growth of congenital craniofacial defects, three general patterns of development may occur: maintenance of the defective growth pattern; catch-up growth, minimizing the defect; or marked worsening of the derangement with increasing age. Of great significance to facial development is the normal closing of the **foramen caecum** in the anterior cranial fossa at the fronto-ethmoid junction (Hoving 1993). Abnormal patency of this foramen, due to non-separation of the neuroectoderm and surface ectoderm during neural tube formation, allows a pathway for neural tissue to herniate into the nasal region, providing the basis of encephaloceles, gliomas and dermoid cysts that cause gross disfigurement of facial structures.

### 5.8.1 The Craniosynostoses

With the ongoing ossification of the calvarial bones during embryogenesis, sutures normally arise at the sites were the osteogenic fronts of the respective bone centres come into close contact. In human fetuses, the first onset of the metopic suture is seen at 15 weeks of gestation, the coronal suture and lambdoid suture at 16 weeks, and the sagittal suture at 18 weeks of gestation (Mathijssen et al. 1999). From this point on, suture development gradually spreads in cranial and caudal direction.

***Craniosynostoses*** are caused by agenesis or premature ossification of one or more of these cranial sutures (Mathijssen et al. 1996). They are the most common developmental disorders of the skull vault, affecting 1 in 2,100–2,500 individuals (Selber et al. 2008; Kweldam et al. 2011). Agenesis and premature closure of calvarial sutures causes the cessation of skull growth in the direction perpendicular to that of the affected suture. In suture agenesis, direct fusion of bone centres takes place at sites where normally sutures arise. This can be observed in isolated and syndromic forms of craniosynostosis, for example in scaphocephaly and Apert syndrome, respectively. In an Apert mouse model (Holmes et al. 2009) a similar observation was made as in a human Apert skull (Mathijssen et al. 1996); the first fusion of the coronal suture was seen at the initial site of contact between the parietal and frontal bones, whereas cranial and caudal to this site a patent coronal suture was present. This contact seems to indicate true agenesis of the suture due to direct fusion of the parietal and frontal bone centres, whereas most part of the suture does develop normally, only to close prematurely shortly afterwards, from the site of fusion in cranial and caudal direction. Likewise, the peripheral parts of the coronal sutures are still visible in most young patients with Apert syndrome but ossify rapidly. The timing of this type of craniosynostosis can be traced back to the time of suture initation, as mentioned before (Mathijssen et al. 1999).

In isolated craniosynostoses no other congenital malformations are present and usually only one suture is closed, whereas craniosynostosis in syndromic cases is accompanied by other anomalies and usually involves more sutures. Non-syndromic craniosynostosis is more frequent than syndromic forms. Sagittal synostosis is the most common of the non-syndromic synostoses (birth prevalence: 1 in 5,000), followed by metopic synostosis (Muenke and Wilkie 2001; Van der Meulen et al. 2009). Depending on which of the sutures is closed prematurely and at what starting time, the skull develops a characteristic shape (Fig. 5.23). The diagnosis of craniosynostosis syndromes is mainly by clinical examination of the presenting craniofacial features. ***Trigonocephaly*** results from premature closure of the metopic suture and causes a triangular shaped forehead with temporal depressions and hypotelorism. ***Scaphocephaly*** (or ***dolichocephaly***)

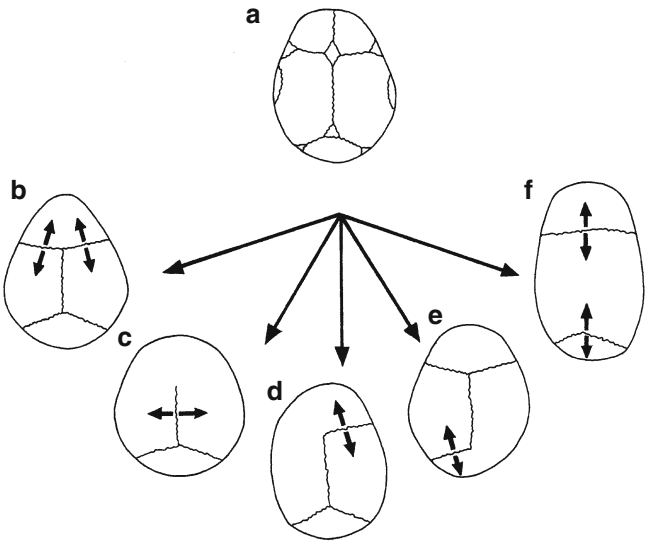


**Fig. 5.23** Premature ossification of the cranial sutures leads to an abnormal head shape: (**a**) normal skull; (**b**) trigonocephaly; (**c**) brachycephaly; (**d**) anterior plagiocephaly; (**e**) posterior plagiocephaly; (**f**) dolichocephaly (After Cohen and MacLean (2000))

occurs after premature closure of the sagittal suture, resulting in a narrow and elongated skull with bossing of the forehead, an occipital bullet and a palpable ridge over the ossified sagittal suture. Unilateral coronal synostosis gives rise to ***anterior plagiocephaly***, with retrusion of the ipsilateral supraorbital rim and forehead and upward displacement of the involved orbit. Synostosis of both coronal sutures leads to a broad skull with retrusion of the supraorbital rim (***brachycephaly***). Premature closure of a lambdoid suture (***posterior plagiocephaly***) is very rare and causes a displacement of the ipsilateral posterior skull base with caudal displacement of the ear and mastoid, and facial scoliosis. Complex synostosis, in which two or more sutures are involved, can lead to various head shapes depending on the involved sutures, including the most severe skull deformity the cloverleaf (*Kleeblattschädel*) malformation found in thanatophoric dysplasia and severe presentation of Crouzon/Pfeiffer syndrome. ***Pansynostosis*** describes the premature closure of all sutures and this usually does not cause a change in head shape but is likely to induce a decline in growth of the head circumference and increased intracranial pressure. The only clue that may be present on clinical examination is a bulge of the skull at the site of the former anterior fontanel; as this is the last part of the skull to ossify, the brain utilizes this last resort for its expansion. Pansynostosis is particularly common in Crouzon syndrome.

Craniosynostosis is associated with increased intracranial pressure (ICP), with a suture specific risk of approximately 12 % for sagittal synostosis, 9 % for metopic synostosis and 10 % for unicoronal synostosis (Renier et al. 1982; 2000; Gault et al. 1992; Thompson et al. 1995; Mathijssen et al. 2006; Florisson et al. 2010). These percentages may rise significantly with postponing surgery beyond the age of 1; reducing these risks on elevated ICP is the main goal of surgery by expanding the intracranial volume. The risk on elevated ICP is much higher for syndromic craniosynostosis and is estimated to be 83 % for Apert syndrome (Marucci et al. 2008), 50–70 % for Crouzon syndrome (Thompson et al. 1995; De Jong et al. 2009) and 20–35 % for Saethre-Chotzen syndrome (Kress et al. 2006; De Jong et al. 2009; Woods et al. 2009). Muenke syndrome appears to be the exception with a risk of only 5 % (Kress et al. 2006; De Jong et al. 2009). Other associated malformations in syndromic craniosynostosis are ventriculomegaly (non-progressive enlargement of the cerebral ventricles), Chiari I malformation (herniation of the cerebellar tonsils below the foramen magnum of more than 5 mm), impaired vision and hearing, obstructive sleep apnea, behavioural disturbances, facial deformities such as exorbitism, midface hypoplasia and upper eyelid ptosis, and anomalies of the hand and feet.

In general, no genetic causes for isolated sagittal or metopic suture synostosis are found, although a recent publication showed copy number variations or mutations in the *FREM1* gene in eight out of 109 patients with metopic suture synostosis (Vissers et al. 2011). However, six of these eight patients demonstrated midface hypoplasia, suggesting that these patients do not represent a true isolated craniosynostosis. In a large genome-wide association study on 130 patients with isolated sagittal suture synostosis and their parents, a robust association was found with *BMP2* and *BBS9* genes that are involved in skeletal development (Justice et al. 2012). By contrast, an increasing number of genes involved in craniosynostosis syndromes are recognized and listed in Table 5.5.

The ***classic craniosynostosis syndromes*** are inherited as autosomal dominant traits and include Apert (ligand-independent Ser252Trp or Pro253Arg fibroblast growth factor receptor (*FGFR2*) mutations), Saethre-Chotzen (*TWIST1* mutation or deletion), Crouzon/Pfeiffer (ligand-dependent *FGFR2* mutations and rarely of *FGFR1* or F*GFR3*) and Muenke syndromes (P250R *FGFR3* mutation) (Figs. 5.24, 5.25 and 5.26). The *FGFR* mutations are gain of function mutations, whereas those in *TWIST1* are loss of function mutations. Many de novo *FGFR* mutations encode highly recurrent missense substitutions, which arise exclusively from the father and are associated with increased paternal age (Glaser et al. 2000; Goriely and Wilkie 2012; Rannan-Eliya et al. 2004). Crouzon and Pfeiffer syndromes can be associated with exactly the same mutations in *FGFR2* gene, indicating that they probably represent a variance of phenotype rather than two separate disorders.

The coronal synostosis is most likely to be affected in syndromic cases of craniosynostosis. The reason for this is probably related to the fact that the coronal suture develops

**Table 5.5** Overview of the more common syndromic craniosynostoses

| Craniosynostosis syndrome/OMIM number | Main features | Involved sutures | Inheritance | Gene defect |
|---|---|---|---|---|
| Apert syndrome/101200 | Intellectual disability, midface deficiency, proptosis, down-slanting palpebral fissures, complex symmetrical syndactyly of hands and feet (either of digits I–V or II–IV) | Bilateral coronal sutures | AD (most cases new mutations) | *FGFR2* |
| Crouzon syndrome/123500 | Midface hypoplasia, exorbitism, ventriculomegaly, Chiari I | Bilateral coronal, then all sutures; may have a postnatal onset | AD | Mainly *FGFR2* (Reardon et al. 1994); *FGFR3* (Meyers et al. 1995); very seldom *FGFR1* (Muenke et al. 1994) |
| Pfeiffer syndrome/101600 | Severe presentation of Crouzon syndrome, often with broad thumbs and toes is frequently referred to as Pfeiffer syndrome | | | |
| Saethre-Chotzen syndrome/101400 | Low-set frontal hairline, ptosis, variable brachydactyly and cutaneous syndactyly | Coronal, uni- or bilateral | AD | *TWIST1 (*Howard et al. 1997; El Ghouzi et al. 1997) |
| Muenke syndrome/602849, 600593 | Macrocephaly, uni- or bicoronal synostosis, temporal widening, brachydactyly, behavioural disturbances | None, uni- or bicoronal synostosis | AD | *P250R FGFR3* (Muenke et al. 1997) |
| Boston type craniosynostosis/12310.001 | Variable craniosynostosis; supraorbital recession; short first metatarsals | | AD | *MSX2* (Jabs et al. 1993) |
| Beare-Stevenson syndrome/123790 | Variable craniosynostosis, cutis gyrata, acanthosis nigricans | | Usually sporadic mutations | *FGFR2* (Przylepa et al. 1996) |
| Craniofrontonasal syndrome | Hypertelorism, orbital dystopia, bifid nose, ridging of nails | Uni- or bicoronal synostosis | AD | *EFNB1* (Twigg et al. 2004) |
| TCF12 | Appears to be isolated | Uni- or bicoronal synostosis | | *TCF12* (Sharma et al. 2013) |
| ERF | Mild midface hypoplasia and exorbitism, behavioural or learning disabilities, Chiari I | Complex synostosis | | *ERF* (Twigg et al. 2013) |
| Carpenter syndrome | Obesity, polydactyly, syndactyly, brachydactyly, molar agenesis, hypogenitalism, cardiac defects, learning disability | Metopic and sagittal synostosis | AR | *RAB23* (Jenkins et al. (2007); *rarely MEGF8* (Twigg et al. 2012) |
| Greig syndrome | Polydactyly, syndactyly | Metopic synostosis | AD | *GLI3* (McDonald-McGinn et al. 2010) |
| IL11RA | Maxillary hypoplasia, delayed tooth eruption, supernumerary teeth | All sutures affected with variable skull shapes | AR | *IL11RA* (Nieminen et al. 2011) |

between the frontal bone and the parietal bone which have a different origin, being derived from neural crest and mesoderm, respectively. Within the centre of the sutures a population of undifferentiated cells maintain the patency of the suture by proliferation, whereas growth of the bone plates is provided by osteogenic differentiation at their periphery (Morriss-Kay and Wilkie 2005). In mice, *twist1* is expressed in mesenchymal cells within the area of the coronal suture even before suture development begins (Rice et al. 2000). TWIST1 expression precedes the FGFR expression, and FGFRs are particularly expressed at the bony edges of the frontal and parietal bones (Johnson et al. 2000). The *TCF12* gene was recently discovered to be involved in coronal suture synostosis and its protein acts synergistically with TWIST1 (Sharma et al. 2013). FGFRs and their ligands are involved in controlling the levels of cell proliferation and differentiation


**Fig. 5.24** Dysmorphology of the head in Apert (**a**, **b**), Crouzon (**c**, **d**), and Pfeiffer (**e**, **f**) syndromes (Courtesy Michiel Vaandrager, Rotterdam)

(Iseki et al. 1999). In a mouse model with the Apert mutation Ser252Trp in FGFR2 it was demonstrated that expression of the mutation in only mesoderm was sufficient to cause craniosynostosis, whereas expression in just the neural-crest derived cells did not (Holmes and Basilico 2012). This study also excludes suggested etiological roles for the dura mater and skull base changes in craniosynostosis. The activating FGFR2 mutation in this mouse model particularly seems to allow the recruitment of osteoprogenitor cells at the site of suture initiation, thus causing fusion of the approaching bones (Holmes et al. 2009). The more common syndromic craniosynostoses will be briefly discussed.

***Apert syndrome*** or acrocephalosyndactyly (Apert 1906) is characterized by bilateral coronal suture synostosis (Fig. 5.24a, b) and an enlarged anterior fontanel that extends in between the frontal bones up to the nasal bones at birth, exorbitism, hypertelorism, strabismus, midfacial hypoplasia, and symmetrical complex syndactyly of the hands and feet (Cohen and Kreiborg 1993, 1995). Intellectual disability is common and often severe. Conductive hearing loss is frequent. Non-progressive ventriculomegaly and agenesis of the corpus callosum are common CNS malformations (Cohen and Kreiborg 1990; Clinical Case 5.4). Almost all cases with Apert syndrome are associated with either of two *FGFR2* mutations, Ser252Trp or Pro253Arg (Park et al. 1995; Wilkie et al. 1995). Rare genetic causes of Apert are a 1.93 kb deletion and a 5′ truncated Alu insertion in FGFR2 (Bochukova et al. 2009).

**Fig. 5.25** Dysmorphology of the head in Saethre-Chotzen syndrome with a *TWIST* mutation (Courtesy I. Marieke de Heer, Rotterdam)

***Crouzon syndrome*** (Crouzon 1912; Kreiborg 1981) is characterized by bicoronal craniosynostosis in which eventually all calvarial sutures can be involved (Fig. 5.24c, d). At birth, the sutures can still be patent with pansynostosis occurring in the first few years of life. Other characteristic findings are midfacial hypoplasia, exorbitism, hypertelorism and unaffected limbs or broad thumbs and halluces. Crouzon syndrome is most commonly caused by mutations in the *FGFR2* gene (Jabs et al. 1994; Reardon et al. 1994; Passos-Bueno et al. 1999). ***Pfeiffer syndrome*** (Pfeiffer 1964; Cohen 1993) appears to be the severe presentation of similar FGFR2 mutations and this diagnosis is particularly used in patients with a cloverleaf skull and/or patients with broad thumbs and halluces. Patients with Crouzon syndrome are particularly at risk for developing Chiari I malformation.

Typical characterics of the ***Saethre-Chotzen syndrome*** (Saethre 1931; Chotzen 1932) are bilateral coronal synostosis (Fig. 5.25), hypertelorism, unilateral or bilateral ptosis of the upper eyelids, low-set hairline, hearing loss, brachydactyly and soft tissue syndactyly. Saethre-Chotzen syndrome has been linked to the *TWIST1* gene on chromosome 7p21.1. Mutations in and variably sized deletions of this gene can be found in patients with clinical features of Saethre-Chotzen syndrome. The clinical spectrum of genetic abnormalities of the *TWIST1* gene is highly variable. In a large five-generation family with characteristics of Saethre-Chotzen syndrome as well as of the blepharophimosis-ptosis-epicanthus inversus syndrome, only two patients of the family had craniosynostosis (de Heer et al. 2004). *TWIST1* deletions often also include part of the surrounding chromosome 7p and, patients with large *TWIST* deletions may suffer from mental retardation, de Heer et al. (2004). Distinction with Muenke syndrome may be difficult based on phenotype and also a resemblance with TCF12 related craniosynostosis occurs. Before the discovery of the P250R mutation in FGFR3 gene (Muenke et al. 1997), most patients with Muenke syndrome were clinically classified as Saethre-Chotzen syndrome. ***Muenke syndrome*** is characterized by an enlarged skull without synostosis or with unicoronal or bicoronal synostosis, and a rather high incidence of disturbed behaviour.

***Craniofrontonasal syndrome*** is an X-linked disorder that is often associated with coronal synostosis, hypertelorism, and ridging of the nails (Cohen 1979; Gorlin et al. 2001). Its genetic cause is found in loss of function mutations in *EFNB1* (Twigg et al. 2004; Twigg et al. 2006; Wallis et al. 2008). Males are usually only mildly affected with hypertelorism. Proving the presence of an EFNB1 mutation may be hampered because of mosaicism.

Infants suffering from ***thanatophoric dwarfism*** or ***dysplasia*** usually die shortly after birth, at least partially because of respiratory insufficiency. The patients show severe skeletal abnormalities, including a form of craniosynostosis with trilocular configuration of the skull

known as cloverleaf skull (*Kleeblattschädel*) and typical facial dysmorphology (Clinical Case 5.5). Temporal lobe abnormalities are a consistent abnormality (Knisely and Ambler 1988; Norman et al. 1995). Mutations in *FGFR3* have been described by Tavormina et al. (1995); Clinical Case 5.5.

## Clinical Case 5.3. Prenatal Diagnosis of Apert Syndrome

Prenatal diagnosis of ***Apert syndrome***, including amniocentesis with confirmation of the gene mutation is rare, as many cases are not diagnosed until delivery. The best diagnostic clue on ultrasonography is an abnormal calvarial shape with severe syndactyly of hands and feet. Frontal bossing with midfacial hypoplasia in combination with polyhydramnios are findings that become more prominent later in pregnancy. Most prenatally detected cases of Apert syndrome were reported in the third trimester since the craniofacial and digital abnormalities and polyhydramnios associated with Apert syndrome are then more obvious (Athanasiadis et al. 2008; Pooh 2009). A recent case is shown as Case Report.

**Case Report**. The non-consanguineous parents, the mother 37 years of age, the father 45, already have a healthy boy. During routine 20-weeks pregnancy ultrasonography elsewhere, no congenital abnormalities were found. When positive dyscongruence was noticed at 28 weeks, an ultrasound was made to evaluate growth. Macrosomia was confirmed, but also enlarged cerebral ventricles were seen (Fig. 5.26). At 29 weeks and 5 days, amniocentesis was performed and the tests revealed a *pSer252Trp FGFR2* mutation, indicating Apert syndrome. Delivery was scheduled at a children's hospital given the high risk of obstructive sleep apnea. After induction of labour at 38 weeks, a boy was born with somewhat atypical craniofacial features for Apert syndrome. Besides the bilateral coronal suture synostosis, the metopic suture was also closed prematurely, resulting in hypotelorism instead of the usually encountered hypertelorism. Midface hypoplasia with exorbitism was marked and complex syndactyly of both hands and feet was present. At the age of 2 months, papilledema was detected through fundoscopy and the boy developed epilepsy. MRI showed a normal corpus callosum and hypoplasia of the septum pellucidum.

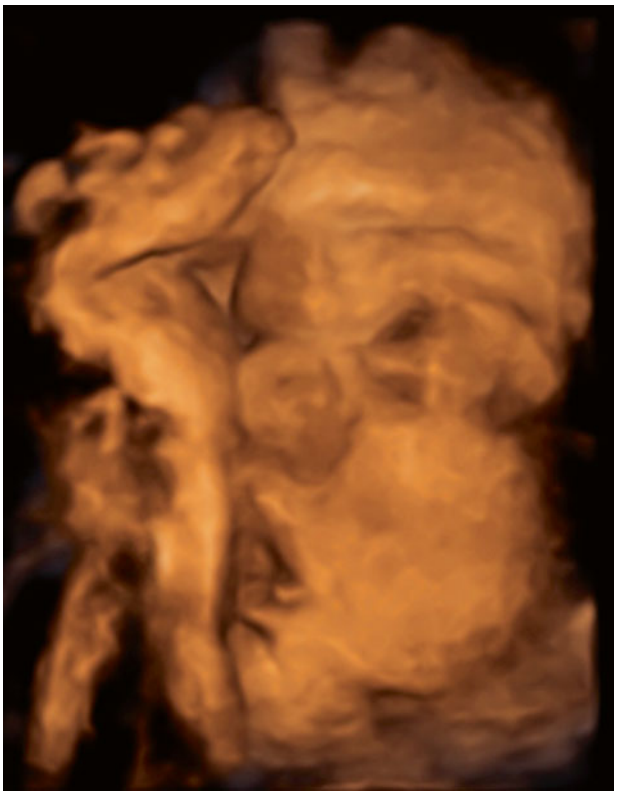

**Fig. 5.26** 3D-Ultrasonography at 36 weeks of gestation, showing an abnormal calvarial shape, exorbitism and complex syndactyly of the hand (Courtesy Remke Dullemond, Rotterdam)

This case was kindly provided by Remke C Dullemond (Rotterdam).

## References

Athanasiadis AP, Zafrakas M, Polychronou P, Florentin-Arar L, Papasozomenou P, Norbury G, Bontis JN (2008) Apert syndrome: the current role of prenatal ultrasound and genetic analysis in diagnosis and counseling. Fetal Diagn Ther 24:495–498

Pooh RK (2009) Neuroscan of congenital brain abnormality. In: Pooh R, Kurjak A (eds) Fetal Neurology. Jaypee, St Louis, pp 59–139

## Clinical Case 5.4. Apert Syndrome

***Apert syndrome***, described by Apert (1906) as acrocephalosyndactyly, is characterized by bilateral coronal suture synostosis, related skull malformations, intellectual disability, complex syndactyly of the hands and feet, and frequently deafness and optic atrophy (Apert 1906; Cohen and Kreiborg 1995). The most frequently associated cerebral malformations are hypoplasia of the corpus callosum and the septum pellucidum, and ventricular enlargement (Cohen and Kreiborg 1990; see Case Report).

**Case Report**. After an uneventful pregnancy, a boy was born as the seventh child in a family with six healthy children. He was born at term with a birth weight of 3,724 g. He had a dysmorphic head with a prominent forehead, retraction of the glabella and upper nose bridge, midfacial hypoplasia and low-implanted ears. There was bilateral choanal atresia. The posterior part of the head was flat with a broad neck. There was symmetric complex syndactyly of the fingers 2–5 of the hands and of toes 1–5. The boy died from severe cardiorespiratory failure due to the following complex malformations of the heart: abnormal venous return of systemic vessels with a persistent left vena cava superior draining through the coronary sinus into the right atrium; hypoplasia of the left ventricle and aorta; bicuspid aortic valve; aortic coarctation, and a persistent patent ductus arteriosus. Head circumference was 36.5 cm (P50) with a shorter-than-normal anteroposterior diameter. This was reflected in a shortened brain with relatively small parieto-occipital lobes (Fig. 5.27a). There was partial agenesis of the corpus callosum, the posterior part of which was absent. Moreover, the septum pellucidum was absent. The pyramids were hypoplastic, and were flanked by rather large, somewhat plump inferior olives (Fig. 5.27b).

This case was kindly provided by Pieter Wesseling (Nijmegen).

## References

Apert E (1906) De l'acrocéphalosyndactylie. Bull Soc Méd (Paris) 23:1310–1330

Cohen MM Jr, Kreiborg S (1990) The central nervous system in the Apert syndrome. Am J Med Genet 35:36–45

Cohen MM Jr, Kreiborg S (1995) Hands and feet in the Apert syndrome. Am J Med Genet 57:82–96

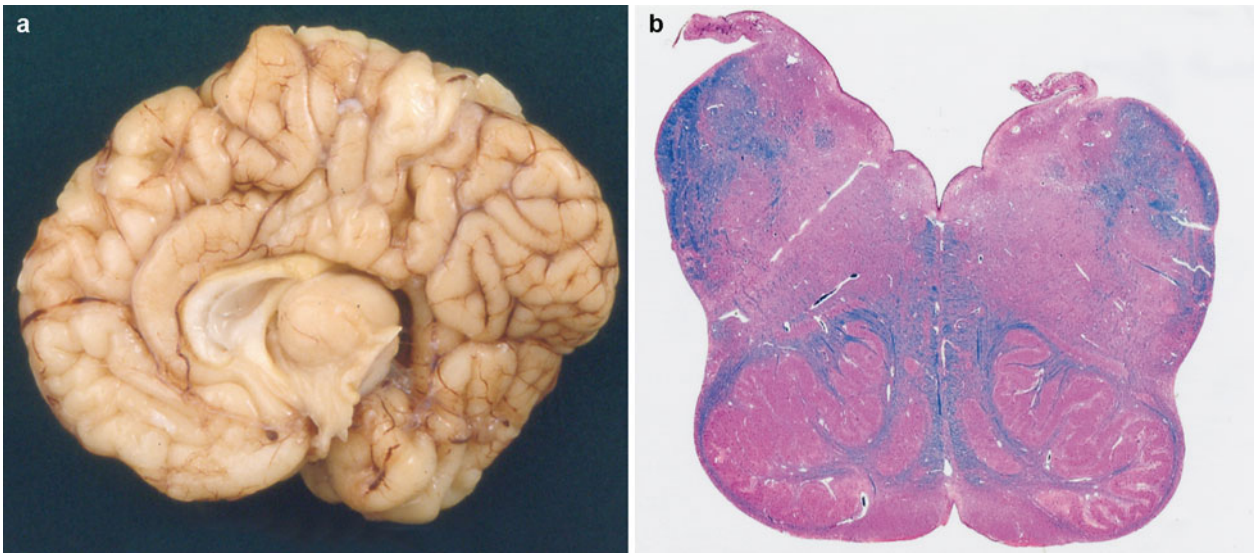


**Fig. 5.27** Apert syndrome: (**a**) medial view of the brain, showing the short anteroposterior diameter of the brain, a relatively small parietal-occipital lobe, incomplete corpus callosum, and absent septum pellucidum; (**b**) Luxol Fast Blue stained section through the medulla oblongata, showing large inferior olives and hypoplastic pyramids (Courtesy Pieter Wesseling, Nijmegen)

## Clinical Case 5.5. Thanatophoric Dysplasia

***Thanatophoric dysplasia*** is the most common form of lethal skeletal dysplasia. The name is derived from the Greek *thanatus* (death) and *phorus* (seeking). Holtermüller and Wiedemann (1960) described a form of craniosynostosis with trilocular configuration of the skull and severe internal hydrocephalus as '*Kleeblattschädel*' (cloverleaf skull) as an isolated anomaly but also in combination with generalized skeletal dysplasia. Different mutations at the FGFR3 locus give rise to distinct phenotypes (Cohen 1997; Hall and Lopez-Rangel 1997; Itoh et al. 2013). Abnormalities in the CNS mainly affect the temporal lobe. A fetus and a newborn are shown as Case Reports.

**Case Reports**:

**Case 1**: Fetal ultrasonography at the 18th week of gestation revealed the presence of thanatophoric dysplasia with characteristic bone features (Fig. 5.28a, b). The female fetus was stillborn at the 21st week of gestation, showing marked shortening of the long bones, a small

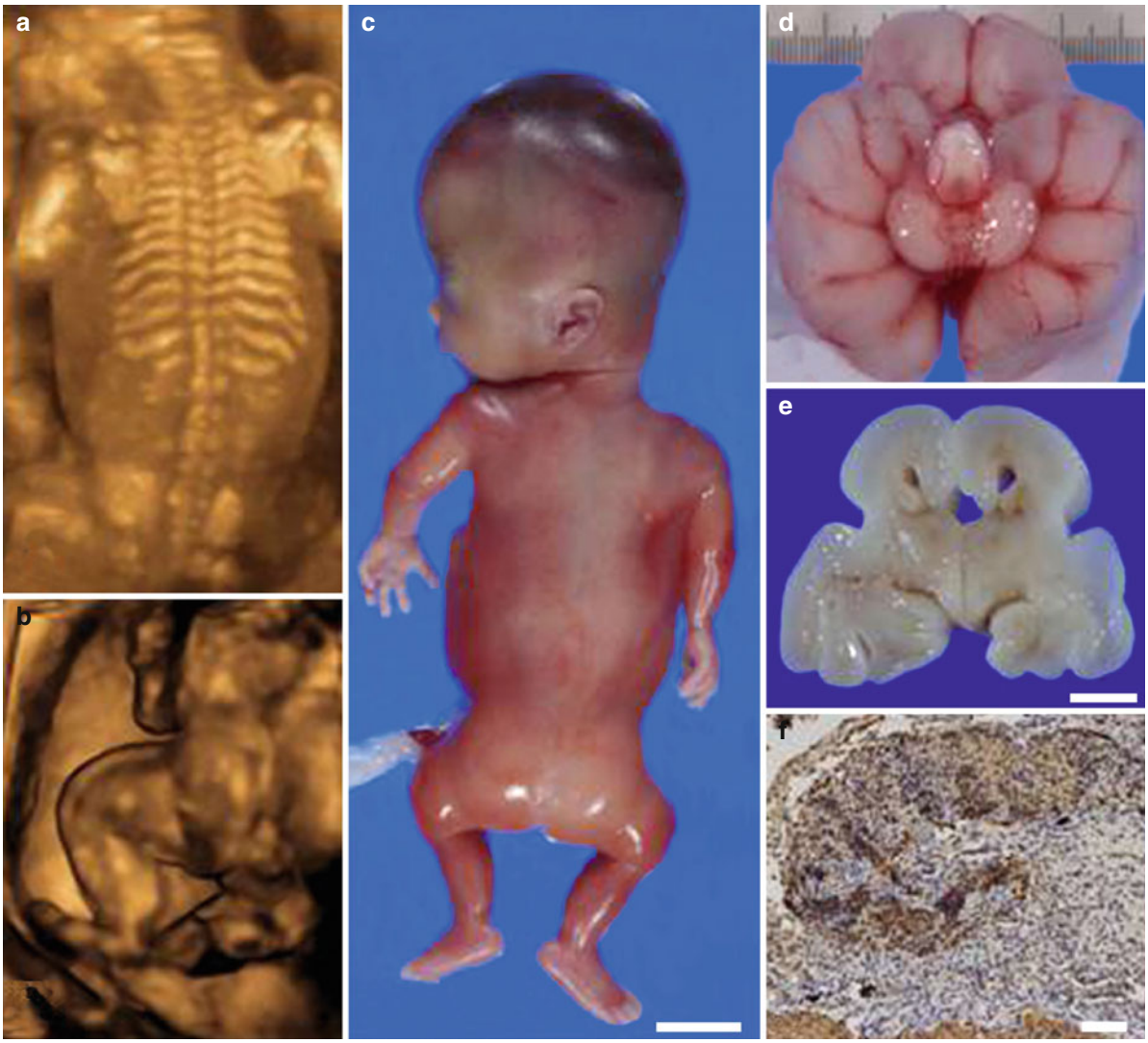


**Fig. 5.28** A fetal case of thanatophoric dysplasia: (**a**, **b**) 3D-ultrasonography of the fetal body at the 18th week of gestation, showing relatively short vertebral size (**a**) and curved and short femurs (**b**); (**c**) macroscopic features at the 21st week of gestation with marked shortening of the long bones, a small thorax and curved short femurs but without a cloverleaf skull; (**d**) macroscopy of the brain; (**e**) a series of coronal sections of the brain; the right temporal lobe was enlarged and hyperconvoluted with broad gyri and deep sulci; (**g**) abnormal gyri of the right temporal cortex and dysplastic hippocampus, showing polymicrogyria and small nests of heterotopia; (**f**, **h**) hippocampal dysplasia (**h**) and subarachnoidal heterotopia in the entorhinal cortex (**f**; doublecortin immunohistochemistry); (**i**) temporal lobe showing heterotopic neuronal nest and a thick subventricular zone immunoreactive for Ki-67; the scale bars are 2 cm (**c**), 1 cm (**e**), 80 µm (**f**), 300 µm (**h**) and 600 µm (**i**), respectively (Courtesy Kyoko Itoh, Kyoto)

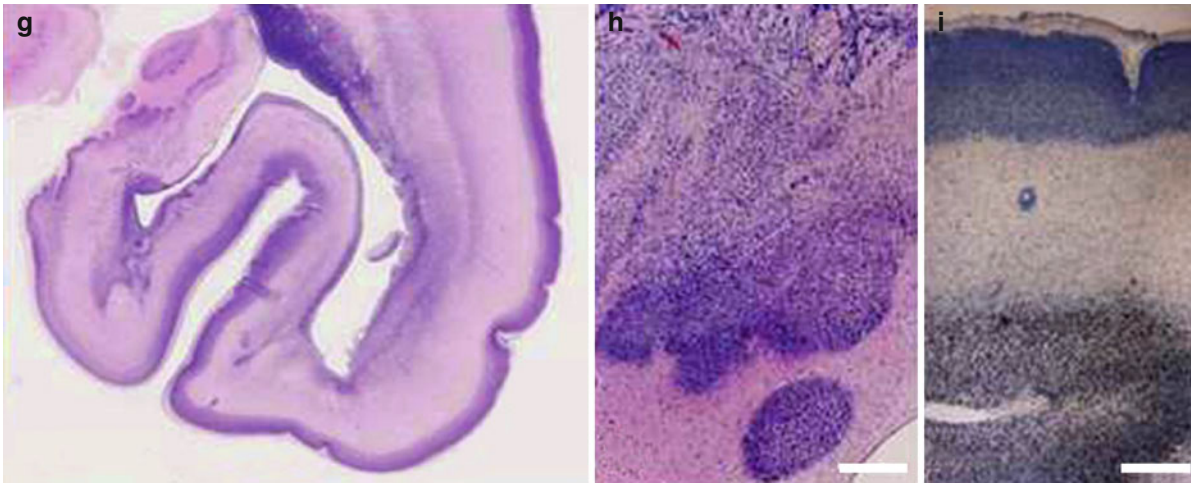


**Fig. 5.28** (continued)

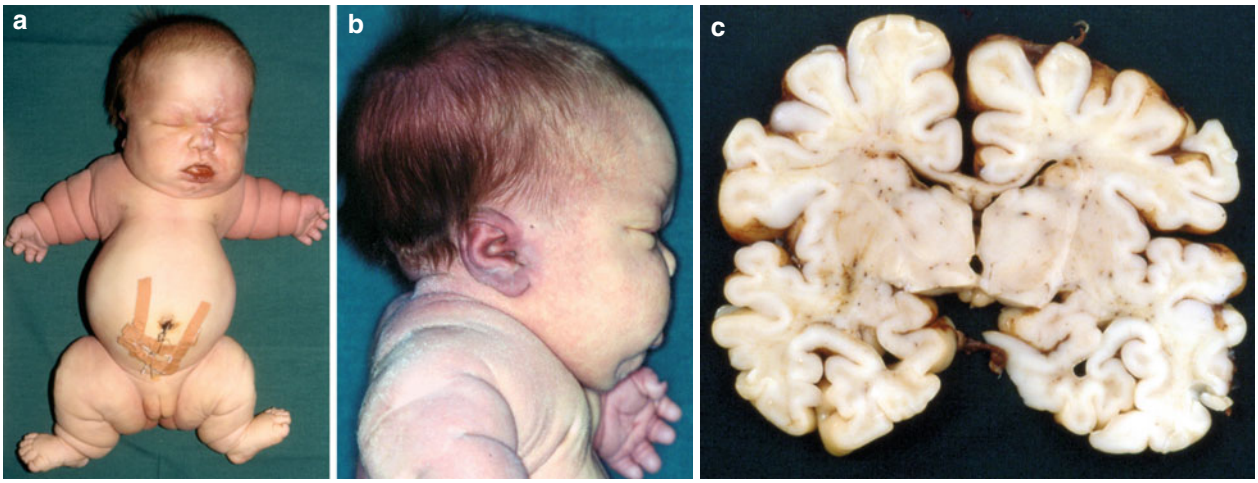


**Fig. 5.29** Thanatophoric dysplasia: frontal (**a**) and lateral (**b**) views of the full-term neonate; (**c**) transverse section through the brain showing the lack of normal enrolling of the hippocampus on both sides (Courtesy Martin Lammens, Nijmegen)

thorax and curved short femurs, but no cloverleaf skull yet (Fig. 5.28c). Both temporal lobes were enlarged and hyperconvoluted with broad gyri and deep sulci (Fig. 5.28d, e), which were composed of focal polymicrogyria-like shallow sulci and heterotopic neuroblastic cells in the intermediate and marginal zones (Fig. 5.28g). The cytoarchitecture from the entorhinal cortex to Ammon's horn was disorganized (Fig. 5.28h) with leptomeningeal glioneuronal heterotopia, immunoreactive for doublecortin (Fig. 5.28f) and nestin. Abundant precursor cells, immunoreactive for nestin and Ki-67 were observed with scattered mitoses in the thickened inner intermediate and subventricular zones of the temporal and occipital lobes (Fig. 5.28i). Genetic analysis revealed a point mutation at C8526T (R248C) in exon 7 of *FGFR3*.

**Case 2**: This girl was the second child of a 31-year-old healthy mother. After an uneventful pregnancy, apart from breech position, she was born by Caesarean section at 41 weeks of gestation. Birth weight was 4,200 g and crown-heel-length 42 cm (much less than P3). The skull was broad and large with frontal bossing (Fig. 5.29a, b; head circumference was 40 cm; much greater than P97). There was micromelia with phonehorn-formed long bones, a small and short thorax, and hypoplastic lungs. The baby died after 3 days. The babygram showed the typical configuration of thanatophoric dysplasia. The brain was megalencephalic and weighed 551 g (normal 420 ± 33 g). Both hippocampi lacked normal enrolling (Fig. 5.29c). A leptomeningeal neuroglial ectopia was found in the left hippocampal region.

The first case was kindly provided by Kyoko Itoh (Kyoto) and the second one by Martin Lammens (Antwerpen).

## References

Cohen MM Jr (1997) Short-limb skeletal dysplasias and craniosynostosis – what do they have in common. Pediatr Radiol 27:442–446

Hall JG, Lopez-Rangel M (1997) Bone dysplasias, nontraditional mechanisms of inheritance and monozygotic twins. Pediatr Radiol 27:422–427

Holtermüller K, Wiedemann HR (1960) Kleeblattschädel Syndrom. Med Monatsschr 14:439–446

Itoh K, Pooh R, Kanemura Y, Yamasaki M, Fushiki S (2013) Brain malformation with loss of normal FGFR3 expression in thanatophoric dysplasia type 1. Neuropathology 33: 663–666

### 5.8.2 Cranial Base Abnormalities

Abnormalities of the cranial base, and of the cervicooccipital junction in particular, account for some serious neurological problems in infants and children (Aicardi 1998). The Chiari malformations are discussed in Chap. 4. Most cases of ***basilar impression*** are congenital and may be familial (Bull et al. 1955; Coria et al. 1983), but acquired cases occur. The degree of impression is variable. In ***platybasia***, the base of the skull is flat. Partial forms exist and are often associated with various abnormalities of the atlas and condylar processes (Bull et al. 1955; Wackenheim 1967). Underlying neural anomalies are hydrosyringomyelia, fibrous bands compressing the lower brain stem, abnormal vessels and kinking of the medulla. Decompression of the posterior fossa can considerably improve the anatomy of the spinal cord (Menezes et al. 1980). A ***narrow foramen magnum*** is common in achondroplasia (Reid et al. 1987; Nelson et al. 1988). In many craniosynostosis syndromes, the cranial base is deformed (Van der Meulen et al. 1990). Recently, a smaller foramen magnum in Crouzon syndrome was shown to be caused by premature closure of the intra-occipital synchondroses (Rijken et al. 2013). ***Cervical vertebral blocks*** occur most commonly in Klippel-Feil syndrome (Chap. 6).

## References

Abu-Issa R, Smyth G, Smoak I, Yamamura K, Meyers EN (2002) *Fgf8* is required for pharyngeal arch and cardiovascular development in the mouse. Development 129:4613–4625

Acampora D, Mazan S, Lallemand Y, Avantaggiato V, Maury M, Simeone A, Brûlet P (1995) Forebrain and midbrain regions are deleted in *Otx2−/−* mutants due to a defective anterior neuroectoderm specification during gastrulation. Development 121: 3279–3290

Acampora D, Avantaggiato V, Tuorte F, Briata P, Corte G, Simeone A (1998) Visceral endoderm-restricted translation of *Otx1* mediates recovery of *Otx2* requirements for specification of anterior neural plate and normal gastrulation. Development 125: 5091–5104

Acampora D, Merlo GR, Paleari L, Zerega B, Postiglione MP, Mantero S et al (1999) Craniofacial, vestibular and bone defects in mice lacking the *Distal-less*-related gene *Dlx5*. Development 126: 3795–3809

Acloque H, Adams MS, Fishwick K, Bronner-Fraser M, Nieto MA (2009) Epithelial-mesenchymal transitions: the importance of changing cell state in development and disease. J Clin Invest 119:1438–1449

Adelmann HB (1925) The development of the neural folds and cranial ganglia in the rat. J Comp Neurol 39:19–171

Adelmann HB (1936) The problem of cyclopia. Q Rev Biol 11:116–182, and 284–304

Ahlgren SC, Bronner-Fraser M (1999) Inhibition of sonic hedgehog signaling in vivo results in craniofacial neural crest cell death. Curr Biol 9:1304–1314

Aicardi J (1998) Diseases of the nervous system in childhood, 2nd edn. Mac Keith, London

Aleksic S, Budzilovich G, Greco MA, McCarthy J, Reuben R, Margolis S et al (1984) Intracranial lipomas, hydrocephalus and other CNS anomalies in oculoauriculo-vertebral dysplasia (Goldenhar-Gorlin syndrome). Childs Brain 11:285–297

Alexander T, Nolte C, Krumlauf R (2009) Hox genes and segmentation of the hindbrain and axial skeleton. Annu Rec Cell Dev Biol 25:431–456

Anson BJ, Bast TH, Cauldwell EW (1948) The development of the auditory ossicles, the otic capsule and the extracapsular tissues. Ann Otol Rhinol Laryngol 57:603–632

Anson BJ, Hanson JS, Richany SF (1960) Early embryology of the auditory ossicles and associated structures in relation to certain anomalies observed clinically. Ann Otol Rhinol Laryngol 69:427–447

Apert E (1906) De l'acrocéphalosyndactylie. Bull Soc Méd (Paris) 23:1310–1330

Aybar MJ, Mayor R (2002) Early induction of neural crest cells: lessons learned from frog, fish and chick. Curr Opin Genet Dev 12:452–458

Aybar MJ, Nieto MA, Mayor R (2003) *Snail* precedes *Slug* in the genetic cascade required for the specification and migration of *Xenopus* neural crest. Development 130:483–494

Bachiller D, Klingensmith J, Shneyder N, Tran U, Anderson R, Rossant J, De Robertis EM (2003) The role of chordin/Bmp signals in mammalian pharyngeal development and DiGeorge syndrome. Development 130:3567–3578

Badano JL, Mitsuma N, Beales PL, Katsanis N (2006) The ciliopathies: an emerging class of human genetic disorders. Annu Rev Genomics Hum Genet 7:125–148

Bajpai R, Chen DA, Rada-Iglesias A, Zhang J, Xiong Y, Helms J et al (2010) CHD7 cooperates with PBAF to control multipotent neural crest formation. Nature 463:958–962

Barber BA, Rastegar M (2010) Epigenetic control of Hox genes during neurogenesis, development, and disease. Ann Anat 192: 261–274

Bardeen R (1910) Die Entwicklung des Schädels, des Zungenbeins und des Kehlkopfskeletts. In: Keibel F, Mall FP (eds) Handbuch der

Entwicklungsgeschichte des Menschen. I. Band. Hirzel, Leipzig, pp 402–456
Bartelmez GW, Blount MP (1954) The formation of neural crest from the primary optic vesicle in man. Contrib Embryol Carnegie Inst 35:55–91
Basch ML, Bronner-Fraser M, Garcia-Castro ML (2006) Specification of the neural crest occurs during gastrulation and requires Pax7. Nature 441:218–222
Batten EH (1958) The origin of the acoustic ganglion in the sheep. J Embryol Exp Morphol 6:597–615
Beales PL, Elcioglu N, Woolf AS, Parker D, Flinter FA (1999) New criteria for improved diagnosis of Bardet-Biedl syndrome: results of a population survey. J Med Genet 36:437–446
Belloni E, Muenke M, Roessler E, Traverso G, Siegel-Bartelt J, Frumkin A et al (1996) Identification of Sonic hedgehog as a candidate gene responsible for holoprosencephaly. Nat Genet 14: 353–356
Bendavid C, Dupé V, Rochard L, Gicquel I, Dubourg C, David V (2010) Holoprosencephaly: an update on cytogenetic abnormalities. Am J Med Genet C 154C:86–92
Berry SM, Gosden C, Snijders RJM, Nicolaides KH (1990) Fetal holoprosencephaly. Associated malformations and chromosomal defects. Fetal Diagn Ther 5:92–99
Beverdam A, Brouwer A, Reijnen M, Korving J, Meijlink F (2001) Severe nasal clefting and abnormal embryonic apoptosis in Alx3/Alx4 double mutant mice. Development 128:3975–3986
Bixler D, Ward R, Gale DD (1985) Agnathia-holoprosencephaly: a developmental field complex involving face and brain. Report of 3 cases. J Craniofac Genet Dev Biol Suppl 1:241–249
Blaas H-GK, Eik-Nes SH, Vainio T, Isaksen CV (2000) Alobar holoprosencephaly at 9 weeks gestational age visualized by two- and three-dimensional ultrasound. Ultrasound Obstet Gynecol 15: 62–65
Blaas H-GK, Eriksson AG, Salvesen KÅ, Isaksen CV, Christensen B, Møllerløkken G, Eik-Nes SH (2002) Brains and faces in holoprosencephaly: pre-and postnatal description of 30 cases. Ultrasound Obstet Gynecol 19:24–38
Bochukova EG, Roscioli T, Hedges DJ, Taylor IB, David DJ et al (2009) Rare mutations of FGFR2 causing Apert syndrome: identification of the first partial gene deletion, and an Alu element insertion from a new subfamily. Hum Mutat 30:204–211
Bockman DE, Redmond M, Kirby ML (1989) Alteration of early vascular development after ablation of cranial neural crest. Anat Rec 225:209–217
Bolande RP (1974) The neurocristopathies: a unifying concept of disease arising in neural crest development. Hum Pathol 4:409–429
Boshart L, Vlot EA, Vermeij-Keers C (2000) Epithelio-mesenchymal transformation in the embryonic face: implications for craniofacial malformations. Eur J Plast Surg 23:217–223
Bovolenta P, Mallamaci A, Boncinelli E (1996) Cloning and characterization of two chick homeobox genes, members of the *Six/sine oculis* family, expressed during eye development. Int J Dev Biol 1(Suppl):738–748
Bronner ME, Le Douarin NM (2012) Development and evolution of the neural crest: an overview. Dev Biol 366:2–9
Brown SA, Warburton D, Brown LY, Yu C, Roeder ER, Stengel-Rutkowski S et al (1998) Holoprosencephaly due to mutation in *ZIC2*, a homologue of *Drosophila odd-paired*. Nat Genet 20: 180–183
Brugmann SA, Cordero DR, Helms JL (2010) Craniofacial ciliopathies: a new classification for craniofacial disorders. Am J Med Genet A 152A:2995–3006
Bull JS, Nixon WL, Pratt RT (1955) Radiological criteria and familial occurrence of primary basilar impression. Brain 78:229–247
Bush JO, Jiang R (2012) Palatogenesis: morphogenetic and molecular mechanisms of secondary palate development. Development 139:231–243
Cano A, Perez-Moreno MA, Rodrigo I, Locascio A, Blanco MJ, del Barrio MG et al (2000) The transcription factor snail controls epithelial-mesenchymal transitions by repressing E cadherin expression. Nat Cell Biol 2:78–83
Capecchi MR (1997) The role of *Hox* genes in hindbrain development. In: Cowan WM, Jessell TM, Zipursky SL (eds) Molecular and cellular approaches to neural development. Oxford University Press, New York, pp 334–355
Cargile CB, McIntosh I, Clough MV, Rutberg J, Yaghmai R, Goodman BK et al (2000) Delayed membranous ossification of the cranium associated with familial translocation (2;3) (p15;q12). Am J Med Genet 92:328–335
Celik T, Simsek PO, Sozen T, Ozyuncu O, Utine GE, Talim B et al (2012) PRRX1 is mutated in an otocephalic newborn infant conceived by consanguineous parents. Clin Genet 81: 294–297
Chassaing N, Sorrentino S, Davis EE, Martin-Coignard D, Iacovelli A, Paznekas W et al (2012) OTX2 mutations contribute to the otocephaly-dysgnathia complex. J Med Genet 49:373–379
Chiang C, Litingtung Y, Lee E, Young KE, Corden JL, Westphal H, Beachy PA (1996) Cyclopia and defective axial patterning in mice lacking *Sonic hedgehog* gene function. Nature 383: 407–413
Chisaka O, Capecchi MR (1991) Regionally restricted developmental defects resulting from targeted disruption of the mouse homeobox gene *Hox-1.5*. Nature 350:473–479
Chotzen F (1932) Eine eigenartige familiäre Entwicklungsstörung (Akrocephalosyndactylie, Dysostosis craniofacialis und Hypertelorismus). Monatsschr Kinderheilk 55:97–122
Cohen MM Jr (1979) Craniofrontonasal dysplasia. Birth Defects 15: 85–89
Cohen MM Jr (1989a) Perspectives on holoprosencephaly: part I. Epidemiology, genetics, and syndromology. Teratology 40: 211–235
Cohen MM Jr (1989b) Perspectives on holoprosencephaly: part III. Spectra, distinctions, continuities, and discontinuities. Am J Med Genet 34:271–288
Cohen MM Jr (1993) Pfeiffer syndrome update, clinical subtypes, and guidelines for differential diagnosis. Am J Med Genet 45: 300–307
Cohen MM Jr (2002) Malformations of the craniofacial region: evolutionary, embryonic, genetic, and clinical perspectives. Am J Med Genet 115:245–268
Cohen MM Jr, Kreiborg S (1990) The central nervous system in the Apert syndrome. Am J Med Genet 35:36–45
Cohen MM Jr, Kreiborg S (1993) An updated pediatric perspective on the Apert syndrome. Am J Dis Child 147:989–993
Cohen MM Jr, Kreiborg S (1995) Hands and feet in the Apert syndrome. Am J Med Genet 57:82–96
Cohen MM Jr, MacLean RE (eds) (2000) Craniosynostosis: diagnosis, evaluation, and management, 2nd edn. Oxford University Press, New York
Cohen MM Jr, Shiota K (2002) Teratogenesis of holoprosencephaly. Am J Med Genet 109:1–15
Cohen MM Jr, Sulik KK (1992) Perspectives on holoprosencephaly: part II. Central nervous system, craniofacial anatomy, syndrome commentary, diagnostic approach, and experimental studies. J Craniofac Genet Dev Biol 12:196–244
Comijn J, Brex G, Vermassen P, Verschueren K, van Grunsven L, Bruyneel E et al (2001) The two-handed E box binding zinc finger proptein SIP1 downregulates E-cadherin and induces invasion. Mol Cell 7:1267–1278
Condie BG, Capecchi MR (1994) Mice with targeted disruptions in the paralogous genes *hoxa-3* and *hoxd-3* reveal synergistic interactions. Nature 370:304–307
Conley ME, Beckwith JB, Mancer JFK, Tenckhoff L (1979) The spectrum of the DiGeorge syndrome. J Pediatr 94:883–890

Cordero DR, Brugmann S, Chu Y, Bajpai R, Jame M, Helms JA (2011) Cranial neural crest cells on the move: their roles in craniofacial development. Am J Med Genet A 155A:270–279

Coria F, Quintana F, Rebollo M, Combarras O, Berciano J (1983) Occipital dysplasia and Chiari type I deformity in a family. Clinical and radiological study of three generations. J Neurol Sci 62: 147–158

Couly GF, Le Douarin NM (1985) Mapping of the early neural primordium in quail-chick chimeras. I. Developmental relationships between placodes, facial ectoderm, and prosencephalon. Dev Biol 110:422–439

Couly GF, Le Douarin NM (1987) Mapping of the early neural primordium in quail-chick chimeras. II. The prosencephalic neural plate and neural folds: implications for the genesis of cephalic human congenital abnormalities. Dev Biol 120:198–214

Couly GF, Le Douarin NM (1988) The fate map of the cephalic neural primordium at the presomitic to the 3-somite stage in the avian embryo. Development (Suppl) 103:101–113

Couly GF, Le Douarin NM (1990) Head morphogenesis in embryonic avian chimeras: evidence for a segmental pattern in the ectoderm corresponding to the neuromeres. Development 108:543–558

Couly GF, Coltey PM, Le Douarin NM (1992) The developmental fate of the cephalic mesoderm in quail-chick chimeras. Development 114:1–15

Couly GF, Coltey PM, Le Douarin NM (1993) The triple origin of skull in higher vertebrates: a study in quail-chick chimeras. Development 117:409–429

Couly G, Grapin-Bottom A, Coltey PM, Ruhin B, Le Douarin NM (1998) Determination of the identity of the derivatives of the cephalic neural crest: incompatibility between Hox gene expression and lower jaw development. Development 125:3445–3459

Couly G, Creuzet S, Bennaceur S, Vincent C, Le Douarin NM (2002) Interactions between Hox-negative cephalic neural crest cells and the foregut endoderm in patterning the facial skeleton in the vertebrate haed. Development 129:1061–1073

Cousley RRJ, Calvert ML (1997) Current concepts in the understanding of hemifacial microsomia. Br J Plast Surg 50:536–551

Creuzet S, Couly G, Vincent C, Le Douarin NM (2002) Negative effect of *Hox* gene expression on the development of the neural crest-derived facial skeleton. Development 129:4301–4313

Creuzet S, Schuler B, Couly G, Le Douarin NM (2004) Reciprocal relationships between Fgf8 and neural crest cells in facial and forebrain development. Proc Natl Acad Sci U S A 101:4843–4847

Creuzet S, Couly G, Le Douarin NM (2005) Patterning the neural crest derivatives during development of the vertebrate head: insights from avian studies. Proc Natl Acad Sci U S A 103:14033–14038

Croen LA, Shaw GM, Lammer EJ (1996) Holoprosencephaly: epidemiologic and clinical characterists of a California population. Am J Med Genet 64:465–472

Crouzon O (1912) Dysostose craniofaciale héréditaire. Bull Med Soc Med Hôp (Paris) 33:545–555

D'Amico-Martel A, Noden DM (1983) Contributions of placodal and neural crest cells to avian cranial peripheral ganglia. Am J Anat 66:445–468

Daft PA, Johnston MC, Sulik KK (1986) Abnormal heart and great vessel development following acute ethanol exposure in mice. Teratology 33:93–104

Dassot-Le Moal F, Wilson M, Mowat D, Collot N, Niel F, Goossens M (2007) ZFHX1B mutations in patients with Mowat-Wilson syndrome. Hum Mutat 28:313–321

de Heer IM, Hoogeboom AJM, Eussen HJ, Vaandrager JM, de Klein A (2004) Deletion of the TWIST gene in a large five-generation family. Clin Genet 65:396–399

de Jong T, Bannink N, Bredero-Boelhouwer HH, Van Veelen ML, Bartels MC, Hoeve LJ et al (2009) Long-term functional outcome in 167 patients with syndromic craniosynostosis; defining a syndrome-specific risk profile. J Plast Reconstr Aesthet Surg 63:1635–1641

DeMyer WE (1967) The median-cleft syndrome. Differential diagnosis of cranium bifidum occultum, hypertelorism, and median cleft nose, lip, and palate. Neurology 17:961–971

DeMyer WE, Zeman W, Palmer CG (1963) Familial holoprosencephaly (arhinencephaly) with median cleft palate. Neurology 13: 913–918

DeMyer WE, Zeman W, Palmer CG (1964) The face predicts the brain: diagnostic significance of median facial anomalies for holoprosencephaly (arhinencephaly). Pediatrics 34:256–263

Depew MJ, Simpson CA, Morallo M, Rubinstein JLR (2005) Reassessing the *Dlx* code: the genetic regulation of branchial arch skeletal pattern and development. J Anat (Lond) 207:501–561

DiGeorge AM (1965) Discussion on a new concept of the cellular basis of immunology. J Pediatr 67:907

Dixon MJ, Marres HAM, Edwards SJ, Dixon J, Cremers CWRJ (1994) Treacher Collins syndrome: correlation between clinical and genetic linkage studies. Clin Dysmorphol 3:96–103

Dixon J, Hovanes K, Shiang R, Dixon MJ (1997) Sequence analysis, identification of evolutionary conserved motifs and expression analysis of murine tcof1 provide further evidence for a potential function for the gene and its human homologue, TCOF1. Hum Mol Genet 6:727–737

Dixon J, Brakebusch C, Fässler R, Dixon MJ (2000) Increased levels of apoptosis in the prefusion neural folds underlie the craniofacial disorder, Treacher Collins syndrome. Hum Mol Genet 9: 1473–1480

Dixon J, Jones NC, Sandell LL, Jayasinghe SM, Crane J, Rey JP, Dixon MJ, Trainor PA (2006) Tcof1/Treacle is required for neural crest cell formation and proliferation deficiencies that cause craniofacial abnormalities. Proc Natl Acad Sci U S A 103: 13403–13408

Dixon J, Trainor PA, Dixon MJ (2007) Treacher Collins syndrome. Orthod Craniofac Res 10:88–95

Dixon MJ, Marazita ML, Beaty TH, Murray JC (2011) Cleft lip and palate: understanding genetic and environmental influences. Nat Rev Genet 12:167–178

Domené S, Roessler E, El-Jaick KB, Snir M, Brown JL, Vélez JI et al (2008) Mutations in the human SIX3 gene in holoprosencephaly are loss of function. Hum Mol Genet 17:3919–3928

Donnenfeld AE, Packer RJ, Zackai EH, Chee CM, Sellinger B, Emanuel BS (1989) Clinical, cytogenetic, and pedigree findings in 18 cases of Aicardi syndrome. Am J Med Genet 32:461–467

Driscoll DA, Burdoff ML, Emanuel BS (1992a) A genetic etiology for the DiGeorge syndrome: consistent deletions and microdeletions of 22q11. Am J Hum Genet 50:924–933

Driscoll DA, Spinner ND, Burdoff ML (1992b) Deletions and microdeletions of 22q11.2 in velo-cardiofacial syndrome. Am J Med Genet 44:261–268

Duband JL, Monier F, Delannet M, Newgreen D (1995) Epithelium-mesenchyme transition during neural cell development. Acta Anat (Basel) 154:63–78

Duhamel B (1966) Morphogenèse Pathologique. Masson, Paris

Dupin E, Coelho-Aguiar JM (2013) Isolation and differentiation properties of neural crest stem cells. Cytometry A 83A:38–47

Durbec PL, Larsson-Blomberg LB, Schuchardt A, Constantini F, Pachnis V (1996) Common origin and developmental dependence on c-ret of subsets of enteric and sympathetic neuroblasts. Development 122:349–358

Eagleson GW, Harris WA (1990) Mapping of the presumptive brain regions in the neural plate of *Xenopus laevis*. J Neurobiol 21: 427–440

Eagleson HW, Ferreiro B, Harris WA (1995) Fate of the anterior neural ridge and the morphogenesis of the *Xenopus* brain. J Neurobiol 28: 146–158

El Ghouzi V, Le Merrer M, Perrin-Schmitt F, Lajeunie E, Benit P, Renier D et al (1997) Mutations in the *TWIST* gene in Saethre-Chotzen syndrome. Nat Genet 15:42–46

El-Jaick KB, Powers SE, Bartholin L, Myers KR, Hahn J, Orioli IM et al (2007) Functional analysis of mutations in TG1F associated with holoprosencephaly. Mol Genet Metab 90:97–111

Emanuel BS, McDonald-McGinn D, Saitta SC, Zackai EH (2001) The 22q11.2 deletion syndrome. Adv Pediatr 48:39–73

Etchevers HC, Vincent C, Le Douarin NM, Couly GF (2001) The cephalic neural crest provides pericytes and smooth muscle cells to all blood vessels of the face and forebrain. Development 128:1059–1068

Etchevers HC, Amiel J, Lyonnet S (2006) Molecular basis of human neurocristopathies. Adv Exp Med Biol 589:213–234

Evrard L, Vanmuylder N, Dourov N, Hermans C, Biermans J, Werry-Huet A, Rooze M, Louryan S (2000) Correlation of HSP110 expression with all-trans retinoic acid-induced apoptosis. J Craniofac Genet Dev Biol 20:183–192

Favier B, Dollé P (1997) Developmental functions of mammalian *Hox* genes. Mol Hum Reprod 3:115–131

Ferrante MI, Giorgio G, Feather SA, Dulfone A, Wright V, Ghiani M et al (2001) Identification of the gene for oral-facial-digital type I syndrome. Am J Hum Genet 68:569–576

Ferrante MI, Zullo A, Barra A, Bimonte S, Messadeq N, Studer M et al (2006) Oral-facial-digital type I protein is required for primary cilia formation and left-right axis specification. Nat Genet 38:112–117

Ferrante MI, Romio L, Castro S, Collin JE, Goulding DA, Stemple DL et al (2009) Convergent extension movements and ciliary function are mediated by odf1, a zebrafish orthologue of the human oral-facial-digital type 1 syndrome gene. Hum Mol Genet 18: 289–303

Florisson JMG, Van Veelen MLC, Bannink N, Van Adrichem LNA, Van der Meulen JJNM, Bartels MC, Mathijssen IM (2010) Papilledema in isolated single-suture craniosynostosis: prevalence and predictive factors. J Craniofac Surg 21:20–24

Franceschetti A, Klein D (1949) Mandibulo-facial dysostosis: new hereditary syndrome. Acta Ophthalmol 27:144–224

Francis-West PH, Robson L, Evans DJR (2003) Craniofacial development: the tissue and molecular interactions that control development of the head. Adv Anat Embryol Cell Biol 169:1–144

Frank DU, Fotheringham LK, Brewer JA, Muglia LJ, Tristani-Firouzi M, Capecchi MR, Moon AM (2002) An *Fgfg8* mouse mutant phenocopies human 22q11 deletion syndrome. Development 129:4591–4603

Furness JB, Costa M (1987) The enteric nervous system. Churchill Livingstone, Edinburgh

Gammill LS, Bronner-Fraser M (2003) Neural crest specification: migrating into genomics. Nat Rev Neurosci 4:795–805

Gasser RF (2006) Evidence that some events of mammalian embryogenesis can result from differential growth, making migration unnecessary. Anat Rec B 289B:53–63

Gault DT, Renier D, Marchac D, Jones BM (1992) Intracranial pressure and intracranial volume in children with craniosynostosis. Plast Reconstr Surg 90:377–381

Geelen JAG, Langman J (1977) Closure of the neural tube in the cephalic region of the mouse embryo. Anat Rec 189:625–640

Gendron-Maguire M, Mallo M, Zhang M, Gridley T (1993) *Hoxa-2* mutant mice exhibit homeotic transformation of skeletal elements derived from cranial neural crest. Cell 75:1317–1331

Glaser RL, Jiang W, Boyadjiev SA, Tran AK, Zachary AA, Van Maldergem L et al (2000) Paternal origin of FGFR2 mutations in sporadic cases of Crouzon syndrome and Pfeiffer syndrome. Am J Hum Genet 66:768–777

Goldberg R, Motzkin B, Marion R, Scambler PJ, Shprintzen RJ (1993) Velocardiofacial syndrome. A review of 120 patients. Am J Med Genet 45:313–319

Golden JA (1998) Holoprosencephaly: a defect in brain patterning. J Neuropathol Exp Neurol 57:991–999

Golden JA, Chernoff GF (1993) Intermittent pattern of neural tube closure in two strains of mice. Teratology 47:73–80

Golden JA, Chernoff GF (1995) Multiple sites of anterior neural tube closure in humans: evidence from anterior neural tube defects (anencephaly). Pediatrics 95:506–510

Golding J, Trainor P, Krumlauf R, Gassman M (2000) Defects in pathfinding by cranial neural crest cells in mice lacking the Neuregulin receptor ErbB4. Nat Cell Biol 2:103–109

Goriely A, Wilkie AOM (2012) Paternal age effects mutations and selfish spermatogonial selection: causes and consequences for human disease. Am J Hum Genet 90:175–200

Gorlin RJ, Cohen MM Jr, Hennekam RCM (eds) (2001) Syndromes of the head and neck, 4th edn. Oxford University Press, Oxford

Goulding EH, Pratt RM (1986) Isotretinoin teratogenicity in mouse whole embryo culture. J Craniofac Genet Dev Biol 6: 99–112

Graham A, Begbie J (2000) Neurogenic placodes: a common front. Trends Neurosci 23:313–316

Graham A, Shimeld SM (2013) The origin and evolution of the ectodermal placodes. J Anat (Lond) 222:32–40

Graham A, Smith A (2001) Patterning the pharyngeal arches. Bioessays 23:54–61

Graham A, Heyman I, Lumsden A (1993) Even-numbered rhombomeres control the apoptotic elimination of neural crest cells from odd-numbered rhombomeres in the chick hindbrain. Development 119:233–245

Graham A, Francis-West P, Brickell P, Lumsden A (1994) The signalling molecule BMP4 mediates apoptosis in the rhombencephalic neural crest. Nature 372:684–686

Graham A, Begbie J, McGonnell I (2004) Significance of the cranial neural crest. Dev Dyn 229:5–13

Graham A, Okabe M, Quinlan R (2005) The role of the endoderm in the development and evolution of the pharyngeal arches. J Anat (Lond) 207:479–487

Graw J (2010) Eye development. Curr Top Dev Biol 90:343–386

Gripp KW, Wotton D, Edwards MC, Roessler E, Ades L, Meinecke P et al (2000) Mutations in *TGIF* cause holoprosencephaly and link *NODAL* signalling to human neural axis determination. Nat Genet 25:205–208

Hall JG, Pallister PD, Clarren SK, Beckwith JB, Wiglesworth FW, Fraser FC et al (1980) Congenital hypothalamic hamartoblastoma, hypopituitarism, imperforate anus, and postaxial polydactyly: a new syndrome? I. Clinical, causal, and pathogenetic considerations. Am J Med Genet 7:47–74

Hanson JR, Anson BJ, Strickland EM (1962) Branchial sources of the auditory ossicles in man. Arch Otolaryngol 76:100–122, and 200–215

Harville EW, Wilcox AJ, Lie RT, Vindemes H, Abyholm F (2005) Cleft lip and palate versus cleft lip only: are they distinct defects? Am J Epidemiol 162:448–453

Hatta K, Kimmel CB, Ho RK (1991) The cyclops mutation blocks specification on the floor plate of the zebrafish central nervous system. Nature 350:339–341

Hatta K, Puschel AW, Kimmel CB (1994) Midline signaling in the primordium of the zebrafish anterior CNS. Proc Natl Acad Sci U S A 91:2061–2065

Hay ED (1995) An overview of epithelio-mesenchymal transformation. Acta Anat (Basel) 154:8–20

Heaton ND, Garrett JR, Howard ER (1988) The enteric nervous system. In: Bannister R (ed) Autonomic failure. A textbook of clinical disorders of the autonomic nervous system, 2nd edn. Oxford University Press, Oxford, pp 238–263

Helms JA, Kim CH, Hu D, Minkoff R, Thaller C, Eichele G (1997) Sonic hedgehog participates in craniofacial morphogenesis and is down-regulated by teratogenic doses of retinoic acid. Dev Biol 187:25–35

Hide T, Hatakeyama J, Kimura-Yoshida C, Tian E, Takeda N, Ushio Y et al (2002) Genetic modifiers of otocephalic phenotypes in *Otx2* heterozygous mutant mice. Development 129:4347–4357

Hinrichsen K (1985) The early development of morphology and patterns of the face in the human embryo. Adv Anat Embryol Cell Biol 98:1–79

Hinrichsen KV (1990) Gesichtsentwicklung. In: Hinrichsen KV (ed) Humanembryologie. Springer, Berlin/Heidelberg/New York, pp 650–692

His W (1868) Untersuchungen über die erste Anlage des Wirbelthierleibes. Die erste Entwickelung des Hünchens im Ei. Vogel, Leipzig

His W (1885) Anatomie menschlicher Embryonen, III: Zur Geschichte der Organe. Vogel, Leipzig

Hochstetter F (1891) Ueber die Bildung der inneren Nasengänge oder primitiven Choanen. Verh Anat Ges (Anat Anz Suppl) 6: 145–151

Holmes G, Basilico C (2012) Mesodermal expression of Fgfr2S252W is necessary and sufficient to induce craniosynostosis in a mouse model of Apert syndrome. Dev Biol 368:283–293

Holmes G, Rothschild G, Basu Roy U, Deng CX, Mansukhani A, Basilico C (2009) Early onset of craniosynostosis in an Apert mouse model reveals critical features of this pathology. Dev Biol 328: 273–284

Hörstadius S (1950) The neural crest. Oxford University Press, Oxford

Hoving EW (1993) Frontoethmoidal encephaloceles. A study of their pathogenesis. Thesis, University of Groningen, The Netherlands

Howard ER, Garrett JR (1970) Histochemistry and electron microscopy of rectum and colon in Hirschsprung disease. Proc R Soc Med 63:20–22

Howard TD, Paznekas WA, Green ED, Chiang LC, Ma N, Ortiz de Luna RI et al (1997) Mutations in *TWIST*, a basic helix-loop-helix transcription factor, in Saethre-Chotzen syndrome. Nat Genet 15:36–41

Hsia YE, Bratu M, Herbordt A (1971) Genetics of the Meckel syndrome (dysencephalia splanchnocystica). Pediatrics 48:237–247

Hu D, Helms JA (1999) The role of sonic hedgehog in normal and abnormal craniofacial morphogenesis. Development 126: 4873–4884

Huang J, Rajagopal R, Liu Y, Dattilo LK, Shaham O, Ashery-Padan R, Beebe DC (2011) The mechanisms of lens placode formation: a case of matrix-mediated morhogenesis. Dev Biol 355:32–42

Hunt P, Gulisano M, Cook M, Sham MH, Faiella A, Wilkinson D et al (1991) A distinct *Hox* code for the branchial region of the vertebrate head. Nature 353:861–864

Iseki S, Wilkie AOM, Morriss-Kay GM (1999) *FGFR1* and *FGFR2* have distinct differentiation- and proliferation-related roles in the developing mouse skull vault. Development 126: 5611–5620

Jabs EW (2002) Genetic etiologies of craniosynostosis. In: Mooney MP, Siegel MI (eds) Understanding craniofacial anomalies: the etiopathogenesis of craniosynostoses and facial clefting. Wiley-Liss, New York, pp 125–146

Jabs EW, Muller U, Li X, Ma L, Luo W, Haworth IS et al (1993) A mutation in the homeodomain of the human MSX2 gene in a family affected with autosomal dominant craniosynostosis. Cell 75: 443–450

Jabs EW, Li X, Scott AF, Meyers G, Chen W, Eccles M et al (1994) Jackson-Weiss and Crouzon syndromes are allelic with mutations in fibroblast growth factor receptor 2. Nat Genet 8:275–279

Jacobson C, Granström G (1997) Clinical appearance of spontaneous and induced first and second branchial arch syndromes. Scand J Plast Reconstr Hand Surg 31:125–136

Jeanty P, Zaleski W, Fleischer AC (1991) Prenatal sonographic diagnosis of lipoma of the corpus callosum in a fetus with Goldenhar syndrome. Am J Perinatol 8:89–90

Jellinger K, Gross H, Kaltenbäck E, Grisold W (1981) Holoprosencephaly and agenesis of the corpus callosum: frequency of associated malformations. Acta Neuropathol (Berl) 55:1–10

Jenkins D, Seelow D, Jehee FS, Perlyn CA, Alonso LG, Bueno DF et al (2007) *RAB23* mutations in Carpenter syndrome imply an unexpected role for hedgehog signaling in cranial-suture development and obesity. Am J Hum Genet 80:1162–1170

Jiang R, Lan Y, Norton CR, Sundberg JP, Gridley T (1998) The *slug* gene is not essential for mesoderm or neural crest development in mice. Dev Biol 198:277–285

Jirásek JE (2001) An atlas of the human embryo and fetus. Parthenon, New York

Johnson D, Iseki I, Wilkie AOM, Morriss-Kay GM (2000) Expression patterns of *TWIST* and *FGFR1-2* and *-3* in the developing mouse coronal suture suggest a key role for *TWIST* in suture initiation and biogenesis. Mech Dev 91:341–345

Johnson JM, Moonis G, Green GE, Carmody R, Burbank HN (2011a) Syndromes of the first and second branchial arches, part 1: embryology and characteristic defects. AJNR Am J Neuroradiol 32: 14–19

Johnson JM, Moonis G, Green GE, Carmody R, Burbank HN (2011b) Syndromes of the first and second branchial arches, part 2: syndromes. AJNR Am J Neuroradiol 32:230–237

Johnston MC, Bronsky PT (1995) Prenatal craniofacial development: new insights on normal and abnormal mechanisms. Crit Rev Oral Biol Med 6:368–422

Johnston MC, Bronsky PT (2002) Craniofacial embryogenesis: abnormal developmental mechanisms. In: Mooney MP, Siegel MI (eds) Understanding craniofacial anomalies: the etiopathogenesis of craniosynostoses and facial clefting. Wiley-Liss, New York, pp 61–124

Jones MC (1990) The neurocristopathies: reinterpretation based upon the mechanism of abnormal morphogenesis. Cleft Palat J 27: 136–140

Jones KL (1997) Smith's recognizable patterns of human malformation, 5th edn. Saunders, Philadelphia

Jones NC, Lynn ML, Gaudenz K, Sakai D, Aoto K, Rey JP et al (2008) Prevention of the neurocristopathy Treacher Collins syndrome through inhibition of p53 function. Nat Med 14:125–133

Jongmans MC, Admiraal RJ, van der Donk KP, Vissers LE, Baas AF, Kapusta L et al (2006) CHARGE syndrome: the phenotypic spectrum of mutations in the CHD7 gene. J Med Genet 43:306–314

Jugessur A, Farlie PG, Kilpatrick N (2009) The genetics of isolated orofacial clefts: from genotypes to subphenotypes. Oral Dis 15:437–453

Juriloff DM, Sulik KK, Roderick TH, Hogan BK (1985) Genetic and developmental studies of a new mouse mutation that produces otocephaly. J Craniofac Genet Dev Biol 5:121–145

Justice CM, Yagnik G, Kim Y, Peter I, Wang Jabs E, Erazo M et al (2012) A genome-wide association study identifies susceptibility loci for nonsyndromic sagittal craniosynostosis near *BMP2* and within *BBS9*. Nat Genet 44:1360–1364

Kanagasuntheram R (1967) A note on the development of the tubotympanic recess in the human embryo. J Anat (Lond) 101:731–741

Kang S, Graham JM, Haskins-Olney A, Biesecker LG (1997) Gli3 Frameshift mutations cause autosomal dominant Pallister-Hall syndrome. Nat Genet 15:266–268

Kayserili H, Uz E, Niessen C, Vargel I, Alanay Y, Tuncbilek G et al (2009) ALX4 dysfunction disrupts craniofacial and epidermal development. Hum Mol Genet 18:4357–4366

Kayserili H, Altunoglu U, Ozgur H, Basaran S, Uyguner ZO (2012) Mild nasal malformations and parietal foramina caused by homozygous ALX4 mutations. Am J Med Genet A 158A:236–244

Kelbermann D, Tyson J, McInemey AM, Malcolm S, Winter RM, Bitner-Glindricz M (2000) Mapping of a locus for autosomal dominant hemifacial microsomia. J Med Genet 37(Suppl 1):S76

Kelley RI, Hennekam RCM (2001) Smith-lemli-opitz syndrome. In: Scriver CR, Beaudet al, Sly WS, Valle D (eds) The metabolic and molecular bases of inherited disease, 8th edn. McGraw-Hill, New York, pp 6183–6201

Kelley RI, Roessler E, Hennekam RCM, Feldman GL, Kosaki K, Jones MC et al (1996) Holoprosencephaly in RSH/Smith-Lemli-Opitz syndrome: does abnormal cholesterol metabolism affect the function of *Sonic Hedgehog*? Am J Med Genet 66: 478–484

Kimura C, Takeda N, Suzuki M, Oshimura M, Aizawa S, Matsuo I (1997) *Cis*-acting elements conserved between mouse and pufferfish *Otx2* genes govern the expression in mesencephalic neural crest cells. Development 124:3929–3941

Kirby ML (1987) Cardiac morphogenesis: recent research advances. Pediatr Res 21:219–224

Kirby ML, Waldo KL (1990) Role of neural crest in congenital heart disease. Circulation 82:332–340

Kjaer I, Keeling JW, Fischer-Hansen B (1999) The prenatal human cranium – normal and pathologic development. Munksgaard, Copenhagen

Kleinhaus S, Boley SJ, Sheran M, Sieber WK (1979) Hirschsprung's disease. A survey of the members of the academy of pediatrics. J Pediatr Surg 14:588–597

Kleinsasser O, Schlothane R (1964) Die ohrenbildung im rahmen der thalidomide-embryopathie. Z Laryngol Rhinol Otol 43:344–367

Knecht AK, Bronner-Fraser M (2002) Induction of the neural crest: a multigenic process. Nat Rev Genet 3:453–461

Knisely AS, Ambler MW (1988) Temporal-lobe abnormalities in thanatophoric dysplasia. Pediatr Neurosci 14:169–176

Kreiborg S (1981) Crouzon syndrome. A clinical and roentgencephalometric study. Scand J Plast Reconstr Surg 18(Suppl):1–198

Kress W, Schropp C, Lieb G, Petersen B, Busse-Ratzka M, Kunz J et al (2006) Saethre-Chotzen syndrome caused by TWIST1 gene mutations: functional differentiation from Muenke coronal synostosis syndrome. Eur J Hum Genet 14:39–48

Kubota Y, Ito K (2000) Chemotactic migration of mesencephalic neural crest cells in the mouse. Dev Dyn 217:170–179

Kulesa PM, Fraser SE (1998) Neural crest cell dynamics revealed by time-lapse video microscopy of whole embryo chick explant cultures. Dev Biol 204:327–344

Kulesa PM, Fraser SE (2000) In ovo time-lapse analysis after dorsal neural tube ablation shows rerouting of chick hindbrain neural crest. Development 127:2843–2852

Kurtz AB, Wapner RJ, Rubin CS, Cole-Beuglet C, Ross D, Goldberg BB (1980) Ultrasound criteria for in utero diagnosis of microcephaly. J Clin Ultrasound 8:11–16

Kweldam CF, Van der Vlugt JJ, Van der Meulen JJNM (2011) The incidence of craniosynostosis in the Netherlands, 1997–2007. J Plast Reconstr Aesthet Surg 64:583–588

LaBonne C, Bronner-Fraser M (1999) Molecular mechanisms of neural crest formation. Annu Rev Cell Dev Biol 15:81–112

LaBonne C, Bronner-Fraser M (2000) Snail-related transcriptional repressors are required in *Xenopus* for both the induction of the neural crest and its subsequent migration. Dev Biol 221:195–205

Lammer EJ, Opitz JM (1986) The DiGeorge anomaly as a developmental field defect. Am J Med Genet Suppl 2:113–127

Lammer EJ, Chen DT, Hoar RM, Agnish ND, Benke PJ, Braun JT et al (1985) Retinoic acid embryopathy. N Engl J Med 313:837–841

Laue K, Pogoda H-M, Daniel PB, van Haeringen A, Alanay Y, von Ameln S et al (2011) Craniosynostosis and multiple skeletal anomalies in humans and zebrafish result from a defect in the localized degradation of retinoic acid. Am J Hum Genet 89: 595–606

Le Douarin NM (1969) Particularités du noyau interphasique chez la caille japonaise (*Coturnix coturnix japonica*). Utilisation de ces particularités comme 'marquage biologique' dans les recherches sur les interactions tissulaires et les migrations cellulaires au cours de l'ontogenèse. Bull Biol Fr Belg 103:435–452

Le Douarin NM (1973) A Feulgen-positive nucleolus. Exp Cell Res 77:459–468

Le Douarin NM (2004) The avian embryo as a model to study the development of the neural crest: a long and still ongoing story. Mech Dev 121:1089–1102

Le Douarin NM, Dupin E (2012) The neural crest in vertebrate evolution. Curr Opin Genet Dev 22:381–389

Le Douarin NM, Kalcheim C (1999) The neural crest, 2nd edn. Cambridge University Press, Cambridge

Le Douarin NM, Teillet M-A (1973) The migration of neural crest cells to the wall of the digestive tract in avian embryo. J Embryol Exp Morphol 30:1–48

Le Douarin NM, Couly G, Creuzet SE (2012) The neural crest is a powerful regulator of pre-otic brain development. Dev Biol 366:74–82

Le Lièvre CS, Le Douarin NM (1975) Mesenchymal derivatives of the neural crest: analysis of chimaeric quail and chick embryos. J Embryol Exp Morphol 34:125–154

Lemire RJ, Cohen MM Jr, Beckwith JB, Kokich VG, Siebert JR (1981) The facial features of holoprosencephaly in anencephalic human specimens. I. Historical review and associated malformations. Teratology 23:297–303

Leussink B, Brouwer A, El Khattabi M, Poelmann RE, Gittenberger-de Groot AC, Meijlink F (1995) Expression patterns of the paired-related homeobox genes MHox/Prx1 and S8/Prx2 suggest roles in development of the heart and the forebrain. Mech Dev 52:51–64

Lindsay EA (2001) Chromosomal microdeletions: dissecting *del22q11* syndrome. Nat Rev Genet 2:858–868

Lindsay EA, Baldini A (2001) Recovery from arterial growth delay reduces penetrance of cardiovascular defects in mice deleted for the DiGeorge syndrome region. Hum Mol Genet 10:997–1002

Lindsay EA, Botta A, Jurcic V, Carattini-Rivera S, Cheah YC, Rosenblatt HM et al (1999) Congenital heart disease in mice deficient for the DiGeorge syndrome region. Nature 401:379–383

Lindsay EA, Vitelli F, Su H, Morishima M, Huyuh T, Pramparo T et al (2001) Tbx1 haploinsufficiency in the DiGeorge syndrome region causes aortic arch defects in mice. Nature 410:97–101

Linker C, Bronner-Fraser M, Mayor R (2000) Relationship between gene expression domains of Xsnail, Xslug and Xtwist and cell movement in the prospective neural crest of *Xenopus*. Dev Biol 224:215–225

Liu Q, Yang ML, Li ZJ, Bax XF, Wang XK, Lu L et al (2007) A simple and precise classification for cleft lip and palate: a five-digit numerical recording system. Cleft Palate Craniofac J 44:465–468

Liu Q, Spusta SC, Mi R, Lassiter RNT, Stark MR, Höke A et al (2012) Human neural crest cells derived from human ESCs and induces pluripotent stem cells: induction, maintenance and differentiation into functional Schwann cells. Stem Cells Transl Med 1: 266–278

Lleras-Forero L, Streit A (2012) Development of the sensory nervous system in the vetrebrate head: the importance of time. Curr Opin Genet Dev 22:315–322

Locascio A, Nieto MA (2001) Cell movements during vertebrate development: integrated tissue behaviour versus individual cell migration. Curr Opin Genet Dev 11:464–469

Luijsterberg AJM, Vermeij-Keers C (2011) Ten years recording common oral clefts with a new descriptive system. Cleft Palate Craniofac J 48:173–182

Luijsterberg AJ, Rozendaal AM, Vermeij-Keers C (2014) Classifying common oral clefts: a new approach after descriptive registration. Cleft Palate Craniofac J (in press)

Lumsden A, Guthrie S (1991) Alternating patterns of cell surface properties and neural crest cell migration during segmentation of the chick embryo. Development (Suppl) 2:9–15

Maarse W, Rozendaal AM, Pajkrt E, Vermeij-Keers C, Mink van der Molen AB, Van den Boogaard MJ (2012) A systematic review of associated structural and chromosomal defects in oral clefts: when is prenatal genetic analysis indicated? J Med Genet 49:490–498

Macca M, Franco B (2006) The molecular basis of oral-facial-digital syndrome, type 1. Am J Med Genet C 151C:318–325
Manley NR, Capecchi MR (1995) The role of *Hoxa-3* in mouse thymus and thyroid development. Development 121:1989–2003
Mark M, Ghyselinck NB, Chambon P (2004) Retinoic acid signalling in the development of branchial arches. Curr Opin Genet Dev 14:591–598
Marres HAM, Cremers CWRJ, Dixon MJ, Huygen PLM, Joosten FBM (1995) The Treacher Collins syndrome: a clinical, radiological and genetic linkage study of two pedigrees. Arch Otolaryngol Head Neck Surg 121:509–514
Marsh KL, Dixon MJ (2001) Treacher Collins syndrome. In: Scriver CR, Beaudet al, Sly WS, Valle D (eds) The metabolic & molecular bases of inherited disease, 8th edn. McGraw-Hill, New York, pp 6147–6152
Marucci DD, Dunaway DJ, Jones BM, Hayward RD (2008) Raised intracranial pressure in Apert syndrome. Plast Reconstr Surg 122:1162–1168
Mathijssen IMJ, Vaandrager JM, Van der Meulen JC, Pieterman H, Sonneveld JW, Kreiborg S, Vermeij-Keers C (1996) The role of bone centers in the pathogenesis of craniosynostosis: an embryologic approach using CT measurements in isolated craniosynostosis and Apert and Crouzon syndromes. Plast Reconstr Surg 98:17–26
Mathijssen IMJ, Van Splunder J, Vermeij-Keers C, Pieterman H, De Jong THR, Mooney MP, Vaandrager JM (1999) Tracing craniosynostosis to its developmental stage through bone center displacement. J Craniofac Genet Dev Biol 19:57–63
Mathijssen I, Arnaud E, Lajeunie E, Marchac D, Renier D (2006) Postoperative cognitive outcome for synostotic frontal plagiocephaly. J Neurosurg 105(1 Suppl Pediatr):16–20
Matsunaga E, Shiota K (1977) Holoprosencephaly in human embryos: epidemiologic studies of 150 cases. Teratology 16:261–272
Matsuo I, Kuratani S, Kimura C, Takeda N, Aizawa S (1995) Mouse *Otx2* functions in the formation and patterning of rostral head. Genes Dev 9:2646–2658
Mavrogiannis LA, Antonopoulou I, Baxova A, Kutilek S, Kim CA, Sugayama SM et al (2001) Haploinsufficiency of the human homeobox gene ALX4 causes skull ossification defects. Nat Genet 27:17–18
Mayor R, Theveneau E (2013) The neural crest. Development 140: 2247–2251
Mayor R, Morgan R, Sargent MG (1995) Induction of the prospective neural crest of *Xenopus*. Development 121:767–777
McDonald-McGinn DM, Feret H, Nah HD, Bartlett SP, Whitaker LA, Zacka EH (2010) Metopic craniosynostosis due to mutations in Gli3: a novel association. Am J Med Genet A 152A: 1654–1660
Meijlink F, Beverdam A, Brouwer A, Oosterveen TC, ten Berge D (1997) Vertebrate *aristaless*-related genes. Int J Dev Biol 43:651–663
Menezes AH, VanGilder JC, Graf CJ, McDonnell DE (1980) Craniocervical abnormalities: a comprehensive surgical approach. J Neurosurg 53:444–455
Mérida-Velasco JA, Sánchez-Montesinos I, Espín-Ferra J, García-García JD, Roldan-Schilling V (1993) Developmental differences in the ossification process of the human corpus and ramus mandibulae. Anat Rec 235:319–324
Meyers GA, Orlow SJ, Munro IR, Przylepa PA, Wang Jabs E (1995) Fibroblast growth factor receptor 3 (FGFR3) transmembrane mutation in Crouzon syndrome with acanthosis nigricans. Nat Genet 11:462–464
Ming JE, Muenke M (1998) Holoprosencephaly: from Homer to hedgehog. Clin Genet 53:155–163
Ming JE, Kaupas ME, Roessler E, Brunner HG, Golabi M, Tekin M et al (2002) Mutations in PATCHED-1, the receptor of SONIC HEDGEHOG, are associated with holoprosencephaly. Hum Genet 110:297–301
Mo R, Freer AM, Zinyk DL, Crackower MA, Michaud J, Heng HH et al (1997) Specific and redundant functions of Gli2 and Gli3 zinc finger genes in skeletal patterning and development. Development 124:113–123
Morriss-Kay GM, Ward SJ (1999) Retinoids and mammalian development. Int Rev Cytol 188:73–131
Morriss-Kay GM, Wilkie AOM (2005) Growth of the normal skull vault and its alteration in craniosynostosis: insights from human genetics and experimental studies. J Anat (Lond) 207: 637–653
Morriss-Kay GM, Ruberte E, Fukiishi Y (1993) Mammalian neural crest and neural crest derivatives. Ann Anat 175:501–507
Mossey PA, Little J, Munger RG, Dixon MJ, Shaw WC (2009) Cleft lip and palate. Lancet 347:1773–1785
Mowat DR, Croaker GD, Cass DT, Kerr BA, Chaitow J, Ades LC et al (1998) Hirschsprung disease, microcephaly, mental retardation, and cgaracteristic facial features: delineation of a new syndrome and identification of a locus at chromosome 2q22-q23. J Med Genet 35:617–623
Mowat DR, Wilson MJ, Goossens M (2003) Mowat-Wilson syndrome. J Med Genet 40:305–310
Muenke M, Beachy PA (2001) Holoprosencephaly. In: Scriver CR, Beaudet al, Sly WS, Valle D (eds) The metabolic & molecular bases of inherited disease, 8th edn. McGraw-Hill, New York, pp 6203–6230
Muenke M, Wilkie AOM (2001) Craniosynostosis syndromes. In: Scriver CR, Beaudet al, Sly WS, Valle D (eds) The metabolic & molecular bases of inherited disease, 8th edn. McGraw-Hill, New York, pp 6117–6146
Muenke M, Schell U, Hehr A, Robin NH, Losken HW, Schinzel A et al (1994) A common mutation in the fibroblast growth factor receptor 1 gene in Pfeiffer syndrome. Nat Genet 8:269–274
Muenke M, Gripp KW, McDonald-McGinn DM, Gaudenz K, Whitaker LA, Barlett SP et al (1997) A unique point mutation in the fibroblast growth factor receptor 3 gene (FGFR3) defines a new craniosynostosis syndrome. Am J Hum Genet 60:555–564
Müller F, O'Rahilly R (1980) The human chondrocranium at the end of the embryonic period, proper, with particular reference to the nervous system. Am J Anat 159:33–58
Müller F, O'Rahilly R (1983) The first appearance of the major divisions of the human brain at stage 9. Anat Embryol (Berl) 168: 419–432
Müller F, O'Rahilly R (1985) The first appearance of the neural tube and optic primordium in the human embryo at stage 10. Anat Embryol (Berl) 172:157–169
Müller F, O'Rahilly R (1986) The development of the human brain and the closure of the rostral neuropore at stage 11. Anat Embryol (Berl) 175:205–222
Müller F, O'Rahilly R (1988a) The development of the human brain from a closed neural tube at stage 13. Anat Embryol (Berl) 177:203–224
Müller F, O'Rahilly R (1988b) The first appearance of the future cerebral hemispheres in the human embryo at stage 14. Anat Embryol (Berl) 177:495–511
Müller F, O'Rahilly R (1989) Mediobasal prosencephalic defects, including holoprosencephaly and cyclopia, in relation to the development of the human forebrain. Am J Anat 185: 391–414
Müller F, O'Rahilly R (1994) Occipitocervical segmentation in staged human embryos. J Anat (Lond) 185:251–258
Nagai T, Aruga J, Takada S, Günther T, Spörle R, Shughart K, Mikoshiba K (1997) The expression of the mouse *Zic1*, *Zic2*, and *Zic3* genes suggests an essential role for *Zic* genes in body pattern formations. Dev Biol 182:299–313
Nagai T, Aruga J, Minowa O, Sugimoto T, Ohno Y, Noda T, Mikoshiba K (2000) Zic2 regulates the kinetics of neurulation. Proc Natl Acad Sci U S A 97:1618–1623

Nakatsu T, Uwabe C, Shiota K (2000) Neural tube closure in humans initiates at multiple sites: evidence from human embryos and implications for the pathogenesis of neural tube defects. Anat Embryol (Berl) 201:455–466

Nanni L, Ming JE, Bocian M, Steinhaus K, Bianchi DW, de Die-Smulders C et al (1999) The mutational spectrum of the *Sonic hedgehog* gene in holoprosencephaly: SHH mutations cause a significant proportion of autosomal dominant holoprosencephaly. Hum Mol Genet 8:2479–2488

Nanni L, Croen LA, Lammer EJ, Muenke M (2000) Holoprosencephaly: molecular study of a Californian population. Am J Med Genet 90:315–319

Naora H, Kimura M, Otani H, Yokoyama M, Koizumi I, Katiuki M, Tanaka O (1994) Transgenic mouse model of hemifacial microsomia: cloning and characterization of insertional mutation region on chromosome 10. Genomics 23:515–519

Nelson FN, Hecht JT, Horton WA, Butler IJ, Goldie WD, Miner M (1988) Neurological basis of respiratory complications in achondroplasia. Ann Neurol 24:89–93

Newgeen DF, Scheel M, Kaster V (1986) Morphogenesis of sclerotome and neural crest cells in avian embryos: in vivo and in vitro studies on the role of notochordal extracellular material. Cell Tissue Res 244:299–313

Niederreither K, Vermot J, Le Roux I, Schuhbaur B, Chambon P, Dollé P (2003) The regional pattern of retinoic acid synthesis by RALDH2 is essential for the development of the posterior pharyngeal arches and the enteric nervous system. Development 130: 2525–2534

Niederreither K, Dollé P (2008) Retinoic acid development: towards an integrated view. Nat Rev Genet 9:541–543

Nieminen P, Morgan NV, Fenwick AL, Parmanen S, Veistinen L, Mikkola ML et al (2011) Inactivation of IL11 signaling causes craniosynostosis, delayed tooth eruption, and supernumerary teeth. Am J Hum Genet 89:67–81

Nieto MA, Sargent MG, Wilkinson DG, Cooke J (1994) Control of cell behavior during vertebrate development by slug, a zinc finger gene. Science 264:835–839

Nishimura Y (1993) Embryological study of nasal cavity development in human embryos with reference to congenital nostril atresia. Acta Anat (Basel) 147:140–144

Noden DM (1978a) The control of avian cephalic neural crest cytodifferentiation. I. Skeletal and connective tissues. Dev Biol 67: 296–312

Noden DM (1978b) The control of avian cephalic neural crest cytodifferentiation. II. Neural tissues. Dev Biol 67:313–329

Noden DM (1983a) The role of the neural crest in patterning of avian cranial skeletal, connective, and muscle tissues. Dev Biol 96:144–165

Noden DM (1983b) The embryonic origins of avian craniofacial muscles and associated connective tissues. Am J Anat 186:257–276

Noden DM (1991a) Cell movements and control of patterned tissue assembly during craniofacial development. J Craniofac Genet Dev Biol 11:192–213

Noden DM (1991b) Vertebrate craniofacial development: the relation between ontogenetic process and morphological outcome. Brain Behav Evol 38:190–225

Noden DM, Trainor PA (2005) Relations and interactions between cranial mesoderm and neural crest populations. J Anat (Lond) 207:575–601

Norman MG, McGillivray BC, Kalousek DK, Hill A, Poskitt PJ (1995) Congenital malformations of the brain. Pathologic, embryologic, clinical, radiologic and genetic aspects. Oxford University Press, New York

Norris EH (1937) The parathyroid glands and lateral thyroid in man: their morphogenesis, histogenesis, topographic anatomy and prenatal growth. Contrib Embryol Carnegie Inst 26: 247–294

Norris EH (1938) The morphogenesis and histogenesis of the thymus gland in man: in which the origin of Hassall's corpuscle of the human thymus is discovered. Contrib Embryol Carnegie Inst 27: 191–207

O'Gorman S (2005) Second branchial arch lineages of the middle ear of wild-type and *Hoxa2* mutant mice. Dev Dyn 234:124–131

O'Leary DDM, Wilkinson DG (1999) Eph receptors and ephrins in neural development. Curr Opin Neurobiol 9:65–73

O'Rahilly R (1966) The early development of the eye in staged human embryos. Contrib Embryol Carnegie Inst 38:1–42

O'Rahilly R (1973) Developmental stages in human embryos. Part A: embryos of the first three weeks (stages 1 to 9). Carnegie Institution of Washington Publication 631, Washington, DC

O'Rahilly R (1983) The timing and sequence of events in the development of the human eye and ear. Anat Embryol (Berl) 168: 87–99

O'Rahilly R, Gardner E (1971) The timing and sequence of events in the development of the human nervous system during the embryonic period proper. Z Anat Entw Gesch 134:1–12

O'Rahilly R, Müller F (1981) The first appearance of the human nervous system at stage 8. Anat Embryol (Berl) 163:1–13

O'Rahilly R, Müller F (1999) The embryonic human brain. An atlas of developmental stages, 2nd edn. Wiley-Liss, New York

O'Rahilly R, Müller F (2001) Human embryology & teratology, 3rd edn. Wiley-Liss, New York

O'Rahilly R, Müller F (2007) The development of the neural crest in the human. J Anat (Lond) 211:335–351

Ongkosuwito EM, van Vooren J, van Neck JW, Wattel E, Wolvius EB, van Adrichem LN, Kuijpers-Jagtman AM (2013) Changes of mandibular ramal height, during growth in unilateral hemifacial microsomia patients and unaffected controls. J Craniomaxillofac Surg 41:92–97

Ongkosuwito EM, van Neck JW, Wattel E, van Adrichem LN, Kuijpers-Jagtman AM (2014) Craniofacial morphology in unilateral hemifacial microsomia. Br J Oral Maxillofac Surg (in press)

Oostrom CAM, Vermeij-Keers C, Gilbert PM, van der Meulen JC (1996) Median cleft of the lower lip and mandible: case reports, a new embryological hypothesis and subdivision. Plast Reconstr Surg 97:313–319

Opperman LA (2000) Cranial sutures as intramembranous growth sites. Dev Dyn 219:472–485

Osumi-Yamashita N, Iseki S, Noji S, Nohno T, Koyama E, Taniguchi S et al (1992) Retinoic acid treatment induces the ectopic expression of retinoic acid receptor β gene and excessive cell death in the embryonic mouse face. Dev Growth Differ 34:199–209

Pane M, Baranello G, Battaglia D, Donvito V, Carnevale F, Stefanini MC et al (2004) Severe abnormalities of the Pons in two infants with Goldenhar syndrome. Neuropediatrics 35:234–238

Park WJ, Theda C, Maestri NE, Meyers GA, Fryburg JS, Dufresne C, Cohen MM Jr, Jabs EW (1995) Analysis of phenotypic features and FGFR2 mutations in Apert syndrome. Am J Hum Genet 57:321–328

Passos-Bueno MR, Wilcox WR, Jabs EW, Sertie AL, Alonso LG, Kitoh H (1999) Clinical spectrum of fibroblast growth factor receptor mutations. Hum Mutat 14:115–125

Passos-Bueno MR, Ornelas CC, Fanganiello RD (2009) Syndromes of the first and second pharyngeal arches: a review. Am J Med Genet A 149A:1853–1859

Pauli RM, Pettersen JC, Arya S, Gilbert EF (1983) Familial agnathia-holoprosencephaly. Am J Med Genet 14:677–698

Pfeiffer RA (1964) Dominant erbliche Akrocephalosyndactylie. Z Kinderheilk 90:310–320

Phelps PD, Poswillo D, Lloyd GAS (1981) The ear deformities in mandibulofacial synostosis. Clin Otolaryngol 6:15–28

Pingault V, Ente D, Dastot-Le Moal F, Goossens M, Marlin S, Bondurand N (2010) Review and update of mutations causing Waardenburg syndrome. Hum Mutat 31:391–406

Poelmann RE, Dubois SV, Hermsen C, Smits-van Prooije AE, Vermeij-Keers C (1985) Cell degeneration and mitosis in the buccopharyngeal and branchial membranes in the mouse embryo. Anat Embryol (Berl) 171:187–192

Politzer G (1952) Zur normalen und abnormen Entwicklung des menschlichen Gesichtes. Z Anat Entw Gesch 116:332–347

Poswillo D (1973) The pathogenesis of the first and second branchial arch syndrome. Oral Surg 35:302–328

Poswillo D (1975) The pathogenesis of the Treacher Collins syndrome (mandibulofacial dysostosis). Br J Oral Surg 13:1–26

Pratt RM, Goulding EH, Abbott BD (1987) Retinoic acid inhibits migration of cranial neural crest cells in the cultured mouse embryo. J Craniofac Genet Dev Biol 7:205–217

Przylepa KA, Paznekas W, Zhang M, Golabi M, Bias W, Bamshad MJ et al (1996) Fibroblast growth factor receptor 2 mutations in Beare-Stevenson cutis gyrate syndrome. Nat Genet 13:492–494

Qu S, Niswender KD, Ji QS, van der Meer R, Keeney D, Magnuson MA, Wisdom R (1997) Polydactyly and ectopic ZPA formation in Alx-4 mutant mice. Development 124:3999–4008

Rannan-Eliya SV, Taylor IB, de Heer IM, van den Ouweland AMW, Wall SA, Wiklie AOM (2004) Paternal origin of *FGFR3* mutations in Muenke-type craniosynostosis. Hum Genet 115:200–207

Read AP (2001) Waardenburg syndrome. In: Scriver CR, Beaudet al, Sly WS, Valle D (eds) The metabolic & molecular bases of inherited disease. McGraw-Hill, New York, pp 6097–6116

Reardon W, Winter RM, Rutland P, Pulleyn LJ, Jones BM, Malcolm S (1994) Mutations in the fibroblast growth factor receptor 2 gene cause Crouzon syndrome. Nat Genet 8:98–103

Reid CS, Pyeritz RE, Kopits SE, Maria BL, Wang H, McPherson RW et al (1987) Cervicomedullary compression in young patients with achondroplasia: value of comprehensive neurologic and respiratory evaluation. J Pediatr 110:522–530

Renier D, Sainte-Rose C, Marchac D, Hirsch JF (1982) Intracranial pressure in craniosynostosis. Childs Nerv Syst 16:645–658

Renier D, Lajeunie E, Arnaud E, Marchac D (2000) Management of craniosynostosis. Childs Nerv Sys 16:645–658

Rhinn M, Dollé P (2012) Retinoic acid signalling during development. Development 139:843–858

Rice DP, Aberg T, Chan Y, Tang Z, Kettunen PJ, Pakarinen L et al (2000) Integration of FGF and TWIST in calvarial bone and suture development. Development 127:1845–1855

Rijken B, Lequin MH, De Rooi JJ, Van Veelen MLC, Mathijssen IMJ (2013) Foramen magnum size and involvement of its intra-occipital synchondroses in Crouzon syndrome. Plast Reconstr Surg 132: 993e–1000e

Rijli FM, Mark M, Lakharaju S, Dierich A, Dollé P, Chambon P (1993) A homeotic transformation is generated in the rostral branchial region of the head by disruption of *Hoxa-2*, which acts as a selector gene. Cell 75:1333–1349

Rijli FM, Gavalas A, Chambon P (1998) Segmentation and specification in the branchial region of the head: the role of the *Hox* selector genes. Int J Dev Biol 42:393–401

Rittler M, Lopez-Camelo JS, Castilla EE, Bermejo E, Cocchi G, Correa A et al (2008) Preferential associations between oral clefts and other major congenital anomalies. Cleft Palate Craniofac J 45: 525–532

Roessler E, Muenke M (1998) Holoprosencephaly: a paradigm for the complex genetics of brain development. J Inherit Metab Dis 21:481–497

Roessler E, Muenke M (2010) The molecular genetics of holoprosencephaly. Am J Med Genet C 154C:52–61

Roessler E, Belloni E, Gaudenz K, Jay P, Berta P, Scherer SW et al (1996) Mutations in the human *Sonic Hedgehog* gene cause holoprosencephaly. Nat Genet 14:357–360

Roessler E, Du Y-Z, Muller JL, Casas E, Allen WP, Gillessen-Kaesbach G et al (2003) Loss-of-function mutations in the human *GLI2* gene are associated with pituitary anomalies and holoprosencephaly-like features. Proc Natl Acad Sci U S A 100:13424–13429

Roessler E, Ouspenkaia MV, Karkera JD, Vélez JI, Kantipong A, Lacbawan F et al (2008) Reduced NODAL signaling strength via mutation of several pathway members including FOXH1 is linked to human heart defects and holoprosencephaly. Am J Hum Genet 83:18–29

Roessler E, Lacbawan F, Dubourg C, Paulussen A, Herbergs J, Hehr U et al (2009) The full spectrum of holoprosencephaly-associated mutations with the ZIC2 gene in humans predicts loss-of-function as the predominant disease mechanism. Hum Mutat 39:E541–E544

Ronen GM, Andrews WL (1991) Holoprosencephaly as a possible embryonic alcohol effect. Am J Med Genet 40:151–154

Rosa F, Piazza-Hepp T, Goetsch R (1994) Holoprosencephaly with 1st trimester topical isotretinoin. Teratology 49:418–419

Rozendaal AM, Luijsterberg AJ, Ongkosuwito EM, van den Boogaard MJ, de Vries E, Hovius SE, Vermeij-Keers C (2012) Delayed diagnosis and underreporting of congenital anomalies associated with oral clefts in the Netherlands: a national validation study. J Plast Reconstr Aesthet Surg 65:780–790

Rudé FP, Anderson L, Conley D, Gasser RF (1994) Three-dimensional reconstructions of the primary palate region in normal human embryos. Anat Rec 238:108–113

Ryan AK, Goodship JA, Wilson DI, Philip N, Levy A, Seidel H et al (1997) Spectrum of clinical features associated with interstitial chromosome 22q11 deletions: a European collaborative study. J Med Genet 34:798–804

Saethre H (1931) Ein Beitrag zum Turmschädelproblem (Pathogenese, Erblichkeit, und Symptomologie). Deutsch Z Nervenheilk 117: 533–555

Sakai Y (1989) Neurulation in the mouse: manner and timing of neural tube closure. Anat Rec 223:194–203

Sandikcioglu M, Molsted K, Kjaer I (1994) The prenatal development of the human nasal and vomeronasal bones. J Craniofac Genet Dev Biol 14:124–134

Sanlaville D, Verloes A (2007) CHARGE syndrome: an update. Eur J Hum Genet 15:389–399

Sanlaville D, Etchevers HC, Gonzales M, Martinovic J, Clément-Ziza M, Delezoide AL et al (2006) Phenotypic spectrum of CHARGE syndrome in fetuses with CHD7 truncating mutations correlates with expression during human development. J Med Genet 43: 211–217

Santagati F, Rijli FM (2003) Cranial neural crest and the building of the vertebrate head. Nat Rev Neurosci 4:806–818

Sato N, Matsuishi T, Utsunomiya N, Yamashita Y, Horikoshi T, Okudera T, Hashimoto T (1987) Aicardi syndrome with holoprosencephaly and cleft lip and palate. Pediatr Neurol 3:114–116

Sauka-Spengler T, Bronner-Fraser M (2008) A gene regulatory network orchestrates neural crest formation. Nat Rev Mol Cell Biol 9:557–568

Saunders CJ, Zhao W, Ardinger HH (2009) Comprehensive ZEB2 gene analysis for Mowat-Wilson syndrome in a North-American cohort: a suggested approach to molecular diagnostics. Am J Med Genet A 149A:2527–2531

Scambler PJ (1994) DiGeorge syndome and related birth defects. Sem Dev Biol 5:303–310

Scambler PJ (2000) The 22q11 deletion syndromes. Hum Mol Genet 9:2421–2426

Schier AF (2001) Axis formation and patterning in zebrafish. Curr Opin Genet Dev 11:393–404

Schinzel A (1983) Catalogue of unbalanced chromosome aberrations in man. De Gruyter, Berlin

Schneider RA, Hu D, Rubinstein JLR, Maden M, Helms JA (2001) Local retinoid signaling coordinates forebrain and facial morphogenesis by maintaining FGF8 and SHH. Development 128: 2755–2767

Sechrist J, Serbedzija GN, Scherson T, Fraser SE, Bronner-Fraser M (1993) Segmental migration of the hindbrain neural crest does not arise from its segmental generation. Development 118: 691–703

Sedano HO, Cohen MM Jr, Jirásek JE, Gorlin RJ (1970) Frontonasal dysplasia. J Pediatr 76:906–913
Sedlacková E (1967) The syndrome of the congenitally shortened velum. The dual innervation of the soft palate. Folia Phoniatr Logop 19:441–443
Sefton M, Sánchez S, Nieto MA (1998) Conserved and divergent roles for members of the Snail family of transcription factors in the chick and mouse embryo. Development 125:3111–3121
Selber J, Reid RR, Chike-Obi CJ, Sutton LN, Zackai EH, McDonald-McGinn D et al (2008) The changing epidemiologic spectrum of single-suture synostoses. Plast Reconstr Surg 122:527–533
Sergi C, Kamnasaran D (2011) PRRX1 is mutated in a fetus with agnathia-otocephaly. Clin Genet 79:293–295
Sharma VP, Fenwick AL, Brockop MS, McGowan SJ, Goos JAC, Hoogeboom AJM et al (2013) Mutations in *TCF12*, encoding a basic helix-loop-helix partner of TWIST1, are a frequent cause of coronal craniosynostosis. Nat Genet 45:304–307
Sheahan S, Bellamy CO, Hazland SN, Harrison DJ, Prost S (2008) TGFbeta induces apoptosis and EMT in primary mouse hepatocytes, independent of *p53*, *p21*$^{Cip1}$ or *Rb* status. BMC Cancer 8:191
Shin SH, Kogerman P, Lindstom E, Toftgard R, Biesecker LG (1999) GLI3 mutations in human disorders mimic Drosophila cubitus interruptus protein functions and localization. Proc Natl Acad Sci U S A 96:288–304
Shiota K (1993) Teratothanasia: prenatal loss of abnormal conceptuses and the prevalence of various malformations during human gastrulation. Birth Defects 29:189–199
Shprintzen RJ, Goldberg RB, Lewin HL, Sidoti EJ, Berkman MD, Argamaso RV (1978) A new syndrome involving cleft palate, cardiac anomalies, typical facies, and learning disabilities: velo-cardio-facial syndrome. Cleft Palate J 15:56–62
Siebert J, Cohen MM Jr, Sulik KK, Shaw C-M, Lemire RJ (1990) Holoprosencephaly: an overview and atlas of cases. Wiley-Liss, New York
Smith DW, Töndury G (1978) Origin of the calvaria and its sutures. Am J Dis Child 132:662–666
Smits-van Prooije AE, Vermeij-Keers C, Poelmann RE, Mentink MMT, Dubbeldam JA (1985) The neural crest in presomite to 40-somite murine embryos. Acta Morphol Neerl-Scand 23:99–114
Smits-van Prooije AE, Vermeij-Keers C, Dubbeldam JA, Mentink MMT, Poelmann RE (1987) The formation of mesoderm and mesectoderm in presomite rat embryos cultured in vitro, using WGA-Au as a marker. Anat Embryol (Berl) 176:71–77
Smits-van Prooije AE, Vermeij-Keers C, Poelmann RE, Mentink MMT, Dubbeldam JA (1988) The formation of mesoderm and mesectoderm in 5- to 41-somite rat embryos cultured in vitro, using WGA-Au as a marker. Anat Embryol (Berl) 177:245–256
Song J (2007) EMT or apoptosis: a decision for TGF-β. Cell Res 17:289–290
Sperber GH (2001) Craniofacial development. Decker, Hamilton
Sperber GH (2002) Craniofacial embryogenesis: normal developmental mechanisms. In: Mooney MP, Siegel MI (eds) Understanding craniofacial anomalies: the etiopathogenesis of craniosynostosis and facial clefting. Wiley-Liss, New York, pp 31–59
Sperber GH, Gorlin RJ (1997) Head and neck. In: Gilbert-Barness E (ed) Potter's pathology of the fetus and infant. Mosby, St. Louis, pp 1541–1579
Sperber GH, Honore LH, Johnson ES (1986) Acalvaria, holoprosencephaly and facial dysmorphia syndrome. In: Melnick M (ed) Current concepts in craniofacial anomalies. Liss, New York, pp 318–329
Sperber GH, Sperber SM, Guttmann GD (2010) Craniofacial embryogenetics and development. People's Medical Publishing House, Shelton
Spritz RA, Chiang P-W, Oiso N, Alkhateeb A (2003) Human and mouse disorders of pigmentation. Curr Opin Genet Dev 13:284–289
Starck D (1975) Embryologie, 3rd edn. Thieme, Stuttgart
Steventon B, Mayor R (2012) Early neural crest induction requires an initial inhibition of Wnt signals. Dev Biol 365:196–207
Streeter GL (1906) On the development of the membranous labyrinth and the acoustic and facial nerves in the human embryo. Am J Anat 6:139–165
Streeter GL (1918) The histogenesis and growth of the otic capsule and its contained periotic tissue-spaces in the human embryo. Contrib Embryol Carnegie Inst 7:5–54
Streeter GL (1922) Development of the auricle in the human embryo. Contrib Embryol Carnegie Inst 14:111–138
Sulik KK (1996) Craniofacial development. In: Turvey TA, Vig KWL, Fonseca RJ (eds) Facial clefts and synostosis – principles and management. Saunders, Philadelphia, pp 3–27
Sulik KK, Johnston MC, Daft PA, Russell WE (1986) Fetal alcohol syndrome and DiGeorge anomaly: critical ethanol exposure periods for craniofacial malformations as illustrated in an animal model. Am J Med Genet 2:191–194
Sulik KK, Johnston MC, Smiley SJ, Speight HS, Jarvis BE (1987) Mandibulofacial dysostosis (Treacher Collins syndrome): a new proposal for its pathogenesis. Am J Med Genet 27: 359–372
Sulik KK, Cook CS, Webster WS (1988) Teratogens and craniofacial malformations: relationship to cell death. Development 103: 213–231
Sun X, Meyers EN, Lewandoski M, Martin GR (1999) Targeted disruption of Fgf8 causes failure of cell migration in the gastrulating mouse embryo. Genes Dev 13:1834–1846
Tan S-S, Morriss-Kay G (1985) The development and distribution of the cranial neural crest in the rat embryo. Cell Tissue Res 240:403–416
Tavormina PL, Shiang R, Thompson LM, Zhu YZ, Wilkin DJ, Lachman RS et al (1995) Thanatophoric dysplasia (Type I and II) caused by distinct mutations in fibroblast growth factor receptor 3. Nat Genet 9:321–328
Taylor AI (1968) Autosomal trisomy syndrome: a detailed study of 27 cases of Edwards' syndrome and 27 cases of Patau's syndrome. J Med Genet 5:227–252
ten Berge D, Brouwer A, El Bahi S, Guénet JL, Robert B, Meijlink F (1998a) Mouse *Alx3*: an *aristaless*-like homeobox gene expressed during embryogenesis in ectomesenchyme and lateral plate mesoderm. Dev Biol 199:11–25
ten Berge D, Brouwer A, Korving J, Martin JF, Meijlink F (1998b) *Prx1* and *Prx2* in skeletogenesis: roles in the craniofacial region, inner ear and limbs. Development 125:3831–3842
ten Berge D, Brouwer A, Korving J, Reijnen MJ, van Raaij EJ, Verbeek F et al (2001) *Prx1* and *Prx2* are upstream regulators of sonic hedgehog and control cell proliferation during mandibular arch morphogenesis. Development 128:2929–2938
ten Donkelaar HJ, Vermeij-Keers C, Lohman AHM (2007) Hoofd en hals. In: ten Donkelaar HJ, Lohman AHM, Moorman AFM (eds) Klinische Anatomie en Embryologie, 3rd edn. Elsevier, Maarssen, pp 545–727 (in Dutch)
ten Donkelaar HJ, Němcová V, Lammens M, Overeem S, Keyser A (2011) The autonomic nervous system. In: ten Donkelaar HJ (ed) Clinical neuroanatomy: brain circuitry and its disorders. Springer, Heidelberg/Berlin/New York, pp 564–602
Thauvin-Robinet C, Cossee M, Cornier-Daire V, Van Maldergem L, Toutain A, Alembik Y et al (2006) Clinical, molecular, and genotype-phenotype correlation studies from 25 cases of oral-facial-digital syndrome type 1: a French and Belgian collaborative study. J Med Genet 45:54–61
Thauvin-Robinet C, Franco B, Saugier-Veber P, Aral B, Gigot N, Donzel A et al (2009) Genomic deletions of OFD1 account for 23 % of oral-facial-digital type 1 syndrome after negative DNA sequencing. Hum Mutat 30:E320–E329
The Treacher Collins Syndrome Collaborative Group (1996) Positional cloning of a gene involved in the pathogenesis of Treacher Collins syndrome. Nat Genet 12:130–136

Theveneau E, Mayor R (2012) Neural crest delamination and migration: from neuroepithelium-to-mesenchyme transition to collective cell migration. Dev Biol 366:34–54

Thiery JP, Sleeman JP (2006) Complex networks orchestrate epithelial-mesenchymal transitions. Nat Rev Mol Cell Biol 7:131–142

Thompson H, Tucker AS (2013) Dual origin of the epithelium of the mammalian middle ear. Science 339:1453–1456

Thompson DNP, Malcolm GP, Jones BM, Harkness WJ, Hauward RD (1995) Intracranial pressure in single-suture craniosynostosis. Pediatr Neurosurg 22:235–240

Thompson H, Ohazama A, Sharpe PT, Tucker AS (2012) The origin of the stapes and relationship to the otic capsule and oval window. Dev Dyn 241:1396–1404

Tint OS, Irons M, Elias ER, Batta AK, Frieden R, Chen TS, Salen G (1994) Defective cholesterol biosynthesis associated with Smith-Lemli-Opitz syndrome. N Engl J Med 330: 107–113

Tobin JL, Di Franco M, Eichers E, May-Simers H, Garcia M, Yan J et al (2008) Inhibition of neural crest migration underlies craniofacial dysmorphology and Hirschsprung's disease in Bardet-Biedl syndrome. Proc Natl Acad Sci U S A 105:6714–6719

Trainor PA (2010) Craniofacial birth defects: the role of neural crest cells in the etiology and pathogenesis of Treacher Collins syndrome and the potential for prevention. Am J Med Genet A 152A: 2984–2994

Trainor PA, Krumlauf R (2000) Patterning the cranial neural crest: Hindbrain segmentation and *Hox* gene plasticity. Nat Rev Neurosci 1:116–124

Trainor PA, Tan S-S, Tam PPL (1994) Cranial paraxial mesoderm: regionalisation of cell fate and impact on craniofacial development in mouse embryos. Development 120:2397–2408

Trainor PA, Sobieszczuk D, Wilkinson D, Krumlauf R (2002) Signalling between the hindbrain and paraxial tissues dictates neural crest migration pathways. Development 129:433–442

Treacher Collins E (1900) Cases with symmetrical congenital notches in the outer part of each lower lid and defective development of the malar bones. Trans Ophthalmol Soc UK 20:190–192

Twigg S, Kan R, Babbs C, Bochukova EG, Robertson SR, Wall SA et al (2004) Mutations of ephrin-B1 (*EFNB1*), a marker of tissue boundary formation, cause craniofrontonasal syndrome. Proc Natl Acad Sci U S A 101:8652–8657

Twigg SRF, Matsumoto K, Kidd AMJ, Goriely A, Taylor IB, Fisher RB et al (2006) The origin of EFNB1 mutations in craniofrontonasal syndrome: frequent somatic mosaicism and explanation of the paucity of carrier males. Am J Hum Genet 78: 999–1010

Twigg SRF, Versnel SL, Nurnberg G, Lees MM, Bhat M, Hammond P et al (2009) Frontorhiny, a distinctive presentation of frontonasal dysplasia caused by recessive mutations in the ALX3 homeobox gene. Am J Hum Genet 84:698–705

Twigg SRF, Lloyd D, Jenkins D, Elcioglu NE, Cooper CDO, Al-Sannaa N et al (2012) Mutations in multidomain protein MEGF8 identify a Carpenter syndrome subtype associated with defective lateralization. Am J Hum Genet 91:897–905

Twigg SRF, Vorgia E, McGowan SJ, Preaki I, Fenwick AL, Sharma VP et al (2013) Reduced dosage of *ERF* causes complex craniosynostosis in humans and mice and links ERK1/2 signalling to regulation of osteogenesis. Nat Genet 45:308–313

Van de Putte T, Franess A, Nelles L, van Grunsven LA, Huylebroeck D (2007) Neural crest-specific removal of Zfhx1b in mouse leads to a wide range of neurocristopathies reminiscent of Mowat-Wilson syndrome. Hum Mol Genet 16:1423–1436

Van De Water TR, Noden DM, Maderson PFA (1988) Embryology of the ear: outer, middle and inner. Otol Med Surg 1:3–27

Van der Meulen J, Mazzola R, Stricker M, Raphael B (1990) Classification of craniofacial malformations. In: Stricker M, Van der Meulen JC, Raphael B, Mazzola R, Tolhurst DE, Murray JE (eds) Craniofacial malformations. Churchill Livingstone, Edinburgh, pp 149–309

Van der Meulen JJNM, van der Hulst R, van Adrichem LNA, Arnaud E, Chin-Song D, Duncan C et al (2009) The increase of metopic synostosis: a pan-European observation. J Craniofac Surg 20: 283–286

van Gijn DR, Tucker AS, Cobourne MT (2013) Craniofacial development. Current concepts in the molecular basis of Treacher Collins syndrome. Br J Oral Maxillofac Surg 61:384–388

van Oostrom CG (1972) De initiële regionale ectoderm-ontwikkeling in het kopgebied bij de muis. Thesis, University of Amsterdam (in Dutch)

Varga ZM, Wegner J, Westerfield M (1999) Anterior movement of ventral diencephalic precursors separates the primordial eye field in the neural plate and requires cyclops. Development 126:5533–5546

Veitch E, Begbie J, Schilling TF, Smith MM, Graham A (1999) Pharyngeal arch patterning in the absence of neural crest. Curr Biol 9:1481–1484

Verloes A (2005) Updated diagnostic criteria for CHARGE syndrome: a proposal. Am J Med Genet A 133A:306–308

Verloes A, Dodinval P, Beco L, Bonnivert J, Lambotte C (1990) Lambotte syndrome: microcephaly, holoprosencephaly, intrauterine growth retardation, facial anomalies, and early lethality – a new sublethal multiple congenital anomaly/mental retardation syndrome in four sibs. Am J Med Genet 37:119–123

Vermeij-Keers C (1972) Transformations in the facial region of the human embryo. Adv Anat Embryol Cell Biol 46:1–30

Vermeij-Keers C (1990) Craniofacial embryology and morphogenesis: normal and abnormal. In: Stricker M, van der Meulen JC, Raphael B, Mazzola R, Tolhurst DE (eds) Craniofacial malformations. Churchill-Livingstone, Edinburgh, pp 27–60

Vermeij-Keers C, Poelmann RE (1980) The neural crest: a study on cell degeneration and the improbability of cell migration in mouse embryo. Neth J Zool 30:74–81

Vermeij-Keers C, Mazzola RF, van der Meulen JC, Stricker M, Raphael B (1983) Cerebro-craniofacial and craniofacial malformations: an embryological analysis. Cleft Palate J 20:128–145

Vermeij-Keers C, Poelmann RE, Smits-van Prooije AE, van der Meulen JC (1984) Hypertelorism and the median cleft face syndrome. An embryological analysis. Ophthalmic Paediatr Genet 4:97–105

Vermeij-Keers C, Poelmann RE, Smits-van Prooije AE (1987) 6.5-mm human embryo with a single nasal placode: cyclopia or hypotelorism? Teratology 36:1–6

Vermot J, Niederreither K, Garnier JM, Chambon P, Dollé P (2003) Decreased embryonic retinoic acid synthesis results in a DiGeorge syndrome phenotype in newborn mice. Proc Natl Acad Sci U S A 100:1763–1768

Verwoerd CDA, van Oostrom CG (1979) Cephalic neural crest and placodes. Adv Anat Embryol Cell Biol 58:1–75

Vieille-Grosjean I, Hunt P, Gulisano M, Boncinelli E, Thorogood P (1997) Branchial HOX gene expression and human craniofacial development. Dev Biol 183:49–60

Vissers LE, van Ravenswaaij CM, Admiraal R, Hurst JA, de Vries BB, Janssen IM et al (2004) Mutations in a new member of the chromodomain family cause CHARGE syndrome. Nat Genet 36: 955–957

Vissers LE, Cox TC, Maga AM, Short KM, Wiradjaja F, Janssen IM et al (2011) Heterozygous mutations of *FREM1* are associated with an increased risk of isolated metopic craniosynostosis in humans and mice. PLoS Genet 7:e1002278

Vitelli F, Taddei I, Morishima M, Meyers EN, Lindsay EA, Baldini A (2002) A genetic link between *Tbx1* and fibroblast growth factor signaling. Development 129:4605–4611

Waardenburg PJ (1951) A new syndrome combining developmental anomalies of the eyelids, eyebrows and nose root with pigmentary

defects of the iris and head hair and with congenital deafness. Am J Hum Genet 3:195–253
Wackenheim A (1967) Les dysplasies des condyles occipitaux. Ann Radiol 11:535–543
Wallis DE, Roessler E, Hehr U, Nanni L, Wiltshire T, Richieri-Costa A et al (1999) Mutations in the homeodomain of the human *SIX3* gene cause holoprosencephaly. Nat Genet 22:196–198
Wallis D, Lacbawan F, Jain M, Der kaloustian VM, Steiner CE, Moeschler JB et al (2008) Additional EFNB1 mutations in craniofrontonasal syndrome. Am J Hum Genet A 146A: 2008–2012
Webster WS, Johnston MC, Lammer EJ, Sulik KK (1986) Isotretinoin embryopathy and the cranial neural crest: an in vivo and in vitro study. J Craniofac Genet Dev Biol 6:211–222
Weller GL Jr (1933) Development of the thyroid, parathyroid and thymus glands in man. Contrib Embryol Carnegie Inst 24:93–142
Whiteford ML, Tolmie JL (1996) Holoprosencephaly in the west of Scotland 1975–1994. J Med Genet 33:578–584
Wiley MJ, Cauwenbergs P, Taylor IM (1983) Effects of retinoic acid on the development of the facial skeleton in hamsters; early changes involving neural crest cells. Acta Anat 116:180–192
Wilkie AOM (1997) Craniosynostosis: genes and mechanisms. Hum Mol Genet 6:1647–1656
Wilkie AOM, Morriss-Kay GM (2001) Genetics of craniofacial development and malformation. Nat Rev Neurosci 2:458–468
Wilkie AO, Slaney SF, Oldridge M, Poole MD, Ashworth GJ, Hockley AD et al (1995) Apert syndrome results from localized mutations of FGFGR2 and is allelic with Crouzon syndrome. Nat Genet 9: 165–172
Willhite CC, Hill RM, Irving AW (1986) Isotretinoin-induced craniofacial malformations in humans and hamsters. J Craniofac Genet Dev Biol 6:193–209
Williams PL et al (eds) (1995) Gray's anatomy, 38th edn. Churchill Livingstone, Edinburgh
Wong GB, Mulliken JB, Benacerraf BR (2001) Prenatal diagnosis of major craniofacial anomalies. Plast Reconstr Surg 108:1316–1333
Woods RH, Ul-Haq E, Wilkie AOM, Jayamohan J, Richard PG, Johnson D et al (2009) Reoperation for intracranial hypertension in TWIST1-confirmed Saethre-Chotzen syndrome: a 15-year review. Plast Reconstr Surg 123:1801–1810
Wraith JE, Super M, Watson GH, Phillips M (1985) Velo-cardio-facial syndrome presenting as holoprosencephaly. Clin Genet 27: 408–410
Wright S, Wagner K (1934) Types of subnormal development of the head from inbred strains of guinea pigs and their bearing on the classification and interpretation of vertebrate monsters. Am J Anat 54:383
Wu YQ, Badano JL, McCaskill C, Vogel H, Potocki L, Shaffer LG (2000) Haploinsufficiency of ALX4 as a potential cause of parietal foramina in the 11p11.2 contiguous gene-deletion syndrome. Am J Hum Genet 67:1327–1332
Wu J, Saint-Jeannet J-P, Klein PS (2003) Wnt-frizzled signaling in neural crest formation. Trends Neurosci 26:40–45
Wuyts W, Cleiren E, Homfray T, Rasore-Quartino A, Vanhoenacker F, Van Hul W (2000a) The ALX4 homeobox gene is mutated in patients with ossification defects of the skull. J Med Genet 37: 916–920
Wuyts W, Reardon W, Preis S, Homfrey T, Rasore-Quartino A, Christians H et al (2000b) Identification of mutations in the *MSX2* homeobox gene in families affected with foramina parietalia permagna. Hum Mol Genet 9:1251–1255
Yagi H, Furutani Y, Hamada H, Sasaki T, Asakawa S, Minoshima S et al (2003) Role of *TBX1* in human del22q11.2 syndrome. Lancet 362:1366–1373
Yutzey KE (2010) DiGeorge syndrome, Tbx1, and retinoic acid signalling come full circle. Circ Res 106:630–632
Zhao Q, Behringer RR, DeCrombrugghe B (1996) Prenatal folic acid treatment suppresses acrania and meroanencephaly in mice mutant for the *Cart1* homeobox gene. Nat Genet 13:275–283
Zuber ME, Gestri G, Viczian AS, Barsacchi G, Harris WA (2003) Specification of the vetrebrate eye by a network of eye field transcription factors. Development 130:5155–5167